

**EGE UNIVERSITY GRADUATE SCHOOL OF  
NATURAL AND APPLIED SCIENCE**

**(PhD THESIS)**

**OPTIMIZATION AND VALIDATION OF  
CENTRI-VOLTAMMETRIC TECHNIQUE  
FOR ULTRATRACE MERCURY ANALYSIS  
IN NATURAL SAMPLES**

**İpek ÜRKMEZ**

**Supervisors: Doç. Dr. H. İsmet GÖKÇEL**

**Prof. Dr. F. Nil ERTAŞ**

**Department of Chemistry**

**Scientific Department Code: 405.03.01**

**Presentation Date: 03.09.2010**

**Bornova - İZMİR**

**2010**



**İpek ÜRKMEZ** tarafından **Doktora** tezi olarak sunulan “**Optimization and Validation of Centri-Voltammetric Technique for Ultratrace Mercury Analysis in Natural Samples**” başlıklı bu çalışma E.Ü. Lisansüstü Eğitim ve Öğretim Yönetmeliği ile E.Ü. Fen Bilimleri Enstitüsü Eğitim ve Öğretim Yönergesi'nin ilgili hükümleri uyarınca tarafımızdan değerlendirilerek savunmaya değer bulunmuş ve 03.09.2010 tarihinde yapılan tez savunma sınavında aday oybirliği ile başarılı bulunmuştur.

**Jüri Üyeleri:**

**İmza**

**Jüri Başkanı : Doç. Dr. H. İsmet GÖKÇEL** .....

**Raportör Üye: Prof. Dr. Ümran YÜKSEL** .....

**Üye : Prof. Dr. Şule AYCAN** .....

**Üye : Doç. Dr. Nuri NAKİBOĞLU** .....

**Üye : Doç. Dr. Zekerya DURSUN** .....



## ÖZET

DOĞAL ÖRNEKLERDE SANTRİ-VOLTAMMETRİK ESER CİVA  
ANALİZİNİN OPTİMİZASYONU VE VALİDASYONU

ÜRKMEZ, İpek

Doktora Tezi, Kimya Anabilim Dalı

Tez Yöneticileri: Doç. Dr. H. İsmet GÖKÇEL

Prof. Dr. F. Nil ERTAŞ

3 Eylül 2010, 136 sayfa

Bu çalışmada, cıva(II) tayini için indirgen reaktif olarak hidrazinin ve taşıyıcı materyal olarak Purolite C100'ün kullanıldığı iki ayrı santri-voltammetrik işlem gerçekleştirilmiştir. Son söz edilen yöntemde yeni tasarlanan “*santri-voltammetrik hücre*” kullanılmıştır.

Hidrazin ve Purolite C100 kullanılarak cıva(II) iyonuna ilişkin en yüksek akım değerlerini elde etmek amacıyla çeşitli deneysel parametrelerin etkileri olası en geniş aralıklarda incelenmiştir. Saptanan optimum koşullarda, sırasıyla  $1.0 \times 10^{-8}$  M ile  $1.0 \times 10^{-10}$  M ve  $1.0 \times 10^{-7}$  M ile  $5.0 \times 10^{-11}$  M Hg(II) derişim aralıklarında kalibrasyon grafikleri logaritmik olarak doğrusal bulunmuştur. Bu doğruların denklemleri:

$$\text{Hidrazin için } \log i_p = -0.3467 \log C_{\text{Hg(II)}} + 6.0912 \quad (R^2: 0.9869)$$

$$\text{Purolite C100 için } \log i_p = -0.3047 \log C_{\text{Hg(II)}} + 5.9119 \quad (R^2: 0.9937)$$

şeklinde. Hidrazin ile altın film elektrot kullanılırken, Purolite C100 ile çalışıldığında yalın camımsı karbon elektrot kullanılması işlem sayısını oldukça azaltmıştır. Tekrarlanabilirlik hidrazin ve Purolite C100 kullanıldığında sırasıyla %1.39 ve %1.78 olarak saptanmıştır. Purolite C100 kullanılması ile  $5.0 \times 10^{-11}$  M gibi eser düzeydeki Hg(II) iyonları ölçülebilmüş ve bu yöntemin geçerliliği gösterilmiştir.

Purolite C100 kullanılarak gerçekleştirilen santri-voltammetrik yöntemin belirtme (LOD) ve saptama alt sınırlarını (LOQ) saptamak için cıvaya ilişkin pik akımlarının ölçülebildiği en seyreltik cıva(II) çözeltilerinde çalışılmıştır. Optimum koşullarda  $5.0 \times 10^{-11}$  M Hg(II) çözeltilisinde ölçülen pik akımlarının ( $n = 7$ ) standart sapmasından LOD ve LOQ sırasıyla  $1.0 \times 10^{-13}$  M ve  $5.8 \times 10^{-12}$  M Hg(II) olarak hesaplanmıştır.

Hidrazin ve Purolite C100'ün kullanıldığı santri-voltammetrik analiz yöntemlerinin doğruluğunu test etmek için  $1.0 \mu\text{g L}^{-1}$  Hg(II) içeren bir standart çözeltilinin ölçüm sonuçları indüktif eşleşmiş plazma kütle spektroskopisi (ICP-MS) ölçüm sonuçlarıyla karşılaştırılmıştır. Amaçlanan yöntemlerin bağıl hatası, ICP-MS yönteminin ki %2.8 iken, sırasıyla %10.3 ve % 6.3 olarak bulunmuştur.

Cd(II), Pb(II), Cu(II) ve Fe(III) iyonlarının cıva(II) tayinine girişim etkileri değerlendirilmiştir. Bu iyonların derişimleri  $1 \times 10^{-9}$  M'dan daha seyreltik olduğunda girişim etkileri görülmemiştir. Purolite C100'ün kullanıldığı santri-voltammetrik analiz yöntemi olası girişim etkileri dikkate alınarak ve standart katma yapılarak kaynak sularına herhangi bir ön işlem yapılmaksızın uygulanmıştır. Bulunan sonuçlar aynı örneklerin indüktif eşleşmiş plazma optik emisyon spektroskopisi sonuçları ile karşılaştırılmıştır. Her iki yöntemle kaynak sularında saptanan cıva(II) derişimlerinin yakınlığı öne sürülen yöntemin doğruluğunu ortaya koymuştur.

**Anahtar sözcükler:** Santri-voltammetri, santrifüj, altın film elektrot, anodik sıyırma voltammetrisi, cıva, hidrazin, Purolite C100



## ABSTRACT

**OPTIMIZATION AND VALIDATION OF  
CENTRI-VOLTAMMETRIC TECHNIQUE FOR ULTRATRACE  
MERCURY ANALYSIS IN NATURAL SAMPLES**

ÜRKMEZ, İpek

PhD in Chemistry

Supervisors: Assoc. Prof. Dr. H. İsmet GÖKÇEL

Prof. Dr. F. Nil ERTAŞ

3 September 2010, 136 pages

In this study, two centri-voltammetric procedures were described for mercury(II) determination by using hydrazine as a reducing agent and Purolite C100 as a carrier material. The latter method was carried out using “*the centri-voltammetric cell*” that was newly introduced.

The conditions were determined to obtain the highest levels of current related to mercury(II) ion with hydrazine and Purolite C100 by studying the largest possible intervals to investigate the effect of various experimental parameters. In the conditions optimized, calibration curves of Hg(II) concentrations ranging from  $1.0 \times 10^{-8}$  M to  $1.0 \times 10^{-10}$  M and  $1.0 \times 10^{-7}$  M to  $5.0 \times 10^{-11}$  M were found in a logarithmically linear fashion, respectively. Their equations were as follows:

$$\text{with hydrazine} \quad \log i_p = -0.3467 \log C_{\text{Hg(II)}} + 6.0912 \quad (R^2: 0.9869)$$

$$\text{with Purolite C100} \quad \log i_p = -0.3047 \log C_{\text{Hg(II)}} + 5.9119 \quad (R^2: 0.9937)$$

While gold film electrode was used with hydrazine, the use of a bare glassy carbon electrode in studies with Purolite C100 has considerably shortened the procedure. The repeatability values were found as 1.39% and 1.78% when hydrazine and Purolite C100 were used, respectively. When Purolite C100 resin was used as a carrier material, Hg(II) levels of as low as  $5 \times 10^{-11}$  M was able to measure and this method was to be validated.

Limit of detection (LOD) and quantification (LOQ) of centri-voltammetric method using Purolite C100 were determined according to the peak currents ( $n = 7$ ) of minimum measurable concentration for Hg(II). Under optimized conditions LOD and LOQ were calculated as  $1.0 \times 10^{-13}$  M and  $5.8 \times 10^{-12}$  M from the standard deviation of peak current values for  $5.0 \times 10^{-11}$  M Hg(II) solution, respectively.

To test the accuracy of the centri-voltammetric analysis methods using hydrazine and Purolite C100, the obtained results for a standard solution containing  $1.0 \mu\text{g L}^{-1}$  Hg(II) were compared with inductively coupled plasma mass spectrometry (ICP-MS) measurements of the same solution. Relative percentage errors of the proposed methods were 10.3% and 6.3%, respectively while that of ICP-MS was 2.8%.

Interferences of Cd(II), Pb(II), Cu(II) and Fe(III) ions on the mercury signal were evaluated. When these ions concentration is more dilute than  $1.0 \times 10^{-9}$  M, it was not observed any interference effect. The developed centri-voltammetric method using Purolite C100 was applied to spring water without any pre-treatment with considering interference effects and standard addition. The obtained results were compared with that of inductively coupled plasma optical emission spectrometric measurements. Proximity of determined mercury(II) concentrations in spring water samples with both methods set forth accuracy of the proposed method.

**Keywords:** centri-voltammetry, centrifugation, gold film electrode, anodic stripping voltammetry, mercury, hydrazine, Purolite C100





## ACKNOWLEDGEMENT

I would like to express my sincere gratitude Doç. Dr. H. İsmet.Gökçel and Prof. Dr. F. Nil Ertay for their kind supervision and great contributions the whole study.

I am also grateful to Prof. Dr. Hüseyin TURAL we are in dept of him encouragement throughout this thesis.

I also would like to express my sincere gratitude to Doç. Dr. Nuri Nakibođlu, Doç. Dr. Zekerya Dursun for their valuable suggestions throughout the study.

I also thank to all of the members of the chemistry department and especially to the members of analytical chemistry division.

I also thank to Yard. Doç. Dr. Ceylan Zafer for helping to AFM imaging studies at Ege University Solar Energy Institute. I wish to thank to Duygu Ođuz Kılıç for helping SEM imaging studies at İzmir Institute of Technology (Centre for Materials Research).

I also thank to Ress. Asst. Melik Kara for helping ICP-MS and ICP-OES measurements at Dokuz Eylül University Environmental Engineering Department (Air Pollution Laboratory).

I would like to thank “ARGE DİZAYN Ltd. Şti.” and Halil İbrahim Göney for helping making centri-voltammetric cell and centrifugal cell, respectively.

Also I would like to thank my dearest friends Ph.D. student Hanife Vardar, Master student Eylem Erdugan for their continuous support and encouragement.

I also thank to Doç. Dr. Müşerref Arda, Ress. Asst. Onur Yayayürük and Özgür Arar for their valuables supports.

I would like to thank my cousin Gökhan Ürkmez, my sister Buket Ürkmez and my friend Özgür Ege for their contributing to at the writing step of the thesis.

Finally, I would like to thank to my parents and my friends for their patience and encouragement education.

İpek ÜRKMEZ

2010, İZMİR



**CONTENTS**

|   | <u>Page</u> |
|---|-------------|
| ÖZET.....   | V           |
| ABSTRACT.....   | VII         |
| ACKNOWLEDGEMENT.....                                  | IX          |
| LIST OF FIGURES.....                                  | XVI         |
| LIST OF TABLES.....                                   | XXV         |
| LIST OF SYMBOLS.....                                  | XXVIII      |
| LIST OF ABBREVIATIONS.....                            | XXX         |
| 1. INTRODUCTION.....                                  | 1           |
| 1.1. Voltammetry.....                                 | 9           |
| 1.1.1. Chronoamperometry.....                         | 13          |
| 1.1.2. Polarography.....                              | 15          |
| 1.1.3. Pulse Voltammetry.....                         | 18          |
| 1.1.3.1. Normal Pulse Voltammetry.....                | 19          |
| 1.1.3.2. Differential Pulse Voltammetry.....          | 20          |
| 1.1.3.3. Square-Wave Voltammetry.....                 | 21          |
| 1.1.3.4. Staircase Voltammetry.....                   | 22          |
| 1.1.4. AC Voltammetry.....                            | 23          |
| 1.1.5. Cyclic Voltammetry.....                        | 24          |
| 1.1.6. Preconcentration and Stripping Techniques..... | 26          |

**CONTENTS (continued)**

|   | <u>Page</u> |
|---|-------------|
| 1.1.6.1. Anodic Stripping Voltammetry.....                              | 27          |
| 1.1.6.2. Cathodic Stripping Voltammetry.....                            | 28          |
| 1.1.6.3. Adsorptive Stripping Voltammetry.....                          | 29          |
| 1.1.6.4. Potentiometric Stripping Voltammetry.....                      | 29          |
| 1.1.7. Working Electrodes in Voltammetry.....                           | 30          |
| 1.1.7.1. Mercury Electrodes.....  | 31          |
| 1.1.7.2. Solid Electrodes.....  | 33          |
| <i>Carbon Electrodes</i> .....  | 33          |
| <i>Glassy Carbon Electrodes</i> .....                                   | 34          |
| <i>Carbon Paste Electrodes</i> .....                                    | 35          |
| <i>Carbon Fiber Electrodes</i> .....                                    | 35          |
| 1.1.7.3. Metal Electrodes.....  | 36          |
| 1.1.7.4. Chemically Modified Electrodes.....                            | 37          |
| 1.2. Sensitive and Selective Voltammetric Determination of Mercury..... | 38          |
| 1.3. Centri-Voltammetry.....  | 44          |
| 1.4. Material for Separation and Preconcentration.....                  | 47          |
| 1.4.1. Ion-Exchange Resins.....   | 47          |
| 1.4.2. Purolite C100 as a Carrier Material.....                         | 53          |
| 1.5. Aim and Scope of Thesis.....                                       | 54          |

**CONTENTS (continued)**

|  | <u>Page</u> |
|--|-------------|
| 2. MATERIALS AND METHODS.....  | 58          |
| 2.1. Apparatus.....  | 58          |
| 2.2. Chemicals and Solutions.....  | 61          |
| 2.3. Procedure.....  | 63          |
| 2.3.1. Procedure in Chapter I.....   | 64          |
| 2.3.1.1. Preparation of Gold Film Electrode.....                               | 64          |
| 2.3.1.2. Reduction and Preconcentration of Mercury(II) Ions.....               | 64          |
| 2.3.1.3. Anodic Stripping of Mercury in the Amalgam.....                       | 65          |
| 2.3.2. Procedure in Chapter II.....  | 65          |
| 2.3.2.1. Pretreatment Applied to Purolite C100 Resin Electrode.....            | 65          |
| 2.3.2.2. Preparation of Home-made Working Electrode.....                       | 66          |
| 2.3.2.3. Sorption and Centri-voltammetric Procedure for Mercury(II) Ions.....  | 66          |
| 3. RESULT AND DISCUSSION.....  | 67          |
| 3.1. Preliminary Investigations for Working Electrodes.....                    | 67          |
| 3.1.1. Activation of Glassy Carbon Electrode.....                              | 67          |
| 3.1.2. Behavior of Gold Film Electrode.....                                    | 68          |
| 3.2. CHAPTER I: Centri-voltammetric Determination of Mercury(II)               |             |
| Using Hydrazine as a Reducing Agent.....                                       | 74          |
| 3.2.1. Effect of Reducing Agent on Centri-voltammetric Mercury Determination.. | 74          |

**CONTENTS (continued)**

|   | <u>Page</u> |
|---|-------------|
| 3.2.2. Effect of pH on Mercury Reduction with Hydrazine.....                | 76          |
| 3.2.3. Effect of Hydrazine Concentration on Mercury Reduction Reaction..... | 78          |
| 3.2.4. Effect of Centrifugation Time (with reducing agent).....             | 80          |
| 3.2.5. Effect of Centrifugation Speed (with reducing agent).....            | 82          |
| 3.2.6. Effect of Stripping Solution Content on Mercury Peak Current.....    | 84          |
| 3.2.7. Resulting Peak Currents of Hg(II) in Optimum Conditions.....         | 88          |
| 3.3. CHAPTER II: Centri-voltammetric Determination of Mercury(II)           |             |
| Using Purolite C100 as a Carrier Material.....                              | 90          |
| 3.3.1. Effect of pH.....  | 91          |
| 3.3.2. Effect of Adsorption Duration.....                                   | 94          |
| 3.3.3. Effect of Amount of Purolite C100.....                               | 96          |
| 3.3.4. Effect of Centrifugation Time (with carrier material).....           | 98          |
| 3.3.5. Effect of Centrifugation Speed (with carrier material).....          | 100         |
| 3.3.6. Effect of Sweep Rate of Potential (with carrier material).....       | 102         |
| 3.3.7. Effect of Sweep Range of Potential (with carrier material).....      | 104         |
| 3.3.8. Resulting Peak Currents of Hg(II) in Optimum Conditions.....         | 106         |
| 3.4. Validation of Centri-voltammetric Methods.....                         | 108         |
| 3.4.1. Linearity and Limit of Detection.....                                | 108         |
| 3.4.2. Accuracy.....  | 112         |

**CONTENTS (continued)**

|  | <u>Page</u> |
|--|-------------|
| 3.4.3. Precision.....  | 112         |
| 3.4.4. Selectivity.....  | 113         |
| 3.5. Analytical Applications.....  | 115         |
| 3.6. Investigation of Surface of Electrodes and Purolite C100 Resin..... | 119         |
| 4. CONCLUSION.....   | 122         |
| REFERENCES.....  | 125         |
| APPENDIX 1.....  | 133         |
| APPENDIX 2.....  | 134         |
| CIRRICULUM VITAE.....  | 135         |

## LIST OF FIGURES

| <u>Figure</u>  | <u>Page</u> |
|--|-------------|
| 1.1. Schematic diagram of a cell for voltammetric measurements: WE working electrodes; RE reference electrode; AE auxiliary electrode. The electrodes are inserted through holes in the cell cover (Wang, 2006). .....                         | 11          |
| 1.2. In chronoamperometric method: (a) potential–time waveform; (b) change in concentration profiles as time progresses; (c) the resulting current–time response (Wang, 2006). .....   | 14          |
| 1.3. Polarograms for 1 M hydrochloric acid ( <i>A</i> ) and $4 \times 10^{-4}$ M $\text{Cd}^{2+}$ in 1 M hydrochloric acid ( <i>B</i> ); $i_d$ represents the limiting current, while $E_{1/2}$ is the half-wave potential (Wang, 2006). ..... | 16          |
| 1.4. Excitation waveform for normal pulse voltammetry (Wang, 2006)....   | 19          |
| 1.5. Excitation signal for differential-pulse voltammetry (Wang, 2006). ...  | 20          |
| 1.6. Square-wave waveform showing the amplitude $E_{sw}$ , step height $\Delta E$ , squarewave period $T$ , delay time $T_d$ , and current measurement times 1 and 2 (Wang, 2006). .....   | 21          |
| 1.7. Potential-time waveform used in staircase voltammetry (Wang, 2006).   | 22          |
| 1.8. Potential-time waveform used in alternating current voltammetry (Wang, 2006). .....   | 24          |
| 1.9. Potential–time excitation signals in a cyclic voltammetric experiment (Wang, 2006). .....   | 25          |
| 1.10. In ASV the potential–time waveform (top) and along with the resulting voltammogram (bottom) (Wang, 2006).....  | 28          |
| 1.11. Stripping potentiograms for a solution containing $100 \mu\text{g L}^{-1}$ tin, cadmium, and lead, with 80 s accumulation at -1.40V (Wang, 2006)..   | 30          |



## LIST OF FIGURES (continued)

| <u>Figure</u>   | <u>Page</u> |
|---|-------------|
| 1.12. Accessible potential windows of platinum, mercury, and carbon electrodes in various supporting electrolytes (Wang, 2006).....   | 31          |
| 1.13. Strong acid cation exchange resin (Mizuike, 1983).....  | 49          |
| 2.1 Metrohm 693 Voltammetric Analyzer (VA) processor and a 694 VA Stand with its own cell. ....   | 58          |
| 2.2. The designed centrifugal cell, A) centrifugal cell (dismounted) B) GCE placed and mounted in centrifugal cell facing upward.....   | 59          |
| 2.3. The designed centri-voltammetric cell and home-made working electrode. ....  | 60          |
| 2.4. (a) Perkin Elmer Optima 2100 DV ICP-OES (New Mexico State University, 2010), (b) The Agilent Technologies 7700 Series ICP-MS (Agilent Technologies, 2010).....   | 61          |
| 3.1. CVs for the GCE (a) before and (b) after activation procedure in 0.1 M HClO <sub>4</sub> solution at 50 mV/s.....  | 68          |
| 3.2. DP voltammograms of GFE in 1.0 M HClO <sub>4</sub> stripping solution in different deposition times. Conditions of formation GFE: 2.5×10 <sup>-5</sup> M Au <sup>3+</sup> , 0.5 M HClO <sub>4</sub> , E <sub>dep</sub> : -400 mV and t <sub>dep</sub> (a) 100, (b) 150, (c) 200, and (d) 300 s.....  | 69          |
| 3.3. Effect of deposition time of GFE on mercury peak current. Hg(II) concentration: 1.0×10 <sup>-9</sup> M, Experimental conditions; m <sub>BH</sub> : 90 mg, t <sub>cent</sub> : 5 min, v <sub>cent</sub> : 3000 rpm, stripping solution content: 1.0 M HClO <sub>4</sub> and 0.35 M HCl. Conditions of formation GFE: 2.5×10 <sup>-5</sup> M Au <sup>3+</sup> , 0.5 M HClO <sub>4</sub> , E <sub>dep</sub> : -400 mV and t <sub>dep</sub> (a) 100, (b) 150, (c) 200, and (d) 300 s. .... | 70          |

## LIST OF FIGURES (continued)

| <u>Figure</u>  | <u>Page</u> |
|--|-------------|
| 3.4. Effect of deposition time of GFE ( $E_{\text{dep}}$ : -400 mV) on mercury peak current which are observed at about 0.5 V.....   | 70          |
| 3.5. DP voltammogram of GFE in 1.0 M HClO <sub>4</sub> stripping solution. Conditions of formation GFE: $2.5 \times 10^{-5}$ M Au <sup>3+</sup> , 0.5 M HClO <sub>4</sub> , $E_{\text{dep}}$ and $t_{\text{dep}}$ -500 mV and 100 s, respectively.....   | 71          |
| 3.6. DP voltammograms of GFE in (a) 0.1 M HClO <sub>4</sub> + 0.05 M KI, (b) 0.1 M HClO <sub>4</sub> + 0.05 M KSCN, (c) 1.0 M HClO <sub>4</sub> + 0.35 M HCl, (d) 1.0 M HClO <sub>4</sub> , (e) 0.01 M HNO <sub>3</sub> , (f) 0.1 M HCl, stripping solution.....   | 72          |
| 3.7. Cyclic voltammogram for the gold film electrode in 0.1 M HClO <sub>4</sub> solution at 50 mV/s and SEM images of GFE electrochemically deposited on a GCE magnified by 20000 and 50000 times.....   | 73          |
| 3.8. The obtained voltammogram for $1.0 \times 10^{-9}$ M Hg(II) by using NaBH <sub>4</sub> . Experimental conditions: <b>pH&lt;1</b> , <b>m<sub>BH</sub></b> : 90 mg, <b>t<sub>cent</sub></b> : 5 min, <b>v<sub>cent</sub></b> : 3000 rpm, stripping solution content: 1.0 M HClO <sub>4</sub> and 0.35 M HCl.....  | 75          |
| 3.9. The obtained voltammogram for $1.0 \times 10^{-9}$ M Hg(II) by using N <sub>2</sub> H <sub>4</sub> . Experimental conditions: <b>pH&lt;1</b> , <b>C<sub>hyd</sub></b> : 0.07 M, <b>t<sub>cent</sub></b> : 7 min, <b>v<sub>cent</sub></b> : 3000 rpm, stripping solution content: 1.0 M HClO <sub>4</sub> and 0.35 M HCl.....  | 75          |
| 3.10. Voltammograms for <b>a</b> ) bare GCE, <b>b</b> ) GFE (Conditions of its formation: $2.5 \times 10^{-5}$ M Au <sup>3+</sup> , 0.5 M HClO <sub>4</sub> ) background current in 0.1 M HClO <sub>4</sub> + 0.35 M HCl, <b>(c, d, e, f)</b> The voltammograms of the blank study for hydrazine in different concentration and pH of reaction medium. Experimental conditions: <b>v<sub>cent</sub></b> : 3000 rpm, <b>t<sub>cent</sub></b> : 7 min, stripping solution content: 1.0 M HClO <sub>4</sub> , 0.35 M HCl..... | 76          |
| 3.11. The voltammograms at lower initial pH values: (a) pH: 1.0, (b) pH <1. Experimental conditions: Hg(II) concentration: $1.0 \times 10^{-9}$ M, <b>C<sub>hd</sub></b> : 0.07 M, <b>v<sub>cent</sub></b> : 3000 rpm, <b>t<sub>cent</sub></b> : 7 min.....  | 77          |

## LIST OF FIGURES (continued)

| <u>Figure</u>   | <u>Page</u> |
|---|-------------|
| 3.12. The influence of concentration of hydrazine on resulting reoxidation peak currents of mercury. Experimental conditions: Hg(II) concentration: $1.0 \times 10^{-9}$ M, <b>pH</b> < 1, $v_{\text{cent}}$ : 3000 rpm, $t_{\text{cent}}$ : 2 min, stripping solution content: 1.0 M HClO <sub>4</sub> and 0.35 M HCl. <b>C<sub>hdy</sub></b> : (a) $1.0 \times 10^{-8}$ , (b) $1.0 \times 10^{-5}$ , (c) $5.0 \times 10^{-3}$ , (d) $2.0 \times 10^{-2}$ , (e) $3.0 \times 10^{-2}$ , (f) $5.0 \times 10^{-2}$ , (g) $7.0 \times 10^{-2}$ , (h) $1.0 \times 10^{-1}$ M..... | 79          |
| 3.13. Effect of hydrazine concentration on the resulting peak currents of $1.0 \times 10^{-9}$ M Hg(II). .....  | 80          |
| 3.14. The influence of the centrifugation time on resulting reoxidation peak currents of mercury. Hg(II) concentration: $1.0 \times 10^{-9}$ M. Experimental conditions; <b>pH</b> < 1, <b>C<sub>hdy</sub></b> : 0.07 M, $v_{\text{cent}}$ : 3000 rpm, stripping solution content: 1.0 M HClO <sub>4</sub> and 0.35 M HCl. $t_{\text{cent}}$ : (a) 2, (b) 5, c) 7, (d) 9, (e) 12 min. ....  | 81          |
| 3.15. The influence of centrifugation time on the resulting peak currents of $1.0 \times 10^{-9}$ M (II). .....   | 82          |
| 3.16. The influence of the centrifugation speed on resulting reoxidation peak currents of mercury. Hg(II) concentration: $1.0 \times 10^{-9}$ M. Experimental conditions; <b>pH</b> < 1, <b>C<sub>hdy</sub></b> : 0.07 M, $t_{\text{cent}}$ : 7 min., stripping solution content: 1.0 M HClO <sub>4</sub> and 0.35 M HCl. $v_{\text{cent}}$ : (a) 500, (b) 1000, (c) 2000, (d) 3000, (e) 3500 rpm.....  | 83          |
| 3.17. The influence of centrifugation time on resulting reoxidation peak currents of $1.0 \times 10^{-9}$ M Hg(II).....   | 84          |
| 3.18. The effect of stripping solution content on resulting reoxidation peak currents, Hg(II) concentration $1 \times 10^{-9}$ M. Experimental conditions: <b>pH</b> < 1, <b>C<sub>hdy</sub></b> : 0.07 M, $v_{\text{cent}}$ : 3000 rpm, $t_{\text{cent}}$ : 7 min, stripping solution content: (a) 1.0 M HClO <sub>4</sub> + 0.35 M HCl, (b) 0.1 M HCl + 0.1 M HNO <sub>3</sub> , (c) 0.1 M HNO <sub>3</sub> , (d) 0.1 M HCl.....  | 85          |

## LIST OF FIGURES (continued)

| <u>Figure</u>   | <u>Page</u> |
|---|-------------|
| 3.19. The effect of HCl concentration in 1.0 M HClO <sub>4</sub> stripping solution on mercury reoxidation peak current, Hg(II) concentration $1 \times 10^{-9}$ M, <b>pH</b> <1, <b>C<sub>hdy</sub></b> : 0.07 M, <b>t<sub>cent</sub></b> : 7min., <b>v<sub>cent</sub></b> : 3000 rpm; HCl concentration: (a) 0.05, (b) 0.10, (c) 0.20, (d) 0.35, (e) 0.45 M.....  | 86          |
| 3.20. The influence of chloride ion concentration in the stripping solution on anodic stripping peaks current values of $1.0 \times 10^{-9}$ M Hg(II).....  | 87          |
| 3.21. The voltammograms obtained under optimum experimental conditions ( <b>C<sub>hdy</sub></b> : 0.07 M, <b>pH</b> < 1 (0.5 M HClO <sub>4</sub> ), <b>t<sub>cent</sub></b> : 7 min, <b>v<sub>cent</sub></b> : 3000 rpm, stripping solution content: 1.0 M HClO <sub>4</sub> and 0.35 M HCl). Hg(II) concentration: (a) $1.0 \times 10^{-10}$ , (b) $1.5 \times 10^{-10}$ , (c) $5.0 \times 10^{-10}$ , (d) $1.0 \times 10^{-9}$ , (e) $5.0 \times 10^{-9}$ M. ....   | 88          |
| 3.22. The calibration graph for Hg(II) ions obtained with hydrazine under the optimal conditions. ....  | 89          |
| 3.23. The voltammograms obtained for (a) blank solution, (b) without centrifugation with Purolite C100 for $1 \times 10^{-7}$ M Hg <sup>2+</sup> , (c) without Purolite C100 with centrifugation for $1 \times 10^{-7}$ M Hg <sup>2+</sup> , (d) without Purolite C100 and centrifugation for $1 \times 10^{-7}$ M Hg <sup>2+</sup> . Related experimental parameters: <b>pH</b> : 7.50, <b>m<sub>r</sub></b> : 6.0 mg, <b>t<sub>ads</sub></b> : 15 min, <b>v<sub>cent</sub></b> : 3000 rpm, <b>t<sub>cent</sub></b> : 10 min. .... | 91          |
| 3.24. The influence of pH on the peak currents of solution containing $1 \times 10^{-7}$ M Hg <sup>2+</sup> in 0.5 M HClO <sub>4</sub> ( <b>m<sub>r</sub></b> : 6.0 mg, <b>t<sub>ads</sub></b> : 20 min, <b>v<sub>cent</sub></b> : 3000 rpm, <b>t<sub>cent</sub></b> : 10 min). <b>pH</b> values: (a) <1, (b) 1.00, (c) 2.50, (d) 4.00, (e) 6.00, (f) 7.50, (g) 9.00, (h) 9.50.....   | 92          |
| 3.25. The influence of pH on the peak currents of solution containing $1 \times 10^{-7}$ M Hg <sup>2+</sup> in 0.5 M HClO <sub>4</sub> .....  | 93          |

## LIST OF FIGURES (continued)

| <u>Figure</u>  | <u>Page</u> |
|--|-------------|
| 3.26. The influence of adsorption duration on the peak currents of solution containing $1 \times 10^{-7}$ M $\text{Hg}^{2+}$ in 0.5 M $\text{HClO}_4$ ( <b>pH</b> : 7.50, <b>m<sub>r</sub></b> : 6.0 mg, <b>v<sub>cent</sub></b> : 3000 rpm, <b>t<sub>cent</sub></b> : 10 min). <b>t<sub>ads</sub></b> : (a) 5, (b) 10, (c)15, (d) 20, (e) 25, (f) 30 min. ....              | 95          |
| 3.27. The influence of adsorption duration on the peak currents of solution containing $1 \times 10^{-7}$ M $\text{Hg}^{2+}$ in 0.5 M $\text{HClO}_4$ ( <b>pH</b> : 7.50, <b>m<sub>r</sub></b> : 6.0 mg, <b>v<sub>cent</sub></b> : 3000 rpm, <b>t<sub>cent</sub></b> : 10 min).....  | 96          |
| 3.28. Dependence of the peak currents on the resin amount for the solution containing $1 \times 10^{-7}$ M $\text{Hg}^{2+}$ in 0.5 M $\text{HClO}_4$ ( <b>pH</b> : 7.50, <b>t<sub>ads</sub></b> : 20 min, <b>v<sub>cent</sub></b> : 3000 rpm, <b>t<sub>cent</sub></b> : 10 min). <b>m<sub>r</sub></b> : (a)1.5, (b) 3.0, (c) 5.0 (d) 6.0, (e)7.0, (f) 8.0, (g) 12.0 mg.....  | 97          |
| 3.29. Dependence of the peak currents on the resin amount for the solution containing $1 \times 10^{-7}$ M $\text{Hg}^{2+}$ in 0.5 M $\text{HClO}_4$ ( <b>pH</b> : 7.50, <b>t<sub>ads</sub></b> : 20 min, <b>v<sub>cent</sub></b> : 3000 rpm, <b>t<sub>cent</sub></b> : 10 min).....   | 98          |
| 3.30. The influence of the centrifugation time on the peak currents for the solution containing $1 \times 10^{-7}$ M $\text{Hg}^{2+}$ in 0.5 M $\text{HClO}_4$ ( <b>pH</b> : 7.50, <b>m<sub>r</sub></b> : 6.0 mg, <b>t<sub>ads</sub></b> : 20 min, <b>v<sub>cent</sub></b> : 3000 rpm). <b>t<sub>cent</sub></b> : (a) 3, (b) 5, (c) 8, (d)10, (e) 12 min. ....               | 99          |
| 3.31. The influence of the centrifugation time on the peak currents for the solution containing $1 \times 10^{-7}$ M $\text{Hg}^{2+}$ in 0.5 M $\text{HClO}_4$ ( <b>pH</b> : 7.50, <b>m<sub>r</sub></b> : 6.0 mg, <b>t<sub>ads</sub></b> : 20 min , <b>v<sub>cent</sub></b> : 3000 rpm).....   | 100         |
| 3.32. The effect of centrifugation speed on the peak currents for the solution containing $1 \times 10^{-7}$ M $\text{Hg}^{2+}$ in 0.5 M $\text{HClO}_4$ ( <b>pH</b> : 7.50, <b>m<sub>r</sub></b> : 6.0 mg, <b>t<sub>ads</sub></b> : 20 min, <b>t<sub>cent</sub></b> : 10 min). <b>v<sub>cent</sub></b> : (a) 500, (b) 1000, (c) 1500, (d) 2000, (e) 2350, (f) 3000 rpm..... | 101         |

## LIST OF FIGURES (continued)

| <u>Figure</u>   | <u>Page</u> |
|---|-------------|
| 3.33. The effect of centrifugation speed on the peak currents for the solution containing $1 \times 10^{-7}$ M $\text{Hg}^{2+}$ in 0.5 M $\text{HClO}_4$ ( <b>pH</b> : 7.50, <b>m<sub>r</sub></b> : 6.0 mg, <b>t<sub>ads</sub></b> : 20 min , <b>t<sub>cent</sub></b> : 10 min).....  | 102         |
| 3.34. The influence of sweep rate centri-voltammetric results for the solution containing $1 \times 10^{-9}$ M $\text{Hg}^{2+}$ in 0.5 M $\text{HClO}_4$ ( <b>pH</b> : 7.50, <b>m<sub>r</sub></b> : 6.0 mg, <b>t<sub>ads</sub></b> : 20 min , <b>t<sub>cent</sub></b> : 10 min, <b>v<sub>cent</sub></b> : 3000 rpm), sweep rate: (a) 10, (b) 20, (c) 30, (d) 40mVs <sup>-1</sup> .....  | 103         |
| 3.35. The influence of sweep rate centri-voltammetric results for the solution containing $1 \times 10^{-9}$ M $\text{Hg}^{2+}$ in 0.5 M $\text{HClO}_4$ ( <b>pH</b> : 7.50, <b>m<sub>r</sub></b> : 6.0 mg, <b>t<sub>ads</sub></b> : 20 min , <b>t<sub>cent</sub></b> : 10 min, <b>v<sub>cent</sub></b> : 3000 rpm).....  | 103         |
| 3.36. The effect of sweep range on the peak currents for the solution containing $1 \times 10^{-9}$ M $\text{Hg}^{2+}$ in 0.5 M $\text{HClO}_4$ ( <b>pH</b> : 7.50, <b>m<sub>r</sub></b> : 6.0 mg, <b>t<sub>ads</sub></b> : 20 min, <b>t<sub>cent</sub></b> : 10 min. <b>v<sub>cent</sub></b> : 3000 rpm), sweep range: (a) -1000 - +800, (b) -800 - +800, (c) -600 - +800, (d) -400 - +800, (e) -200 - +800 mV.....  | 104         |
| 3.37. The effect of sweep range on the peak currents for the solution containing $1 \times 10^{-9}$ M $\text{Hg}^{2+}$ in 0.5 M $\text{HClO}_4$ .....   | 105         |
| 3.38. The effect of Hg(II) concentration on current values obtained with Purolite C100 under the optimized conditions ( <b>pH</b> : 7.50, <b>m<sub>r</sub></b> : 6.0 mg, <b>t<sub>ads</sub></b> : 20 min, <b>v<sub>cent</sub></b> : 3000 rpm, <b>t<sub>cent</sub></b> : 10 min). Hg(II) concentrations: (a) $1 \times 10^{-11}$ , (b) $5 \times 10^{-11}$ , (c) $1 \times 10^{-10}$ , (d) $5 \times 10^{-10}$ , (e) $1 \times 10^{-9}$ , (f) $5 \times 10^{-9}$ , (g) $1 \times 10^{-8}$ , (h) $5 \times 10^{-8}$ , (i) $1 \times 10^{-7}$ M..... | 106         |
| 3.39. The calibration graph for Hg(II) ions in 0.5 M $\text{HClO}_4$ obtained with Purolite C100 under the optimal conditions.....  | 107         |

## LIST OF FIGURES (continued)

| <u>Figure</u>   | <u>Page</u> |
|---|-------------|
| 3.40. The comparison of calibration graphs. Without carrier material: (◆) borohydride and (■) hydrazine as a reducing agent, with carrier material: (▲) Purolite C100. ....   | 109         |
| 3.41. Investigation of interfering effect of some foreign ions for $1 \times 10^{-9}$ M Hg(II). ....  | 115         |
| 3.42. Voltammograms of standard addition experiments for (1) Sample I, (2) Sample I + $1.5 \times 10^{-11}$ M, (3) Sample I + $3.0 \times 10^{-11}$ M, (4) Sample I + $5.0 \times 10^{-11}$ M Hg(II) in the cell.....   | 116         |
| 3.43. Standard addition graph for Sample I.....   | 116         |
| 3.44. Voltammograms of standard addition experiments for (1) Sample II, (2) Sample II + $1.5 \times 10^{-11}$ M, (3) Sample II + $3.0 \times 10^{-11}$ M, (4) Sample II + $5.0 \times 10^{-11}$ M Hg(II) in the cell.....   | 117         |
| 3.45. Standard addition graph for Sample II.....  | 117         |
| 3.46. SEM images of Purolite C100 resin before sorption ( $>45\mu\text{m}$ size) magnified by (a)10000, (c) 30000 times, and after sorption of Hg(II) ions (b) 10000, (d) 30000 times. Under the experimental conditions <b>pH</b> : 7.50, <b>m<sub>r</sub></b> : 6.0 mg, <b>t<sub>ads</sub></b> : 20 min Hg(II) concentration: $5 \times 10^{-8}$ M. ....  | 119         |
| 3.47. SEM images of gold film surface magnified by (a) 20000, (c) 50000, (e)100000 times, and after applied centrifugation procedure to reduced mercury with hydrazine (b) 20000, (d) 50000, (f) 100000 times. Conditions of formation GFE: $2.5 \times 10^{-5}$ M Au <sup>3+</sup> , 0.5 M HClO <sub>4</sub> , <b>E<sub>dep</sub></b> : -500 mV and <b>t<sub>dep</sub></b> : 100 s. Experimental conditions ( <b>C<sub>hdy</sub></b> : 0.07 M, <b>pH</b> < 1 (0.5 M HClO <sub>4</sub> ), <b>t<sub>cent</sub></b> : 7 min, <b>v<sub>cent</sub></b> : 3000 rpm, Hg(II) concentration: $5 \times 10^{-8}$ M. .... | 120         |

**LIST OF FIGURES (continued)**

| <u>Figure</u>   | <u>Page</u> |
|---|-------------|
| 3.48. (a) Phase mode, (c) wave mode, (e) wave mode shaded, (g) wave mode 3D, of AFM images for GFE. (b) Phase mode, (d) wave mode, (f) wave mode shaded, (h) wave mode 3D, of AFM images for GFE after applied centrifugation procedure to reduced mercury with hydrazine, (i) bare GCE. .... | 121         |



## LIST OF TABLES

| <u>Table</u>  | <u>Page</u> |
|---|-------------|
| 1.1. Major mercury species in environmental and biological samples.....   | 3           |
| 1.2. Selected applications of different methods for Hg determination.....   | 6           |
| 1.3. Functional groups reducible at the DME (Wang, 2006).....   | 18          |
| 1.4. Some studies for determinations of mercury using voltammetric techniques with different electrodes.....  | 39          |
| 1.5. Most frequently used ion exchange resins (Mizuike, 1983).....  | 48          |
| 1.6. Selected resins used for separation and/or preconcentration of metal ions. ....  | 50          |
| 1.7. Summary of mercury-selective chelate resins (EPA, 1997).....   | 52          |
| 1.8. Ion exchange treatment for mercury in drinking water (EPA, 1997)...  | 52          |
| 1.9. The physical and chemical properties of Purolite C100 and the standard operating conditions (Purolite Company, 2009).....  | 53          |
| 3.1. The effect of pH on mercury reduction reaction with hydrazine. Hg(II) concentration: $5.0 \times 10^{-9}$ M, $C_{\text{hdy}}$ : 0.1M, $v_{\text{cent}}$ : 3000 rpm, $t_{\text{cent}}$ : 7 min, stripping solution content: 1.0 M HClO <sub>4</sub> and 0.35 M HCl..... | 77          |
| 3.2. The currents of mercury reoxidation peak at lower initial pH values. Hg(II) concentration: $1.0 \times 10^{-9}$ M.....   | 78          |
| 3.3. Effect of hydrazine concentration on the resulting peak currents of $1.0 \times 10^{-9}$ M Hg(II). ....  | 79          |
| 3.4. The influence of centrifugation time on the resulting peak currents of $1.0 \times 10^{-9}$ M Hg(II).....  | 82          |

**LIST OF TABLES (continued)**

| <u>Table</u>   | <u>Page</u> |
|--|-------------|
| 3.5. The influence of centrifugation speed on the resulting peak currents of $1.0 \times 10^{-9}$ M Hg(II). .....  | 84          |
| 3.6. Effect of HCl concentration on resulting peak currents values of $1.0 \times 10^{-9}$ M Hg(II). .....   | 87          |
| 3.7. The list of optimal working conditions for the procedure with reducing agent (Hydrazine).....   | 88          |
| 3.8. The effect of mercury (II) concentration on current values obtained with hydrazine under the optimized conditions.....  | 89          |
| 3.9. The influence of pH on the peak currents of solution containing $1 \times 10^{-7}$ M $\text{Hg}^{2+}$ in 0.5 M $\text{HClO}_4$ .....                            | 93          |
| 3.10. The influence of adsorption duration on the peak currents of solution containing $1 \times 10^{-7}$ M $\text{Hg}^{2+}$ in 0.5 M $\text{HClO}_4$ .....          | 95          |
| 3.11. Dependence of the peak currents on the resin amount for the solution containing $1 \times 10^{-7}$ M in 0.5 M $\text{HClO}_4$ .....                            | 98          |
| 3.12. The influence of the centrifugation time on the peak currents for the solution containing $1 \times 10^{-7}$ M $\text{Hg}^{2+}$ in 0.5 M $\text{HClO}_4$ ..... | 100         |
| 3.13. The effect of centrifugation speed on the peak currents for the solution containing $1 \times 10^{-7}$ M $\text{Hg}^{2+}$ in 0.5 M $\text{HClO}_4$ .....       | 102         |
| 3.14. The influence of sweep rate centri-voltammetric results for the solution containing $1 \times 10^{-9}$ M $\text{Hg}^{2+}$ in 0.5 M $\text{HClO}_4$ .....       | 103         |
| 3.15. The effect of sweep range on the peak currents for the solution containing $1 \times 10^{-9}$ M $\text{Hg}^{2+}$ in 0.5 M $\text{HClO}_4$ .....                | 105         |
| 3.16. The list of optimal working conditions for the procedure with a carrier material (Purolite C100).....  | 106         |

**LIST OF TABLES (continued)**

| <u>Table</u>  | <u>Page</u> |
|---|-------------|
| 3.17. The effect of Hg(II) concentration on current values obtained with Purolite C100 under the optimized conditions.....  | 107         |
| 3.18. Comparison of Centri-Voltammetric method with ASV for $1 \times 10^{-9}$ M $\text{Hg}^{2+}$ .....   | 110         |
| 3.19. Successive current values for $5.0 \times 10^{-11}$ M mercuric ions solution under the optimized conditions for Purolite C100. s: standard deviation. ....              | 111         |
| 3.20. Comparison of the result of accuracy testing.....   | 112         |
| 3.21. Successive current values for $1.0 \times 10^{-9}$ M mercuric ions solution under the optimized conditions for hydrazine and Purolite C100, s: standard deviation. .... | 113         |
| 3.22. The effects of some foreign ions to the signal of $1 \times 10^{-9}$ M Hg(II).....  | 114         |
| 3.23. The results of standard addition to Sample I.....   | 116         |
| 3.24. The results of standard addition to Sample II.....  | 117         |
| 3.25. ICP-OES results of the determination of Cu(II), Pb(II) and Cd(II) in spring water samples. ....   | 118         |
| 3.26. Comparison of the obtained mercury(II) concentrations with Centri-Voltammetry using Purolite C100 and ICP-OES in spring water samples. ....                             | 118         |

## LIST OF SYMBOLS

| <u>Symbol</u>       | <u>Explanation</u>   |
|---------------------|--|
| $A$                 | Surface area of the electrode  |
| $C_O^0$ and $C_R^0$ | Redox species at the electrode surface                                   |
| $d$                 | Density of mercury   |
| $D$                 | Diffusion coefficient  |
| $D_O$               | Diffusion coefficient of the oxidized forms of the electroactive species |
| $D_R$               | Diffusion coefficient of the reduced forms of the electroactive species  |
| $\Delta E$          | Amplitude  |
| $E$                 | Application of a potential   |
| $E^0$               | Standard electrode potential for the redox couple                        |
| $E_{1/2}$           | Half-wave potential  |
| $E_{\text{dep}}$    | Deposition potential   |
| $E_p$               | Peak potential   |
| $E_{pa}$            | Anodic peak potential  |
| $E_{pc}$            | Cathodic peak potential  |
| $F$                 | Faraday constant   |
| $g$                 | Earth's gravitational acceleration                                       |
| $i_{av}$            | Average current  |
| $i_d$               | Limiting diffusion current   |
| $i_p$               | Peak current   |
| $i_{pa}$            | Anodic peak current  |
| $i_{pc}$            | Cathodic peak current  |
| $k^0$               | Rate of the reaction   |

## LIST OF SYMBOLS (continued)

| <u>Symbol</u>     | <u>Explanation</u>                             |
|-------------------|--|
| $m$               | Mass flow rate of mercury                      |
| $m_r$             | Resin amount                                   |
| $m_{\text{BH}}$   | Amount of borohydride                          |
| $N$               | Rotational speed                               |
| $n$               | Number of electrons transferred                |
| $n$               | Successive replicates                          |
| $N_{\text{rpm}}$  | Rotational speed measured                      |
| <b>O</b>          | The oxidized species                           |
| <b>R</b>          | The reduced species                            |
| $R$               | Gas constant                                   |
| $r$               | Rotational radius                              |
| $r_{\text{cm}}$   | Rotational radius measured in centimeters (cm) |
| $s$               | Standard deviation                             |
| $t$               | Time   |
| $T$               | The absolute temperature                       |
| $T$               | Squarewave period                              |
| $t_{\text{cent}}$ | Time of centrifugation                         |
| $T_d$             | Delay time                                     |
| $t_{\text{dep}}$  | Deposition time                                |
| $v_{\text{cent}}$ | Speed of centrifugation                        |
| $x$               | The distance from the electrode surface        |
| $\omega$          | Frequency                                      |
| $\alpha$          | Transfer coefficient                           |
| $\varphi$         | Flux of matter                                 |

**LIST OF ABBREVIATIONS**

| <u>Abbreviation</u> | <u>Explanation</u>                           |
|---------------------|--|
| AAS                 | Atomic absorption spectrometry               |
| AC                  | Alternating current                          |
| AdSV                | Adsorptive stripping voltammetry             |
| AE                  | Auxiliary electrode                          |
| AES                 | Atomic emission spectrometry                 |
| AFM                 | Atomic force microscopy                      |
| AFS                 | Atomic fluorescence spectrometry             |
| ASV                 | Anodic stripping voltammetry                 |
| CME                 | Chemically modified electrode                |
| CSV                 | Cathodic stripping voltammetry               |
| CV                  | Cyclic voltammetry                           |
| CV                  | Cold Vapor                                   |
| DC                  | Direct current                               |
| DCP                 | Direct current plasma                        |
| DME                 | Dropping mercury electrode                   |
| DPV                 | Differential pulse voltammetry               |
| EPA                 | United State Environmental Protection Agency |
| EPMA                | Electron probe micro-analysis                |
| ET                  | Electrothermal                               |
| FI                  | Flow injection                               |
| GCE                 | Glassy Carbon Electrode                      |
| GFE                 | Gold Film Electrode                          |
| HMDE                | Hanging mercury drop electrode               |

**LIST OF ABBREVIATIONS (continued)**

| <u>Abbreviation</u> | <u>Explanation</u>                     |
|---------------------|--|
| HPLC                | High-performance liquid chromatography |
| IC                  | Ion chromatography                     |
| ICP                 | Inductively coupled plasma             |
| LOD                 | Limit of detection                     |
| LOQ                 | Limit of quantification                |
| MFE                 | Mercury film electrode                 |
| MIP                 | Microwave induced plasma               |
| MS                  | Mass spectrometry                      |
| NAA                 | Neutron activation analysis            |
| NPV                 | Normal pulse voltammetry               |
| OES                 | Optical emission spectrometry          |
| PIXE                | Proton induced X-ray emission          |
| PSA                 | Potentiometric stripping analysis      |
| RCF                 | Relative centrifugal force             |
| RE                  | Reference electrode                    |
| rpm                 | Revolutions per minute                 |
| RSD%                | Relative percentage standard deviation |
| RVC                 | Reticulated vitreous carbon            |
| SEM                 | Scanning electron microscopy           |
| SWV                 | Square-wave voltammetry                |
| US                  | Ultrasound                             |
| WE                  | Working electrode                      |
| XRF                 | X-ray fluorescence                     |





## 1. INTRODUCTION

Mercury is a toxic element and occurs naturally as the metallic form and/or its sulfide ores such as cinnabar (HgS). A small concentration of mercury is found throughout the lithosphere, the atmosphere, the hydrosphere and the biosphere. The earth's crust contains  $0.5 \text{ mg kg}^{-1}$ , ambient air may contain  $0.002\text{-}0.02 \text{ } \mu\text{g L}^{-1}$ , and sea water contains about  $0.03 \text{ mg L}^{-1}$ . Mercury is also found in trace amounts in most animal and plant tissues. Recent estimates of global emissions of mercury to the atmosphere are highly variable, ranging from  $2\ 000\text{-}3\ 000 \text{ t year}^{-1}$  to  $6\ 000 \text{ t year}^{-1}$ , because of the uncertainty about natural emission rates. Elementary mercury finds extensive use industrially in lamps, batteries, thermometers, and as amalgams, and especially in the electrolytic manufacture of chlorine and sodium hydroxide (Morita et al., 1998).

Mercury compounds have been used as catalysts, fungicides, herbicides, disinfectants, pigments and for other purposes. The world production was about  $10\ 000 \text{ t}$  in 1973 and about  $6\ 500 \text{ t}$  in 1980. In addition to the production of pure mercury by industrial processes, mercury is released into the environment by human activities such as the combustion of fossil fuels, waste disposal and by industry. Recent estimates of anthropogenic emissions are in the order of  $2\ 000$  to  $3\ 000 \text{ t year}^{-1}$  (Morita et al., 1998).

Mercury cycles in the environment as a result of natural and human (anthropogenic) activities. As it cycles between the atmosphere, land, and water, mercury undergoes a series of complex chemical and physical transformations. In the atmosphere mercury moves in its volatile forms such as elemental vapour or methylmercury, as well as in particulate-bound forms. In the marine and terrestrial environments, inorganic mercury is methylated to methylmercury species which are readily accumulated in marine organisms. A portion of environmental mercury becomes bound to sulfur, producing insoluble HgS which accumulates in sediments. On land, some plants are known to concentrate Hg as less-toxic chemical forms such as elemental Hg droplets or as HgS. To understand the environmental cycling of Hg, it is necessary to know the chemical forms of the element that exist in each compartment.

Mercury and its compounds are considered health hazards, and reports of Hg poisoning because of industrial, agricultural, and laboratory exposure as well as its suicidal use are numerous. Mercury toxicity is caused, mainly, by the fact that it enters the living organism, and reacts with different enzymes inhibiting the catalysis of basic metabolic reactions (WHO, 1990; Public Health Statement, 1990; WHO, 1989). The general population may be exposed to mercury compounds through inhalation of ambient air; consumption of contaminated food, water or soil; and/or dermal exposure to substances containing mercury. In addition, some quantity of mercury is released from dental amalgam (Pavlogeorgatos and Kikilias, 2002).

The toxicity of mercury is known to be highly dependent on its chemical form: organomercury is generally more toxic than inorganic mercury salts. Elementary mercury and insoluble HgS are the least toxic. Mercury accumulated in the tissues of fish is usually in the form of methylmercury, a highly toxic form.

The compounds and other physico-chemical forms of mercury may be classified in different ways, and the term 'speciation' has been used with different meanings by scientists who have different backgrounds and different interests in mercury studies. For toxicologists, for example, it is important to know whether mercury is in an organic form or an inorganic form. Massive human intoxication cases have been reported for methylmercury at Minamata, Japan and in Iraq. As well as toxic monoalkylmercury compounds, dialkylmercury is also known to be toxic. New mercury pollution cases in developing countries have resulted from the use of amalgamation in gold mining and changes of chemical form in the environment have been reported. Thus, from this toxicological point of view, it is apparently necessary to "speciate" mercury. Lindquist et al., (1984) proposed speciation of mercury compounds into three categories, volatile species (Hg), reactive species ( $\text{Hg}^{2+}$ , HgO on aerosol particles,  $\text{Hg}^{2+}$  complexes with  $\text{OH}^-$ ,  $\text{Cl}^-$ ,  $\text{Br}^-$ , and organic acids) and non-reactive species ( $\text{CH}_3\text{Hg}^+$ , and other organomercurial moieties,  $\text{Hg}(\text{CN})_2$ , HgS and  $\text{Hg}^{2+}$  bound to sulfur in fragments of humic matter). For plant physiologists, mercury speciation is related to bioavailability which is related to solubility, stability and interaction with soil. Stable and insoluble forms such as HgS will have different consequences to other

species of mercury. For industrial purposes, it is also necessary to determine specific mercury compounds in commercial products to guarantee product quality and safety. Thus, the processes to identify and determine the individual chemical forms of the element are important. This approach may be called chemical speciation and involves differentiation of the various chemical forms of mercury which together make up its total concentration in a sample. The chemical forms that have been considered important for mercury in biological and environmental samples are listed in Table 1.1.

**Table 1.1.** Major mercury species in environmental and biological samples.

|                           |                 |                |
|---------------------------|-----------------|----------------|
| Elemental mercury         |                 | $Hg^{\circ}$   |
| Inorganic mercury species | Mercurous ion   | $Hg^{+}$       |
|                           | Mercuric ion    | $Hg^{2+}$      |
|                           | Mercury sulfide | $HgS$          |
| Organic mercury species   | Methylmercury   | $CH_3Hg^{+}$   |
|                           | Ethylmercury    | $C_2H_5Hg^{+}$ |
|                           | Phenylmercury   | $C_6H_5Hg^{+}$ |
|                           | Dimethylmercury | $(CH_3)_2Hg$   |

In the geochemical cycling of the element, the physical properties of the mercury species together with any potential carrier are possibly of greatest importance. For example, gaseous mercury can be transferred for long distances in the atmosphere, while particulate-bound mercury is less mobile. Or dissolved mercury can be transported by sea currents while mercury bound to particulates is sedimented. In this respect, mercury may be classified into several species that are determined by physical properties (Morita et al., 1998).

Mercury enters the environment as either ionic mercury [Hg(II)] or elemental mercury [Hg(0)] but undergoes numerous biotic and abiotic transformations. As chemical speciation of mercury greatly affects its toxicity and transport, the fate of mercury in the subsurface is critical to groundwater quality and the public health. The most toxic species, methylmercury, formed from Hg(II)

by anaerobic bacteria, is a public health concern because of its accumulation and biomagnifications in the food chain. Methylmercury interacts less strongly than Hg(II) with soil constituents and is therefore more drifting in the environment (Wiatrowski et al., 2006).

Elementary mercury occurs naturally and is present in the atmosphere. It is a volatile liquid at room temperature and is poorly soluble in water. The vapour pressure of Hg is 0.001201 mmHg at 20°C, and the solubility of Hg in water is about 20 mg L<sup>-1</sup>. HgS is the major mercury ore. This material is almost insoluble in water (10<sup>-5</sup> g L<sup>-1</sup> at 18°C) but can be transformed under strong acidic conditions into a soluble form. Consequently, it evaporates from surface waters and sediments (Morita et al., 1998).

Mercury exhibits valences of +1 and +2 and forms stable salts: the divalent (mercuric) salts are more soluble in water than the monovalent (mercurous) salts. Hg forms covalent bonds with carbon and the resulting compounds show a variety of different physical and toxicological properties. Mono-substituted mercury compounds such as methylmercury (CH<sub>3</sub>-HgX), ethylmercury (C<sub>2</sub>H<sub>5</sub>-HgX) and phenylmercury (C<sub>6</sub>H<sub>5</sub>-HgX) have been commercially synthesized and applied for biocidal use.

Ionic mercury is the least mobile species of mercury. It sorbs to organic matter, clays, humic and fulvic acids, amorphous iron sulfide, and oxides of aluminum, iron, and manganese. In the presence of sulfide, Hg(II) forms mercuric sulfide (HgS), a solid precipitate, but also soluble neutral species that are likely the substrate for methylation. Both abiotic and microbial transformations reduce Hg(II) to Hg(0).

Emissions of Hg from power generating facilities and subsequent atmospheric deposition create a global contamination problem. Mercury is also present in the environment because of current and past industrial activities. The subsurface environment may be contaminated either from mobilization of mercury in geological deposits or from anthropogenic sources. In the United States, nuclear weapons test and burial of waste from weapons manufacturing

contaminated vast tracts of subsurface lands with mercury as well as other metals, organic solvents, and radionuclides (Wiatrowski et al., 2006).

Because of the strong public concern about environmental mercury contamination, a large amount of analytical research has been done on the determination of mercury and its compounds. Most of the papers were related to the determination of the total mercury concentrations in the samples and the literature concerned with mercury speciation is still limited.

The toxic effects of mercury are well known. For that reason, sensitive, fast, reproducible, and accurate analytical methods are required in determination of this element. In routine laboratory measurements, Hg is determined in its atomic form in the vapour phase using atomic spectroscopic methods and electrochemical methods. However, the direct determination of (ultra)trace amounts of mercury in complicated matrices is usually difficult due to matrix interferences and/or lack of sufficient detection ability. Therefore, a preliminary preconcentration and/or separation are required (Cañada Rudner et al., 1998).

A variety of detection methods have been used to detect mercury selectively and sensitively (Table 1.2). Good review papers have been published for the determination of total mercury concentrations in environmental and biological samples. These methods can be listed as follows: gravimetry, micrometry, radiometry, titrimetry, colorimetry, and fluorometry, atomic absorption spectrometry (AAS) (cold vapour, electrothermal etc.), atomic fluorescence spectrometry (AFS), atomic emission spectrometry (AES) [spectrography, inductively coupled plasma-atomic emission spectrometry (ICP-AES), microwave induced plasma-atomic emission spectrometry (MIP-AES), direct current plasma-atomic emission spectrometry (DCP-AES) etc.], neutron activation analysis (NAA), X-ray fluorescence (XRF), electron probe micro-analysis (EPMA), proton induced X-ray emission (PIXE) etc.), mass spectrometry (MS), electrometry (polarography, amperometry, voltammetry etc.), chromatography, and other miscellaneous methods (Morita et al., 1998).

**Table 1.2.** Selected applications of different methods for Hg determination.

US: Ultrasound, CV: Cold Vapor, AAS: Atomic absorption spectrometry, AFS: Atomic fluorescence spectrometry, AES: atomic emission spectrometry, OES: Optical emission spectrometry, MS: Mass spectrometry, ICP: Inductively coupled plasma, MIP: Microwave induced plasma, ET: Electrothermal, FI: Flow injection, HPLC: High-performance liquid chromatography, IC: Ion chromatography

| Matrix  | Sample pre-treatment   | Separation/preconcentration  | Detection Technique | Detection limit (ng L <sup>-1</sup> ) | Ref.                 |
|---|--|--|---------------------|---------------------------------------|----------------------|
| Simulated waste waters and environmental waters | US-assisted decomposition of organic mercury species in the presence of HCl              | CV generation  | FI-CV-AAS           | 400                                   | Capelo et al., 2000  |
| Lake, moorland, river, sea water                | On-line digestion with BrCl at 70 °C   | CV generation and trapping onto gold collector   | FI-CV-AFS           | 0.016                                 | Leopold et al., 2008 |
| Natural waters                                  | Addition of formic acid to favor US-CV generation  | US-CV generation and subsequent in-atomizer trapping on a noble metal coated platform of a graphite tube | ET-AAS              | 30                                    | Gil et al., 2007     |
| River water                                     | On-line digestion with Br <sup>-</sup> /BrO <sub>3</sub> <sup>-</sup> and UV-irradiation | CV generation  | AAS                 | 10                                    | Elsholz et al., 2000 |
| Lake, moorland, river, sea water                | UV-irradiation-assisted degradation of mercury complexes with natural organic compounds  | Trapping onto catalytic active nano-gold collector, thermal desorption                                   | AFS                 | 0.08                                  | Zierhut et al., 2010 |

**Table 1.2.** continued

| <b>Matrix</b>   | <b>Sample pre-treatment</b>  | <b>Separation/preconcentration</b>                                      | <b>Detection Technique</b> | <b>Detection limit<br/>(ng L<sup>-1</sup>)</b> | <b>Ref.</b>                  |
|---|--|---|----------------------------|--|------------------------------|
| River water   | -  | Pre-concentration onto gold-coated silica collector, thermal desorption | FI-AFS                     | 0.18   | Leopold et al., 2009         |
| River water   | Batch oxidative decomposition with BrCl at room temperature                              | CV generation and trapping onto gold collector                          | AFS                        | 0.26   | Labatzke and Schlemmer, 2004 |
| Estuarine water                                       | -  | Trapping onto catalytic active nano-gold collector, thermal desorption  | AFS                        | 0.14   | Zierhut et al., 2009         |
| Estuarine water                                       | US-assisted decomposition of organic mercury species                                     | CV generation   | AAS                        | 500  | Fernandez et al., 2006       |
| Sea water   | On-line digestion with Br <sup>-</sup> /BrO <sub>3</sub> <sup>-</sup> and UV-irradiation | CV generation and trapping onto gold collector                          | AAS                        | 0.5  | Wurl et al., 2000            |
| Rain, potable, and nonpotable water and lake sediment | The sediment river samples were pre-treated microwave oven                               | Home made CV generation and separation                                  | ET-AAS                     | 93 (pg)  | Moreno et al., 2002          |

**Table 1.2.** continued

| <b>Matrix</b>                         | <b>Sample pre-treatment</b>  | <b>Separation/preconcentration</b>   | <b>Detection Technique</b> | <b>Detection limit (ng L<sup>-1</sup>)</b> | <b>Ref.</b>            |
|---------------------------------------|--|--|----------------------------|--|------------------------|
| Tap water                             | Cloud point extraction   | Cloud point extraction   | FI-CV-ICP-OES              | 4  | Wuilloud et al., 2002  |
| Lake water                            | Optional: Addition of formic acid to favor US-CV generation  | US-CV generation   | AAS                        | 100  | Gil et al., 2006       |
| Potable water                         | -  | Amalgamation   | ICP-MS                     | 32   | Allibone et al., 1999  |
| Standard reference material, SRM 2704 | Digested with a mixture of 3.5 mL of HNO <sub>3</sub> -HCl (1:3), then added a 2 mL of KMnO <sub>4</sub> 5% (w:v) solution, followed by the addition of H <sub>2</sub> O <sub>2</sub> (1-2 mL) | Based amalgamation of the generated mercury vapor on gold trap                           | MIP-AES                    | 14   | Murillo et al., 2001   |
| Drinking water and sediment           | The sediment samples were dried at 60 °C, then sieved through a nylon sieve  | Solid-phase extraction on sodium diethyldithiocarbamate immobilized in polyurethane foam | HPLC-ICP-MS                | 4.6  | Santos et al., 2009    |
| Synthetic mixtures and tap water      | As cysteine complexes, reduction system: sodium tetrahydroborate,  | Ion chromatography, CV   | IC-CV-AAS                  | 20   | Sarzanini et al., 1994 |



As shown in Table 1.2; for determination of mercury, various methods whose detection limits can change from 500 to 0.016 ng L<sup>-1</sup> are developed and in wide range of waters, mercury analysis was carried out. Several chromatographic techniques coupled with spectrometric methods have also been used for mercury speciation. Among these, AFS procedure is the preferred detection method due to its sensitivity. Being achieved of this sensitivity analysis is also based on time-consuming pre-treatment, separation and preconcentration operations' which are applied to samples to be performed efficiently. However considering the equipment used, it is pointed out that they are expensive, unmovable and they have complex and specific measurement systems which can work together with a lot of equipments. Moreover, working together with fluid gas and liquids like CV and FI methods contains many challenges. Electrochemical methods, in particularly stripping techniques represent an interesting alternative for mercury determination against aforementioned disadvantages of other methods.

Voltammetric analysis is especially suited for such determination because they offer advantages such as sensitivity, versatility, simplicity, low costs and medium exchange. The recommendation of the United State Environmental Protection Agency (EPA) for the adoption of stripping analysis for the quantification of heavy metals as mercury (EPA Method 7472, 2000) is a very representative example of this application.

### **1.1. Voltammetry**

Voltammetry comprises a group of electroanalytical techniques in which information about the analyte is derived from current-voltage curves-that is, plots of current as a function of applied potential-obtained under conditions that encourage polarization of working electrode. Generally, the working electrodes in voltammetry are characterized by their small surface area which enhances polarization. Such electrodes are generally referred to as microelectrodes. Historically, the field of voltammetry developed from the discovery of polarography by Jaroslav Heyrovský in the early 1920.

Polarography, which is still the most widely used of all voltammetric methods, differs from the others in the respect that a dropping mercury electrode (DME) serves as the microelectrode. By 1950, voltammetry appeared to be a mature and fully developed technique. The decade from 1955 to 1965, however, was marked by the appearance of several major modifications of the original method, which served to overcome many of its limitations. Following this, the advent of low-cost operational amplifiers in the early 1960 made possible the development of relatively inexpensive, commercially available instruments that incorporated many of these important modifications. The result has been a recent resurgence of interest in the applications of voltammetric methods to the qualitative and quantitative determination of organic and inorganic species, which are electroactive (directly analysis) and non-electroactive (indirectly analysis).

Three-electrode cells are commonly used in controlled potential experiments (Figure 1.1). The cell is usually a covered beaker of 5-50 mL volume, and contains the three electrodes (working, reference, and auxiliary), which are immersed in the sample solution. While the working electrode (WE) is the electrode at which the reaction of interest occurs, the reference electrode (RE) provides a stable and reproducible potential (independent of the sample composition), against which the potential of the working electrode is compared. Such “buffering” against potential changes is achieved by a constant composition of both forms of its redox couple, such as Ag/AgCl or Hg/Hg<sub>2</sub>Cl<sub>2</sub>, as common with the silver-silver chloride and the saturated calomel reference electrodes, respectively. To minimize contamination of the sample solution, the reference electrode may be insulated from the sample through an intermediate bridge (double junction reference electrode). An inert conducting material, such as platinum wire or graphite rod, is usually used as the current-carrying auxiliary electrode (AE). The relative position of these electrodes and their proper connection to the electrochemical analyzer should be noted. The three electrodes, as well as the tube used for bubbling, the deoxygenating gas are supported in five holes in the cell cover. Complete systems, integrating the three-electrode cell, built in gas control, and stirrer, along with proper cover, are available commercially (Wang, 2006). In addition to these, home-made three-electrode systems and voltammetric cells can be produced as available for purpose such in this study.

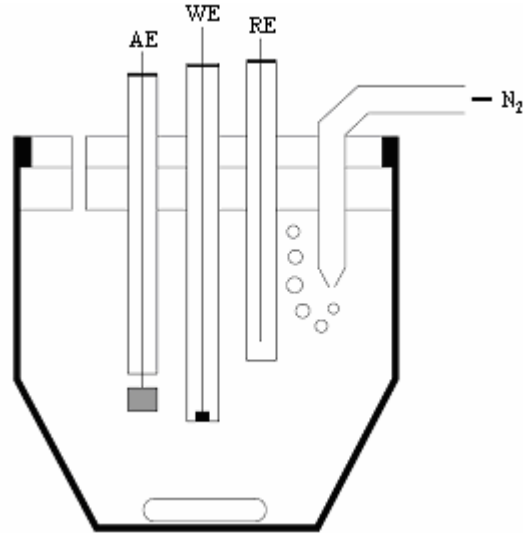


**Figure 1.1.** Schematic diagram of a cell for voltammetric measurements: WE working electrodes; RE reference electrode; AE auxiliary electrode. The electrodes are inserted through holes in the cell cover (Wang, 2006).

In voltammetry, the effects of the applied potential and the behavior of the redox current are described by several well-known laws. The applied potential controls the concentrations of the redox species at the electrode surface ( $C_O^0$  and  $C_R^0$ ) and the rate constant ( $k^0$ ), as described by the Nernst or Butler-Volmer equations, respectively. In the cases where diffusion plays a controlling part, the current resulting from the redox process (known as the faradaic current) is related to the material flux at the electrode-solution interface and is described by Fick's law. The interplay between these processes is responsible for the characteristic features observed in the voltammograms of the various techniques (Settle, 1997).

For a reversible electrochemical reaction (that is, a reaction so fast that equilibrium is always reestablished as changes are made), which can be described by  $\mathbf{O} + ne^- \rightleftharpoons \mathbf{R}$ , the application of a potential  $E$  forces the respective concentrations of  $\mathbf{O}$  and  $\mathbf{R}$  at the surface of the electrode (that is,  $c_O^0$  and  $c_R^0$ ) to a ratio in compliance with the Nernst equation:

$$E = E^0 + \frac{RT}{nF} \ln \frac{c_O^0}{c_R^0} \quad (1.1)$$

where  $R$  is the gas constant ( $8.3144 \text{ J mol}^{-1} \text{ K}^{-1}$ ),  $T$  is the absolute temperature ( $K$ ),  $n$  is the number of electrons transferred,  $F$  is Faraday constant ( $96,485 \text{ C/equiv}$ ), and  $E^0$  is the standard electrode potential for the redox couple. If the potential applied to the electrode is changed, the ratio  $c_R^0/c_O^0$  at the surface will also change so as to satisfy Eq. (1.1). If the potential is made more negative the ratio becomes larger (that is, **O** is reduced) and, conversely, if the potential is made more positive the ratio becomes smaller (that is, **R** is oxidized).

For some techniques it is useful to use the relationship that links the variables for current, potential, and concentration, known as the Butler-Volmer equation:

$$\frac{i}{nFA} = k^0 \{c_O^0 \exp[-\alpha\theta] - c_R^0 \exp[(1-\alpha)\theta]\} \quad (1.2)$$

where  $\theta = nF(E - E^0)/RT$ ,  $k^0$  is the heterogeneous rate constant,  $\alpha$  is known as the transfer coefficient, and  $A$  is the surface area of the electrode. This relationship allows us to obtain the values of the two analytically important parameters,  $i$  and  $k^0$ .

Finally, in most cases the current flow also depends directly on the flux of material to the electrode surface. When new **O** or **R** is created at the surface, the increased concentration provides the force for its diffusion toward the bulk of the solution. Likewise, when **O** or **R** is destroyed, the decreased concentration promotes the diffusion of new material from the bulk solution. The resulting concentration gradient and mass transport is described by Fick's law, which states that the flux of matter ( $\varphi$ ) is directly proportional to the concentration gradient:

$$\varphi = -AD_O(\partial c_O/\partial x) \quad (1.3)$$

where  $D_O$  is the diffusion coefficient of **O** and  $x$  is the distance from the electrode surface. An analogous equation can be written for **R**. The flux of **O** or **R** at the electrode surface controls the rate of reaction, and thus the faradaic current

flowing in the cell. In the bulk solution, concentration gradients are generally small and ionic migration carries most of the current. The current is a quantitative measure of how fast a species is being reduced or oxidized at the electrode surface. The actual value of this current is affected by many additional factors, most importantly the concentration of the redox species, the size, shape, and material of the electrode, the solution resistance, the cell volume, and the number of electrons transferred.

In addition to diffusion, mass transport can also occur by migration or convection. Migration is the movement of a charged ion in the presence of an electric field. In voltammetry, the use of a supporting electrolyte at concentrations 100 times that of the species being determined eliminates the effect of migration. Convection is the movement of the electroactive species by thermal currents, by density gradients present in the solution, or by stirring the solution or rotating the electrode. Convection must be eliminated or controlled accurately to provide controlled transport of the analyte to the electrode (Settle, 1997).

The basis of all controlled-potential techniques is the measurement of the current response to an applied potential. A multitude of potential excitations (including a ramp, potential steps, pulse trains, a sine wave, and various combinations thereof) exists.

### **1.1.1. Chronoamperometry**

Chronoamperometry involves stepping the potential of the working electrode from a value at which no faradaic reaction occurs to a potential at which the surface concentration of the electroactive species is effectively zero (Figure 1.2a). A stationary working electrode and unstirred (quiescent) solution are used. The resulting current–time dependence is monitored. As mass transport under these conditions is solely by diffusion, the current–time curve reflects the change in the concentration gradient in the vicinity of the surface. This involves a gradual expansion of the diffusion layer associated with the depletion of the reactant, and hence decreased slope of the concentration profile as time progresses (see Figure 1.2b). Accordingly, the current (at a planar electrode) decays with time (Figure 1.2c), as given by the *Cottrell equation*

$$i(t) = \frac{nFACD^{1/2}}{\pi^{1/2}t^{1/2}} = kt^{-1/2} \quad (1.4)$$

where  $C$ ,  $D$ , and  $t$  are the concentration, the diffusion coefficient, and time, respectively.

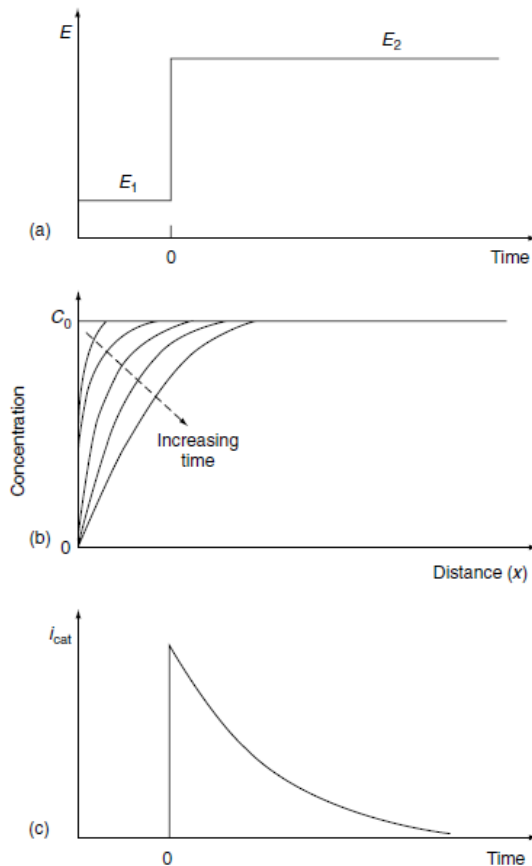


**Figure 1.2.** In chronoamperometric method: (a) potential–time waveform; (b) change in concentration profiles as time progresses; (c) the resulting current–time response (Wang, 2006).

Such an  $it^{1/2}$  constancy is often termed a “Cottrell behavior.” Deviations from such behavior occur at long times (usually over 100 s) as a result of natural convection effects, due to coupled chemical reactions, and when using non-planar electrodes or microelectrodes with high perimeter-to-area ratio. In the latter case, a time-independent current (proportional to the concentration) is obtained for  $t > 0.1$  s, due to a large radial diffusion contribution. Similar considerations apply to spherical electrodes whose current response following potential step contains

time-dependent and time-independent terms. Recall also that for short values of  $t$  ( $t < 50$  ms), the chronoamperometric signal contains an additional background contribution of the charging current. This exponentially decaying charging current represents the main contribution to the response in the absence of an electroactive species (Wang, 2006).

Chronoamperometry is often used for measuring the diffusion coefficient of electroactive species or the surface area of the working electrode. Some analytical applications of chronoamperometry (e.g., *in vivo* bioanalysis) rely on pulsing of the potential of the working electrode repetitively at fixed time intervals. Chronoamperometry can also be applied to the study of mechanisms of electrode processes (Wang, 2006).

### **1.1.2. Polarography**

Polarography is a subclass of voltammetry in which the working electrode is dropping mercury. Because of the special properties of this electrode, particularly its renewable surface and wide cathodic potential range, polarography has been widely used for the determination of many important reducible species. This classical technique had an enormous impact on the progress of electroanalysis (Wang, 2006).

The excitation signal used in conventional (DC) polarography is a linearly increasing potential ramp. For a reduction, the initial potential is selected to ensure that the reaction of interest does not take place. The potential is then scanned cathodically while the current is measured. Such current is proportional to the slope of the concentration–distance profile. At a sufficiently negative potential, reduction of the analyte commences, the concentration gradient increases, and the current rises rapidly to its limiting (diffusion-controlled) value. At this plateau, any analyte particle that arrives at the electrode surface instantaneously undergoes an electron transfer reaction, and the maximum rate of diffusion is achieved. The resulting polarographic wave is shown in Figure 1.3. The current oscillations reflect the growth and fall of the individual drops.

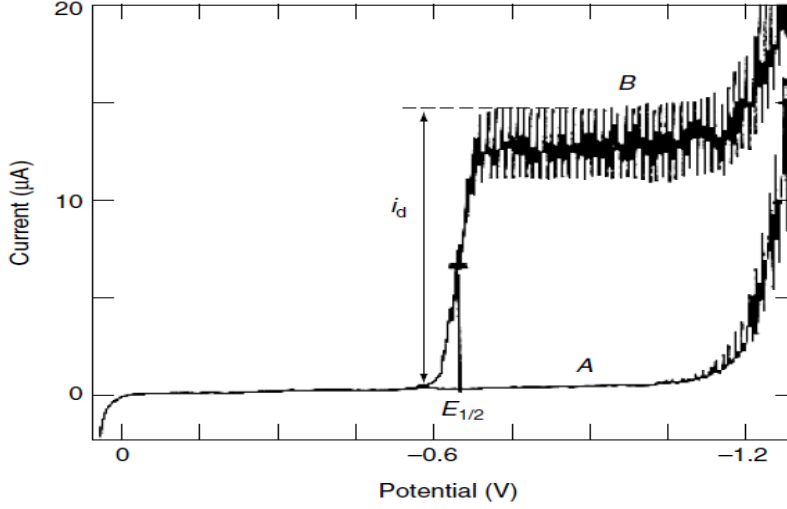


**Figure 1.3.** Polarograms for 1 M hydrochloric acid (A) and  $4 \times 10^{-4}$  M  $\text{Cd}^{2+}$  in 1 M hydrochloric acid (B);  $i_d$  represents the limiting current, while  $E_{1/2}$  is the half-wave potential (Wang, 2006).

To derive the expression for the current response, one must account for the variation of the drop area with time

$$A = 4\pi \left( \frac{3mt}{4\pi d} \right)^{2/3} = 0.85(mt)^{2/3} \quad (1.5)$$

where  $t$  is the time and  $m$  and  $d$  are the mass flow rate and density of mercury, respectively. By substituting the surface area into the Cottrell equation, and replacing  $D$  by  $7/3D$  (to account for the compression of the diffusion layer by the expanding drop), we can obtain the *Ilkovic equation* for the limiting diffusion current:

$$i_d = 708 n D^{1/2} m^{2/3} t^{1/6} C \quad (1.6)$$

Here,  $i_d$  will have units of amperes (A), when  $D$  is in  $\text{cm}^2\text{s}^{-1}$ ,  $m$  is in  $\text{g s}^{-1}$ ,  $t$  is in seconds, and  $C$  is in  $\text{mol cm}^{-3}$ . This expression represents the current at the end of the drop life. The average current over the drop life is obtained by integrating the current of this time period:

$$i_{av} = 607 n D^{1/2} m^{2/3} t^{1/6} C \quad (1.7)$$



To determine the diffusion current, it is necessary to subtract the residual current. This can be achieved by extrapolating the residual current prior to the wave or by recording the response of the deaerated supporting electrolyte (blank) solution. Standard addition or a calibration curve is often used for quantitation. Polarograms to be compared for this purpose must be recorded in the same way.

The potential where the current is one-half of its limiting value is called the *half-wave potential*,  $E_{1/2}$ . The half-wave potential (for electrochemically reversible couples) is related to the formal potential  $E^\circ$  of the electroactive species according to

$$E_{1/2} = E^\circ + \frac{RT}{nF} \log(D_R/D_O)^{1/2} \quad (1.8)$$

where  $D_R$  and  $D_O$  are the diffusion coefficients of the reduced and oxidized forms of the electroactive species, respectively. Because of the similarity in the diffusion coefficients, the half-wave potential is usually similar to the formal potential. Thus, the half-wave potential, which is a characteristic of a particular species in a given supporting electrolyte solution, is independent of the concentration of that species. Therefore, by measuring the half-wave potential, one can identify the species responsible for an unknown polarographic wave. Typical half-wave potentials for several reducible organic functionalities, common in organic compounds, are given in Table 1.3. Compounds containing these functionalities are ideal candidates for polarographic measurements. Since neutral compounds are involved, such organic polarographic reductions commonly involve hydrogen ions. Such reactions can be represented as



where R and  $RH_n$  are oxidized and reduced forms of the organic molecule. For such processes, the half-wave potential will be a function of pH (with a negative shift of about 59 mV/n for each unit increase in pH, due to decreasing availability of protons). Thus, in organic polarography, good buffering is vital for generating reproducible results. Reactions of organic compounds are also often slower and more complex than those for inorganic cations.

**Table 1.3.** Functional groups reducible at the DME (Wang, 2006).

| Class of Compounds                     | Functional          | $E_{1/2}$ (V <sup>a</sup> )<br>Group |
|--|---------------------|--------------------------------------|
| Azo                                    | —N=N—               | -0.4                                 |
| Carbon-carbon double bond <sup>b</sup> | —C=C—               | -2.3                                 |
| Carbon-carbon triple bond <sup>b</sup> | —C≡C—               | -2.3                                 |
| Carbonyl                               | >C=O                | -2.2                                 |
| Disulfide                              | S—S                 | -0.3                                 |
| Nitro                                  | NO <sub>2</sub>     | -0.9                                 |
| Organic halides                        | C—X (X = Br, Cl, I) | -1.5                                 |
| Quinone                                | C=O                 | -0.1                                 |

<sup>a</sup> Against the saturated calomel electrode at pH = 7.

<sup>b</sup> Conjugated with a similar bond or with an aromatic ring.

### 1.1.3. Pulse Voltammetry

In order to increase speed and sensitivity, many forms of potential modulation (other than just a simple staircase ramp) have been tried over the years. Pulse voltammetric techniques, introduced by Barker and Jenkin, are aimed at lowering the detection limits of voltammetric measurements. By substantially increasing the ratio between the faradaic and nonfaradaic currents, such techniques permit convenient quantitation down to the  $10^{-8}$  M concentration level. Because of their greatly improved performance, modern pulse techniques have largely supplanted classical polarography in the analytical laboratory. The various pulse techniques are all based on a sampled current/potential-step (chronoamperometric) experiment. A sequence of such potential steps, each with duration of about 50 ms, is applied onto the working electrode. After the potential is stepped, the charging current decays rapidly (exponentially) to a negligible value, while the faradaic current decays more slowly. Thus, by sampling the current late in the pulse life, an effective discrimination against the charging current is achieved.

The difference between the various pulse voltammetric techniques is the excitation waveform and the current sampling regime. With both normal-pulse and differential-pulse voltammetry, one potential pulse is applied for each drop of mercury when the DME is used (Both techniques can also be used at solid electrodes). By controlling the drop time (with a mechanical knocker), the pulse is synchronized with the maximum growth of the mercury drop. At this point, near

the end of the drop lifetime, the faradaic current reaches its maximum value, while the contribution of the charging current is minimal (based on the time dependence of the components) (Wang, 2006).

### 1.1.3.1. Normal-Pulse Voltammetry

Normal-pulse voltammetry (NPV) consists of a series of pulses of increasing amplitude applied to successive drops at a preselected time near the end of each drop lifetime. Such a normal pulse train is shown in Figure 1.4. Between the pulses, the electrode is kept at a constant (base) potential at which no reaction of the analyte occurs. The amplitude of the pulse increases linearly with each drop. The current is measured about 40 ms after the pulse is applied, at which time the contribution of the charging current is nearly zero. In addition, because of the short pulse duration, the diffusion layer is thinner than that of DC polarography (i.e., greater flux of analyte) and hence the faradaic current is increased. The resulting voltammogram has a sigmoidal shape (Wang, 2006).

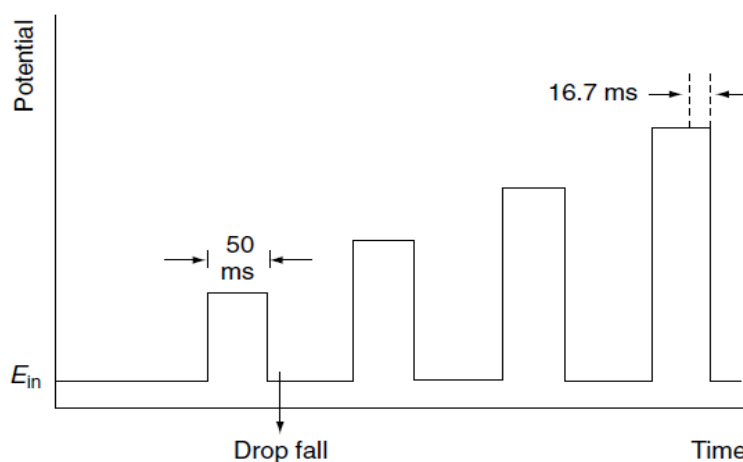


**Figure 1.4.** Excitation waveform for normal pulse voltammetry (Wang, 2006).

### 1.1.3.2. Differential Pulse Voltammetry

Differential pulse voltammetry (DPV) is an extremely useful technique for measuring trace levels of organic and inorganic species. In DPV, fixed magnitude pulses -superimposed on a linear potential ramp- are applied to the working electrode at a time just before the end of the drop (Figure 1.5). The current is

sampled twice, just before the pulse application (at 1) and again late in the pulse life (after  $\sim 40$ ms, at 2, when the charging current has decayed). The first current is instrumentally subtracted from the second, and this current difference [ $\Delta i = i(t_2) - i(t_1)$ ] is plotted against the applied potential. The resulting differential-pulse voltammogram consists of current peaks, the height of which is directly proportional to the concentration of the corresponding analytes (Wang, 2006).

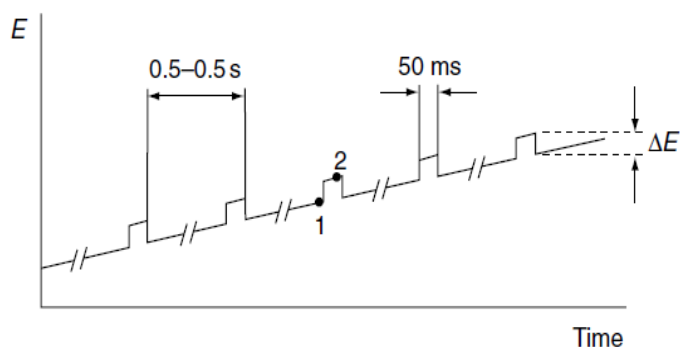


**Figure 1.5.** Excitation signal for differential-pulse voltammetry (Wang, 2006).

The peak potential ( $E_p$ ) can be used to identify the species, as it occurs near the polarographic half-wave potential:

$$E_p = E_{1/2} - \Delta E/2 \quad (1.10)$$

The differential-pulse operation results in a very effective correction of the charging background current. The charging-current contribution to the differential current is negligible.

The peak-shaped response of differential-pulse measurements results also in improved resolution between two species with similar redox potentials. In various situations, peaks separated by 50 mV may be measured. Such quantitation depends not only on the corresponding peak potentials but also on the widths of the peak. The peak-shaped response, coupled with the flat background current, makes the technique particularly useful for analysis of mixtures.

The selection of the pulse amplitude and potential scan rate usually requires a tradeoff among sensitivity, resolution, and speed. For example, larger pulse amplitudes result in larger and broader peaks. Pulse amplitudes of 25-50 mV,

coupled with a scan rate of  $5 \text{ mVs}^{-1}$ , are commonly employed. Irreversible redox systems result in lower and broader current peaks (i.e., inferior sensitivity and resolution) compared with those predicted for reversible systems. In addition to improvements in sensitivity and resolution, the technique can provide information about the chemical form in which the analyte appears (oxidation states, complexation, etc.) (Wang, 2006).

### 1.1.3.3. Square-Wave Voltammetry

Square-wave voltammetry is a large-amplitude differential technique in which a waveform composed of a symmetric square wave, superimposed on a base staircase potential, is applied to the working electrode (Figure 1.6). The current is sampled twice during each square-wave cycle, once at the end of the forward pulse (at  $t_1$ ) and once at the end of the reverse pulse (at  $t_2$ ). Since the square-wave modulation amplitude is very large, the reverse pulses cause the reverse reaction of the product (of the forward pulse). The difference between the two measurements is plotted versus the base staircase potential (Wang, 2006).

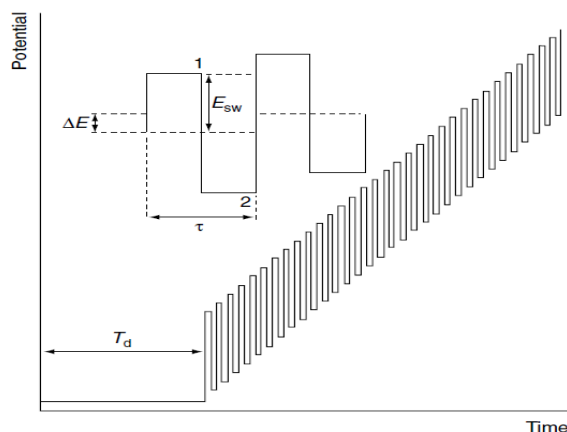


**Figure 1.6.** Square-wave waveform showing the amplitude  $E_{sw}$ , step height  $\Delta E$ , squarewave period  $T$ , delay time  $T_d$ , and current measurement times 1 and 2 (Wang, 2006).

The peak height is directly proportional to the concentration of the electroactive species and direct detection limit as low as  $10^{-8} \text{ M}$  is possible. Square-wave voltammetry has several advantages. Among these are its excellent sensitivity and the rejection of background currents. Another is the speed (for example, its ability to scan the voltage range over one drop during polarography

with the DME). This speed, coupled with computer control and signal averaging, allows for experiments to be performed repetitively and increases the signal to-noise ratio. Applications of square-wave voltammetry include the study of electrode kinetics with regard to preceding, following, or catalytic homogeneous chemical reactions, determination of some species at trace levels, and its use with electrochemical detection in HPLC (Settle, 1997).

#### 1.1.3.4. Staircase Voltammetry

Staircase voltammetry has been proposed as a useful tool for rejecting the background charging current. The potential-time waveform involves successive potential steps of  $\sim 10$  mV height and about 50 ms duration (Figure 1.7). The current is sampled at the end of each step, where the charging current has decayed to a negligible value. Hence, this waveform couples the discrimination against the charging current with the experimental speed of linear scan voltammetry. Such an operation results in a peak-shaped current response, similar to that of linear scan experiments.

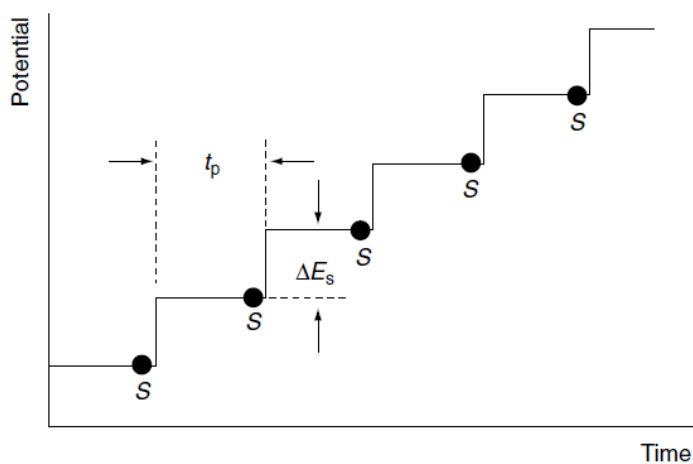


**Figure 1.7.** Potential-time waveform used in staircase voltammetry (Wang, 2006).

Indeed, as the steps become smaller, the equations for the staircase voltammetric response converge with those of linear scan voltammetry. As such, staircase voltammetry can be considered as the digital version of linear scan voltammetry. Similarly, cyclic staircase voltammetric experiments, in which the direction of the potential steps is reversed at a switching potential, result in a

voltammetric response resembling cyclic voltammetry (but with a much reduced charging-current contribution) (Wang, 2006).

#### 1.1.4. AC Voltammetry

Alternating current (AC) voltammetry is a frequency-domain technique which involves the superimposition of a small amplitude AC voltage on a linear ramp (Figure 1.8). Usually the alternating potential has a frequency of 50-100 Hz and amplitude of 10-20 mV. The AC signal thus causes a perturbation in the surface concentration, around the concentration maintained by the DC potential ramp. The resulting AC current is plotted against the potential. Such a voltammogram shows a peak, the potential of which is the same as that of the polarographic half-wave potential (At this region the sinusoid has maximum impact on the surface concentration, i.e., on the current). For a reversible system, such a response is actually the derivative of the DC polarographic response. The height of the AC voltammetric peak is proportional to the concentration of the analyte and, for a reversible reaction, to the square root of the frequency ( $\omega$ ):

$$i_p = \frac{n^2 F^2 A \omega^{1/2} D^{1/2} C \Delta E}{4RT} \quad (1.11)$$

The term  $\Delta E$  is the amplitude. The peak width is independent of the AC frequency, and is  $90.4/n$  mV (at 25°C).

The detection of the AC component allows one to separate the contributions of the faradaic and charging currents. The former is phase-shifted by 45° relative to the applied sinusoidal potential, while the background component is 90° out of phase. The charging current is thus rejected using a phase-sensitive lock-in amplifier (able to separate the in-phase and out-of-phase current components). As a result, reversible electrode reactions yield a detection limit of  $5 \times 10^{-7}$  M.

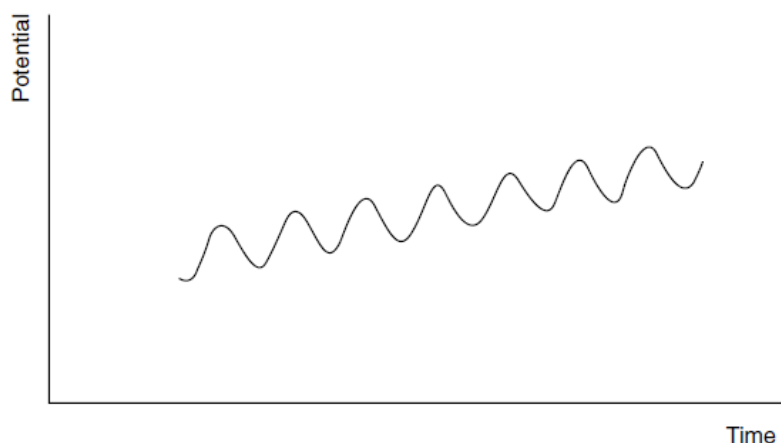


**Figure 1.8.** Potential-time waveform used in alternating current voltammetry (Wang, 2006).

### 1.1.5. Cyclic Voltammetry

Cyclic voltammetry (CV) has become an important and widely used electroanalytical technique in many areas of chemistry. It is rarely used for quantitative determinations, but it is widely used for the study of redox processes, for understanding reaction intermediates, and for obtaining stability of reaction products. This technique is based on varying the applied potential at a working electrode in both forward and reverse directions (at some scan rate) while monitoring the current. For example, the initial scan could be in the negative direction to the switching potential. At that point the scan would be reversed and run in the positive direction. Depending on the analysis, one full cycle, a partial cycle, or a series of cycles can be performed (Settle, 1997).

CV consists of scanning linearly the potential of a stationary working electrode (in an unstirred solution), using a triangular potential waveform (Figure 1.9). Depending on the information sought, single or multiple cycles can be used. During the potential sweep, the potentiostat measures the current resulting from the applied potential. The resulting current-potential plot is termed a *cyclic voltammogram*. The cyclic voltammogram is a complicated, time-dependent function of a large number of physical and chemical parameters (Wang, 2006).



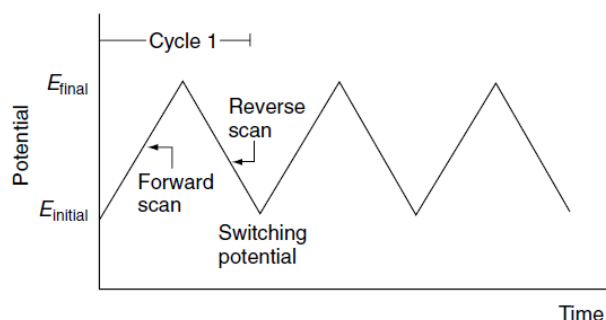


**Figure 1.9.** Potential–time excitation signals in a cyclic voltammetric experiment (Wang, 2006).

The important parameters in a cyclic voltammogram are the peak potentials ( $E_{pc}$ ,  $E_{pa}$ ) and peak currents ( $i_{pc}$ ,  $i_{pa}$ ) of the cathodic and anodic peaks, respectively. If the electron transfer process is fast compared with other processes (such as diffusion), the reaction is said to be electrochemically reversible, and the peak separation is

$$\Delta E_p = |E_{pa} - E_{pc}| = 2.303RT/nF \quad (1.12)$$

Thus, for a reversible redox reaction at 25°C with  $n$  electrons  $\Delta E_p$  should be  $0.0592/n$  V or about 60 mV for one electron. In practice this value is difficult to attain because of such factors as cell resistance. Irreversibility due to a slow electron transfer rate results in  $\Delta E_p > 0.0592/n$  V, greater, say, than 70 mV for a one-electron reaction. The formal reduction potential ( $E^\circ$ ) for a reversible couple is given by

$$E^\circ = \frac{E_{pc} + E_{pa}}{2} \quad (1.13)$$

For a reversible reaction, the concentration is related to peak current by the Randles–Sevcik expression (at 25°C):

$$i_p = 2.686 \times 10^5 n^{3/2} A c^\circ D^{1/2} \nu^{1/2} \quad (1.14)$$

where  $i_p$  is the peak current in amps,  $A$  is the electrode area ( $\text{cm}^2$ ),  $D$  is the diffusion coefficient ( $\text{cm}^2 \text{s}^{-1}$ ),  $A c^\circ$  is the concentration in  $\text{mol cm}^{-3}$ , and  $n$  is the

scan rate in  $\text{Vs}^{-1}$ . Cyclic voltammetry is carried out in quiescent solution to ensure diffusion control. A three-electrode arrangement is used. Mercury film electrodes are used because of their good negative potential range. Other working electrodes include glassy carbon, platinum, gold, graphite, and carbon paste (Settle, 1997).

#### **1.1.6. Preconcentration and Stripping Techniques**

Stripping analysis is an extremely sensitive electrochemical technique for measuring trace metals. Its remarkable sensitivity is attributed to the combination of an effective preconcentration step with advanced measurement procedures that generates an extremely favorable signal-to-background ratio. Since the metals are preconcentrated into the electrode by factors of 100-1000, detection limits are lowered by two to three orders of magnitude compared to solution-phase voltammetric measurements. Hence, four to six metals can be measured simultaneously in various matrices at concentration levels down to  $10^{-10}$  M, utilizing relatively inexpensive instrumentation. The ability to obtain such low detection limits strongly depends on the degree to which contamination can be minimized (Wang, 2006).

The most commonly used variations are anodic stripping voltammetry (ASV), cathodic stripping voltammetry (CSV), adsorptive stripping voltammetry (AdSV) and potentiometric stripping analysis (PSA).

Even though ASV, CSV, AdSV and PSA each have their own unique features, all have two steps in common. First, the analyte species in the sample solution is concentrated onto or into a working electrode. It is this crucial preconcentration step that results in the exceptional sensitivity that can be achieved. During the second step, the preconcentrated analyte is measured or stripped from the electrode by the application of a potential scan. Any number of potential waveforms can be used for the stripping step (that is, differential pulse, square wave, linear sweep, or staircase). The most common are differential pulse and square wave due to the discrimination against charging current. However, square wave has the added advantages of faster scan rate and increased sensitivity relative to differential pulse (Settle, 1997).

The electrode of choice for stripping voltammetry is generally mercury. The species of interest can be either reduced into the mercury, forming amalgams as in anodic stripping voltammetry, or adsorbed to form an insoluble mercury salt layer, as in cathodic stripping voltammetry.

Stripping voltammetry is a very sensitive technique for trace analysis. As with any quantitative technique, care must be taken so that reproducible results are obtainable. Important conditions that should be held constant include the electrode surface, rate of stirring, and deposition time. Every effort should be made to minimize contamination (Settle, 1997).

#### **1.1.6.1. Anodic Stripping Voltammetry**

ASV is most widely used for trace metal determination and has a practical detection limit in the part per-trillion range. This low detection limit is coupled with the ability to determine simultaneously trace metals using relatively inexpensive instrumentation (Settle, 1997).

Metal ions in the sample solution are concentrated into a mercury electrode during a given time period by application of a sufficient negative potential. These amalgamated metals are then stripped (oxidized) out of the mercury by scanning the applied potential in the positive direction. The resulting peak currents,  $i_p$ , are proportional to the concentration of each metal in the sample solution, with the position of the peak potential,  $E_p$ , specific to each metal. The use of mercury limits the working range for ASV to between approximately 0 and -1.2 V versus SCE. The use of thin Hg films or Hg microelectrodes along with pulse techniques such as square-wave voltammetry can substantially lower the limits of detection of ASV (Settle, 1997).

Repetitive ASV runs can be performed with good reproducibility in connection to a short (30–60 s) “electrochemical cleaning” period at the final potential (e.g., +0.1 V using mercury electrodes). The potential–time sequence used in ASV, along with the resulting stripping voltammogram, is shown in Figure 1.10. The voltammetric peak reflects the time-dependent concentration

gradient of the metal in the mercury electrode during the potential scan. Peak potentials serve to identify the metals in the sample. The peak current depends on various parameters of the deposition and stripping steps, as well as on the characteristics of the metal ion and the *electrode geometry* (Wang, 2006).

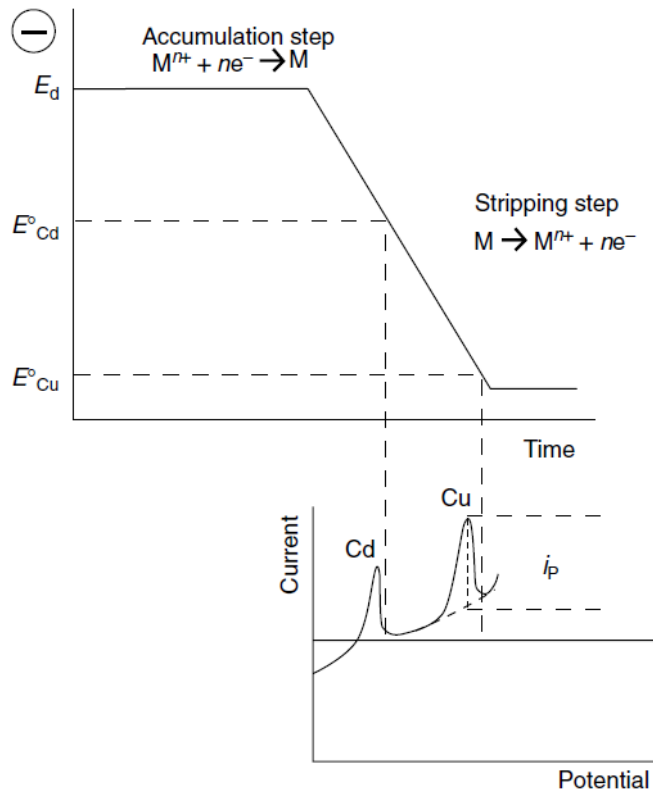


**Figure 1.10.** In ASV the potential–time waveform (top) and along with the resulting voltammogram (bottom) (Wang, 2006).

With more than one metal ion in the sample, the ASV signal may sometimes be complicated by formation of intermetallic compounds, such as ZnCu. This may shift or distort the stripping peaks for the metals of interest. These problems can often be avoided by adjusting the deposition time or by changing the deposition potential (Settle, 1997).

### 1.1.6.2. Cathodic Stripping Voltammetry

CSV can be used to determine substances that form insoluble salts with the mercurous ion. Application of a relatively positive potential to a mercury electrode in a solution containing such substances results in the formation of an

insoluble film on the surface of the mercury electrode. A potential scan in the negative direction will then reduce (strip) the deposited film into solution. This method has been used to determine inorganic anions such as halides, selenide, and sulfide, and oxyanions such as  $\text{MoO}_4^{2-}$  and  $\text{VO}_3^{5-}$ . In addition, many organic compounds, such as nucleic acid bases, also form insoluble mercury salts and may be determined by CSV (Settle, 1997).

### 1.1.6.3. Adsorptive Stripping Voltammetry

AdSV is quite similar to anodic and cathodic stripping methods. The primary difference is that the preconcentration step of the analyte is accomplished by adsorption on the electrode surface or by specific reactions at chemically modified electrodes rather than accumulation by electrolysis. Many organic species have been determined at micromolar and nanomolar concentration levels using AdSV; inorganic species have also been determined. The adsorbed species is quantified by using a voltammetric technique such as DPV or SWV in either the negative or positive direction to give a peak-shaped voltammetric response with amplitude proportional to concentration (Settle, 1997).

### 1.1.6.4. Potentiometric Stripping Analysis

PSA, known also as *stripping potentiometry*, differs from ASV in the method used for stripping the amalgamated metals. In this case, the potentiostatic control is disconnected following the preconcentration, and the concentrated metals are reoxidized by an oxidizing agent [e.g.,  $\text{O}_2$ ,  $\text{Hg(II)}$ ] that is present in the solution:



A stirred solution is used also during the stripping step to facilitate the transport of the oxidant. Alternately, the oxidation can be carried out by passing a constant anodic current through the electrode. During the oxidation step, the variation of the working electrode potential is recorded, and a stripping curve, like the one shown in Figure 1.11a, is obtained. When the oxidation potential of a

given metal is reached, the potential scan is slowed down as the oxidant (or current) is used for its stripping. A sharp potential step thus accompanies the depletion of each metal from the electrode (Wang, 2006).

Modern PSA instruments use microcomputers to register fast stripping events. Such differential display of  $dt/dE$  versus  $E$  is shown in Figure 1.11b. The use of nondeaerated samples represents an important advantage of PSA (over analogous ASV schemes), particularly in field applications. In addition, such potential-time measurements eliminate the need for amplification when microelectrodes are concerned. By obviating the need for stirring or deoxygenating the solution, the coupling of PSA with microelectrodes permits convenient trace analysis of very small samples. PSA is also less susceptible to interfering surfactant effects, and hence can simplify the pretreatment of biological samples (Wang, 2006).

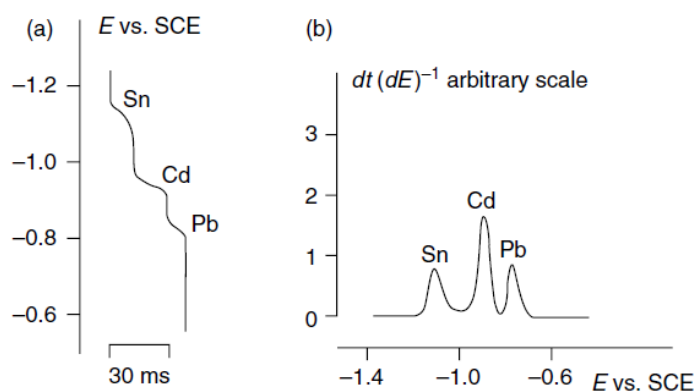


**Figure 1.11.** Stripping potentiograms for a solution containing  $100 \mu\text{g L}^{-1}$  tin, cadmium, and lead, with 80 s accumulation at  $-1.40\text{V}$  (Wang, 2006).

### 1.1.7. Working Electrodes in Voltammetry

The performance of the voltammetric procedure is strongly influenced by the working-electrode material. The working electrode should provide high signal to-noise characteristics, as well as a reproducible response. Thus, its selection depends primarily on two factors: the redox behavior of the target analyte and the background current over the potential region required for the measurement. Other considerations include the potential window, electrical conductivity, surface reproducibility, mechanical properties, cost, availability, and toxicity. A range of

materials have found application as working electrodes for electroanalysis. The most popular are those involving mercury, carbon, or noble metals (particularly platinum and gold). Figure 1.12 displays the accessible potential window of these electrodes in various solutions. The geometry of these electrodes must also be considered (Wang, 2006).

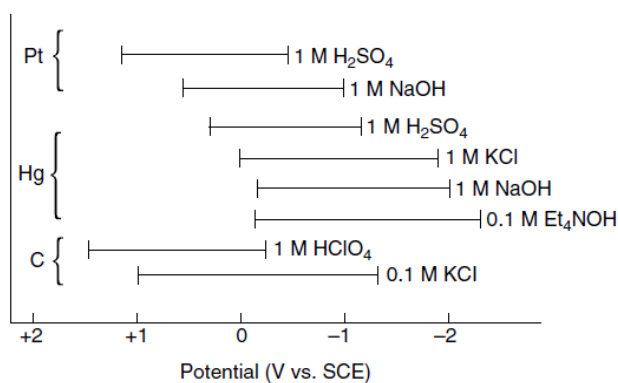


**Figure 1.12.** Accessible potential windows of platinum, mercury, and carbon electrodes in various supporting electrolytes (Wang, 2006).

### 1.1.7.1. Mercury Electrodes

Mercury is a very attractive choice for electrode materials because it has a high hydrogen overvoltage that greatly extends the cathodic potential window (compared to solid electrode materials) and possesses a highly reproducible, readily renewable, and smooth surface. In electrochemical terms, its roughness factor is equal to one (i.e., identical geometric and actual surface areas). Disadvantages of the use of mercury are its limited anodic range (due to the oxidation of mercury) and toxicity.

There are several types of mercury electrodes. Of these, the dropping mercury electrode (DME), the hanging mercury drop electrode (HMDE), and the mercury film electrode (MFE) are frequently used. Related solid amalgam electrodes have been introduced more recently to address concerns related to the toxicity of mercury.

The DME, used in polarography, consists of a 12-20 cm-long glass capillary tubing (with an internal diameter of 30-50 $\mu$ m), connected by a flexible tube to an

elevated reservoir of mercury. The continuous exposure of fresh spherical drops eliminates passivation problems that may occur at stable solid electrodes. More elaborate DMEs, based on a mechanical drop detachment at reproducible time intervals, are used for pulse polarography (Wang, 2006).

The hanging mercury drop electrode is a popular working electrode for stripping analysis and cyclic voltammetry. In this configuration, stationary mercury drops are displaced from a reservoir through a vertical capillary. Early (Kemula-type) HMDE designs rely on a mechanical extrusion (by a micrometer-driven syringe) from a reservoir through a capillary. The mercury reservoir should be completely filled with mercury; air must be fully eliminated. Modern HMDEs employ an electronic control of the drop formation, which offers improved reproducibility and stability. When used in the DME mode, it exhibits a very rapid growth to a given area, which then remains constant (as desired for minimizing charging-current contributions). The performance of HMDEs can be improved by siliconizing the interior bore of the capillary.

The mercury film electrode (MFE), used for stripping analysis or flow amperometry, consists of a very thin (10-100  $\mu\text{m}$ ) layer of mercury covering a conducting and inert support. Because of the adherent oxide films on metal surfaces, and the interaction of metals with mercury, glassy carbon is most often used as a substrate for the MFE. The mercury film formed on a glassy carbon support is actually composed of many droplets. Because they do not have a pure mercury surface, such film electrodes exhibit a lower hydrogen overvoltage and higher background currents. Another useful substrate for the MFE is iridium (because of its very low solubility in mercury and the excellent adherence of the resulting film). Mercury film electrodes are commonly pre-plated by cathodic deposition from a mercuric nitrate solution. An in situ plated MFE is often employed during stripping analysis. This electrode is prepared by simultaneous deposition of the mercury and the measured metals. Most commonly, a disk-shaped carbon electrode is used to support the mercury film. Mercury film ultramicroelectrodes, based on coverage of carbon fiber or carbon microdisk surfaces, have also received a growing attention in recent years (Wang, 2006).



### 1.1.7.2. Solid Electrodes

The limited anodic potential range of mercury electrodes has precluded their utility for monitoring oxidizable compounds. Accordingly, solid electrodes with extended anodic potential windows have attracted considerable analytical interest. Of the many different solid materials that can be used as working electrodes, the most often used is carbon, platinum, and gold. Silver, nickel, and copper can also be used for specific applications (Wang, 2006).

An important factor in using solid electrodes is the dependence of the response on the surface state of the electrode. Accordingly, the use of such electrodes requires precise electrode pretreatment and polishing to obtain reproducible results. The nature of these pretreatment steps depends on the materials involved. Mechanical polishing (to a smooth finish) and potential cycling are commonly used for metal electrodes, while various chemical, electrochemical, or thermal surface procedures are added for activating carbon-based electrodes. Unlike mercury electrodes, solid electrodes present a heterogeneous surface with respect to electrochemical activity. Such surface heterogeneity leads to deviations from the behavior expected for homogeneous surfaces.

Solid electrodes can be stationary or rotating, usually in a planar disk configuration. Other configurations of solid electrodes, including various ultramicroelectrodes and microfabricated screen-printed strips or silicon-based thin-film chips, are attracting increasing attention (Wang, 2006).

#### Carbon Electrodes

Solid electrodes based on carbon are currently in widespread use in electroanalysis, primarily because of their broad potential window, low background current, rich surface chemistry, low cost, chemical inertness, and suitability for various sensing and detection applications. In contrast, electron transfer rates observed at carbon surfaces are often slower than those observed at metal electrodes. Electron transfer reactivity is strongly affected by the origin and

history of the carbon surface. Other factors, besides the surface microstructure, affect the electrochemical reactivity at carbon electrodes. These include the cleanliness of the surface and the presence of surface functional groups. A variety of electrode pretreatment procedures have been proposed to increase the electron transfer rates. The type of carbon, as well as the pretreatment method, thus has a profound effect on the analytical performance. The most popular carbon electrode materials are those involving glassy carbon, carbon paste, carbon fiber, screen-printed carbon strips, carbon films, or other carbon composites (Wang, 2006).

### *Glassy Carbon Electrodes*

Glassy (or “vitreous”) carbon has been very popular because of its excellent mechanical and electrical properties, wide potential window, chemical inertness (solvent resistance), and relatively reproducible performance. The material is prepared by means of a careful controlled heating program of a premodeled polymeric (phenolformaldehyde) resin body in an inert atmosphere. The carbonization process proceeds very slowly over the 300-1200°C temperature range to ensure the elimination of oxygen, nitrogen, and hydrogen. The structure of glassy carbon involves thin, tangled ribbons of cross-linked graphite-like sheets. Because of its high density and small pore size, no impregnating procedure is required. However, surface pretreatment is usually employed to create active and reproducible glassy carbon electrodes (GCE) and to enhance their analytical performance. Such pretreatment is usually achieved by polishing (to a shiny “mirror-like” appearance) with successively smaller alumina particles (down to 0.05  $\mu\text{m}$ ). The electrode should then be rinsed with deionized water before use. Additional activation steps, such as electrochemical, chemical, heat, or laser treatments, have also been used to enhance the performance. The improved electron transfer capability has been attributed to the removal of surface contaminants, exposure of fresh carbon edges, and an increase in the density of surface oxygen groups that act as interfacial surface mediators.

A similar, but yet highly porous, vitreous carbon material, reticulated vitreous carbon (RVC), has found widespread applications for flow analysis and spectroelectrochemistry. RVC is an open-pore (“sponge-like”) material; such a

network combines the electrochemical properties of glassy carbon with many structural and hydrodynamic advantages. These include a very high surface area ( $\sim 66\text{cm}^2\text{cm}^{-3}$  for the 100-ppi grade), 90-97% void volume, and a low resistance to fluid flow (Wang, 2006).

### Carbon Paste Electrodes

Carbon paste electrodes, which use graphite powder mixed with various water-immiscible nonconducting organic binders (pasting liquids), offer an easily renewable and modified surface, low cost, and very low background current contributions. A wide choice of pasting liquids is possible, but practical considerations of low volatility, purity, and economy narrow the choice to a few liquids. These include Nujol (mineral oil), paraffin oil, silicone grease, and bromonaphthalene. The former appears to perform the best. The paste composition strongly affects the electrode reactivity, with the increase in pasting liquid content decreasing the electron transfer rates, as well as the background current contributions. In the absence of pasting liquid, the dry graphite electrode yields very rapid electron transfer rates (approaching those of metallic surfaces). Despite their growing popularity, the exact behavior of carbon paste electrodes is not fully understood. It is possible that some of the electrochemistry observed at these electrodes involves permeation of the pasting liquid layer by the electroactive species (i.e., solvent extraction). Carbon paste represents a convenient matrix for the incorporation of appropriate modifying moieties. The modifier is simply mixed together with the graphite/binder paste (with no need to devise individualized attachment schemes for each modifier). A disadvantage of carbon pastes is the tendency of the organic binder to dissolve in solutions containing an appreciable fraction of organic solvent (Wang, 2006).

### Carbon Fiber Electrodes

The growing interest in ultramicroelectrodes has led to a widespread use of carbon fibers in electroanalysis. Such materials are produced, mainly in the preparation of high-strength composites, by high-temperature pyrolysis of polymer textiles or via catalytic chemical vapor deposition. Different carbon fiber

microstructures are available, depending on the manufacturing process. They can be classified into three broad categories: low-, medium-, and high-modulus types. The latter is most suitable for electrochemical studies because of its well-ordered graphite-like structure and low porosity. Improved electron transfer performance can be achieved by various electrode pretreatments, particularly “mild” and “strong” electrochemical activations, or heat treatment. Most electroanalytical applications rely on fibers of 5-20  $\mu\text{m}$  diameters that provide the desired radial diffusion. Such fibers are typically mounted at the tip of a pulled glass capillary with epoxy adhesive, and are used in cylindrical or disk configurations. Precautions should be taken to avoid contamination of the carbon surface with the epoxy. The main advantage of carbon fiber microelectrodes is their small size (5-30  $\mu\text{m}$  diameters of commercially available fibers) that makes them very attractive for anodic measurements in various microenvironments (Wang, 2006).

### **1.1.7.3. Metal Electrodes**

While a wide choice of noble metals is available, platinum and gold are the most widely used metallic electrodes. Such electrodes offer very favorable electron transfer kinetics and a large anodic potential range. In contrast, the low hydrogen overvoltage at these electrodes limits the cathodic potential window. More severe are the high background currents associated with the formation of surface oxide or adsorbed hydrogen layers. Such films can also strongly alter the kinetics of the electrode reaction, leading to irreproducible data. These difficulties can be addressed with a pulse potential (cleaning–reactivation) cycle, as common in flow amperometry. The surface-layer problem is less severe in nonaqueous media, where noble metals are often an ideal choice. Compared to platinum electrodes, gold ones are more inert, and hence are less prone to the formation of stable oxide films or surface contamination. Gold electrodes are also widely used as substrates for self-assembled organosulfur monolayer or for stripping measurements of trace metals. Other metals, such as copper, nickel, or silver, have been used as electrode materials in connection with specific applications. Bismuth film electrodes (preplated or in situ plated ones) have been shown to be an attractive alternative to mercury films used for stripping voltammetry of trace metals. Alloy electrodes (e.g., platinum–ruthenium, nickel–titanium) are also

being used for addressing adsorption or corrosion effects of one of their components. The bifunctional catalytic mechanism of alloy electrodes (such as Pt-Ru or Pt-Sn ones) has been particularly useful for fuel cell applications (Wang, 2006).

#### **1.1.7.4. Chemically Modified Electrodes**

Chemically modified electrodes (CMEs) represent a modern approach to electrode systems. These electrodes rely on the placement of a reagent onto the surface, to impart the behavior of that reagent to the modified surface. Such deliberate alteration of electrode surfaces can thus meet the needs of many electroanalytical problems, and may form the basis for new analytical applications and different sensing devices. Such surface functionalization of electrodes with molecular reagents has other applications, including energy conversion, electrochemical synthesis, and microelectronic devices (Wang, 2006).

There are different directions by which CMEs can benefit analytical applications. These include acceleration of electron transfer reactions, preferential accumulation, or selective membrane permeation. Such steps can impart higher selectivity, sensitivity, or stability on electrochemical devices. Many other important applications, including electrochromic display devices, controlled release of drugs, electrosynthesis, fuel cells, and corrosion protection, should also benefit from the rational design of electrode surfaces.

One of the most common approaches for incorporating a modifier onto the surface has been coverage with an appropriate polymer film. Polymermodified electrodes are often prepared by casting a solution droplet containing the dissolved polymer onto the surface and allowing the solvent to evaporate, by dip or spin coatings, or via electropolymerization in the presence of the dissolved monomer. The latter method offers precise control of the film thickness (and often the morphology), and is particularly attractive in connection with miniaturized sensor surfaces. Other useful modification schemes include bulk modification of composite carbon materials, covalent (chemical) attachment, sol-gel encapsulation, physical adsorption, and spontaneous chemisorption (Wang, 2006).

## 1.2. Sensitive and Selective Voltammetric Determination of Mercury

A number of papers were devoted to the determination of mercury in different matrixes by voltammetric methods at different solid and modified electrodes. Some of these studies are summarized in Table 1.4. As can be seen here, for Hg(II) analysis generally gold-based working electrodes were preferred. Due to the use of different reference electrodes and different working medium, signals related to Hg(II) ions were observed on different potential values. Generally, it was worked in supporting electrolyte solution containing chloride. Due to the use of stripping techniques quite sensitive results were reached. By using gold microwire electrode and gold nanoparticle modified GCE with ASV methods ultratrace Hg(II) ions ( pM and smaller level) could be determined. Also, it is seen that by using chronopotentiometric stripping analysis method with GCE same detection limits could be attained (Table 1.4).

Gold was found to be the best electrode material for the determination of mercury by especially ASV, with conventional (Ermakov, et al.,2001), film (Okcu et al., 2005; Augelli et al., 2007) and micro (Widmann and Berg, 2005; Salaun and Berg, 2006) electrodes. One reason for the use of gold is its high affinity for mercury, which enhances the preconcentration effect. The main disadvantage of gold electrodes is the well known phenomenon of structural changes of their surface, caused by amalgam formation, and the time-consuming cleaning treatments that are needed to achieve reproducibility (Bonfil et al., 2000).

High sensitivity of stripping techniques results from pre-concentration of the analyte on the small volume of the microelectrode so the accumulation time, for relatively highly concentrated solutions, should be limited for avoiding saturation and the amount of deposited analyte should be kept about 2% of the bulk solution (Monk, 2002). In the case of highly dilute solutions, however, much longer accumulation times and much more deposited analyte can be required to obtain distinguishable signals. In order to attain lower detection limits, alternative ways of accumulation should be searched. Recently, a novel promising method, called centri-voltammetry, that utilized the effect of centrifugal forces was reported for preconcentration of analytes.

**Table 1.4.** Some studies for determinations of mercury using voltammetric techniques with different electrodes.

A: Analyte, WE: working electrode, AE: auxiliary electrode, RE: reference electrode, DPAdSV: differential pulse adsorptive stripping voltammetry, SV: stripping voltammetry, DPASV: differential pulse anodic stripping voltammetry, SWASV: square wave anodic stripping voltammetry, sat.: saturated.

| A   | Electrodes                           |                   |                               | Medium                                 | Methods   | Potential (V)  | Detection limit (M)  |                                 | Ref. |
|---|--------------------------------------|-------------------|-------------------------------|--|---|--|--|---------------------------------|------|
|   | WE                                   | AE                | RE                            |  |   |  |  |                                 |      |
| CH <sub>3</sub> Hg <sup>+</sup><br>Hg(II) | Gold nanoparticle modified<br>GCE    | Glassy<br>carbon  | Ag/AgCl                       | 60 mM HCl                              | ASV   | 0.58   | CH <sub>3</sub> Hg <sup>+</sup><br>0.20 µg L <sup>-1</sup> | Abollino<br>et al.,<br>2009     |      |
| Hg(II)                                    | Gold nanoparticle modified<br>GCE    | Glassy<br>carbon  | Ag/AgCl/<br>KCl (3 M)         | 60 mM HCl                              | ASV   | 0.57   | Hg(II)<br>0.15 ng L <sup>-1</sup>                          | Abollino<br>et al.,<br>2008     |      |
| Hg(II)                                    | Rotating solid gold<br>electrode     | Glassy<br>carbon  | Ag/AgCl                       | diluted HCl                            | ASV   | 0.58   | Hg(II)<br>0.40 µg L <sup>-1</sup>                          | Giacomino<br>et al.,<br>2007    |      |
| Hg(II)                                    | Gold electrode                       | Pt wire           | Ag/AgCl                       | 2.5 mM<br>KCl/KNO <sub>3</sub><br>pH 3 | ASV   | 0.55 (non-chloride-<br>containing medium)<br>0.75 (chloride-<br>containing medium) | Hg(II)   | Watson<br>et al.,<br>1999       |      |
| Hg(II)                                    | Manufactured gold<br>electrode       | Pt spiral<br>foil | Calomel<br>electrode,<br>sat. | 50 mM HCl                              | Chrono-<br>potentiometric<br>stripping analysis | ~ 0.55   | Hg(II)<br>0.30 µg L <sup>-1</sup>                          | Radulescu<br>and Danet,<br>2008 |      |
| Hg(II)                                    | Gold-based screen-printed<br>sensors | Graphite          | Silver                        | 0.1 M HCl                              | SWASV   | ~ 0.40   | Hg(II)<br>0.9 µg L <sup>-1</sup>                           | Meucci<br>et al., 2009          |      |

**Table 1.4.** continued

| A   | Electrodes   |                   |                       | Medium  | Methods                                  | Potential (V) | Detection limit (M)   |  | Ref.                       |
|---|--|-------------------|-----------------------|---|--|---------------|---|--|----------------------------|
|   | WE   | AE                | RE                    |   |  |               |   |  |                            |
| Hg(II)  | Carbon electrodes impregnated with the paraffin and polyethylene | Ag/AgCl, (1M KCl) | Ag/AgCl (1M KCl)      | 0.035 M H <sub>2</sub> SO <sub>4</sub><br>0.002 M KCl | SV                                       |               | Hg(II)  | down to 0.02 μ L <sup>-1</sup>   | Romanenko and Larina, 2005 |
| Hg(II)  | Lectin modified carbon paste electrode                           | Pt                | Ag/AgCl               | 0.1 M NaOH, pH 7                                      | DPAdSV                                   | 0.08          | Hg(II)  | 0.0474 mg L <sup>-1</sup>  | Mojica and Merca, 2005     |
| Hg(II)<br>MeHg <sup>+</sup><br>EtHg <sup>+</sup><br>PhHg <sup>+</sup> | Cu electrode   | Pt                | no noted              | 20 mM sodium tetraborate<br>pH 9.5                    | Amperometric detection                   |               | Hg <sup>2+</sup><br>MeHg <sup>+</sup><br>EtHg <sup>+</sup><br>PhHg <sup>+</sup> | 1.7 μg L <sup>-1</sup><br>2.6 μg L <sup>-1</sup><br>5.1 μg L <sup>-1</sup><br>3.5 μg L <sup>-1</sup> | Kubáň et al., 2007         |
| Hg(II)  | Carbon paste electrode   | Pt wire           | Ag/AgCl/<br>KCl (3 M) | 0.05-0.1M<br>KNO <sub>3</sub><br>pH 2-3               | Linear Scan ASV                          | 0.30          | Hg(II)  | 1.1×10 <sup>-6</sup> M (in the presence of polymer: PEI)   | Osipova et al., 2000       |
| Hg(II)  | GCE  | Pt wire           | Ag/AgCl (3.5 M)       | 0.006 M HCl   | Chrono-potentiometric stripping analysis |               | Hg(II)  | 0.1 ng L <sup>-1</sup>   | Švarc-Gajić et al., 2006   |
| Hg(II)  | Gold film electrode  | Pt                | Ag/AgCl               | 0.1 M HClO <sub>4</sub>                               | SWASV                                    |               | Hg(II)  | 0.04 μg L <sup>-1</sup>  | Wang and Tien, 1994        |



**Table 1.4.** continued

| A      | Electrodes  |                   |  | Medium                                  | Methods          | Potential (V) | Detection limit (M)  | Ref.                     |
|--------|---|-------------------|--|---|------------------|---------------|--|--------------------------|
|        | WE  | AE                | RE   |   |                  |               |  |                          |
| Hg(II) | Tosflex-coated glassy carbon electrode (TCE) or gold disk electrodes                  | Pt coil or Pt net | Ag/AgCl                                      | 0.5 M NaCl<br>0.01 M HCl                | DPASV            | 0.42          | Hg(II)<br>3.35×10 <sup>-10</sup> M (DPASV-Au)<br>3.95×10 <sup>-10</sup> M (DPASV-TCE)                | Ugo et al., 2001         |
| Hg(II) | Gold film electrode   | Pt wire           | Double junction Ag/AgCl/KCl/KNO <sub>3</sub> | 0.1 M HClO <sub>4</sub>                 | DPASV            | 0.58          | Hg(II)<br>0.17 µg L <sup>-1</sup>  | Okçu et al., 2008        |
| Hg(II) | Gold disk electrode   | Pt wire           | Double junction Ag/AgCl                      | 0.1 M HClO <sub>4</sub> /<br>2.5 mM HCl | Osteryoung SWASV |               | Hg(II)<br>22 ng L <sup>-1</sup>  | Wu et al., 1997          |
| Hg(II) | Carbon paste electrodes modified with α- and β-cyclodextrins (CPE <sub>α/β-CD</sub> ) | Graphite bar      | Ag/AgCl                                      | 1 M HClO <sub>4</sub>                   | ASV              | 0.26          | Hg(II)<br>0.42 µM (at CPE)<br>0.09 µM (at CPE <sub>α-CD</sub> )<br>0.05 µM (at CPE <sub>β-CD</sub> ) | Roa-Morales et al., 2005 |
| Hg(II) | Gold microwire electrodes   | Iridium wire      | Double junction Ag/AgCl/KCl (3 M)            | 0.01 M HCl                              | SWASV            | ~ 0.51        | Hg(II)<br>6 pM   | Salaun and Berg, 2006    |

**Table 1.4.** continued

| A      | Electrodes  |               |                    | Medium  | Methods | Potential (V) | Detection limit (M)   | Ref.                        |
|--------|---|---------------|--------------------|---|---------|---------------|---|-----------------------------|
|        | WE  | AE            | RE                 |   |         |               |   |                             |
| Hg(II) | Gold electrode  | Glassy carbon | Ag/AgCl (sat. KCl) | 2 M HClO <sub>4</sub> + 1 M HCl                                     | ASV     | ~ 0.68        | Hg(II) 0.45 µg L <sup>-1</sup>  | Vladimirovna, 2006          |
| Hg(II) | Gold nanoparticles/ carbon nanotubes  | Pt wire       | Ag/AgCl (sat. KCl) | 0.1 M HClO <sub>4</sub>   | DPASV   | 0.63          | Hg(II) 0.06 µg L <sup>-1</sup>  | Xu et al., 2008             |
| Hg(II) | Polythymine oligonucleotide modified gold electrode   | Pt wire       | Ag/AgCl (sat. KCl) | 10 mM HEPES, pH 7.2, 1 M NaClO <sub>4</sub>                         | DPASV   | 0.78          | Hg(II) 60 pM  | Wu et al., 2010             |
| Hg(II) | Carbon paste electrode modified by a natural 2:1 phyllosilicate clay functionalized with either amine or thiol groups | Pt wire       | Ag/AgCl/ KCl (3 M) | 0.1 M NaCl<br>0.01 M HCl  | DPASV   | ~ 0.00        | Hg(II) 8.7×10 <sup>-8</sup> M (the amine-functionalized clays)<br>6.8×10 <sup>-8</sup> M (the thiol-functionalized clays) | Tonle et al., 2005          |
| Hg(II) | Gold electrode  | Pt wire       | Ag/AgCl (sat. KCl) | 0.01 M EDTA-Na <sub>2</sub> + 0.06 M NaCl + 2.0 M HClO <sub>4</sub> | SWASV   | 0.52          | Hg(II) 0.15 µg L <sup>-1</sup>  | Locatelli and Melucci, 2010 |

**Table 1.4.** continued

| A      | Electrodes   |               |  | Medium   | Methods                 | Potential (V) | Detection limit (M)              | Ref.                       |
|--------|--|---------------|--|--|-------------------------|---------------|----------------------------------|----------------------------|
|        | WE   | AE            | RE   |  |                         |               |                                  |                            |
| Hg(II) | Chemically modified GCE  | Pt            | Calomel electrode, sat.                        | 0.01 M NaSCN                                       | DPASV                   | 0.06          | Hg(II) 0.1 $\mu\text{g mL}^{-1}$ | Sousa and Bertazzoli, 1996 |
| Hg(II) | Epoxy-resin impregnated graphite electrode coated with gold                                  | Pt            | Ag/AgCl  | 0.1 M HClO <sub>4</sub> + 0.003 M HCl              | DPASV                   | ~-0.65        | Hg(II) 0.46 ng                   | Korolczuk, 1997            |
| Hg(II) | Gold foil  | Pt wire       | Ag/AgCl  | 2.5 mM KCl/KNO <sub>3</sub> pH 3                   | SV                      | 0.30          |                                  | Watson et al, 1999         |
| Hg(II) | Rotating gold disk electrode   | Pt wire       | Ag/AgCl (1M KCl)                               | 10 mM HNO <sub>3</sub> , 10 mM NaCl                | Subtractive mode of ASV | ~-0.64        | Hg(II) 50 pM                     | Bonfil et al., 2000        |
| Hg(II) | Modified with a gold(III)/pyrrolidine-dithiocarbamate complex thick film graphite electrodes | Glassy carbon | Ag/AgCl/KCl (3 M)                              | 0.1 M H <sub>2</sub> SO <sub>4</sub> + 0.004 M HCl | ASV                     | ~-0.50        | Hg(II) 5 ng L <sup>-1</sup>      | Faller et al, 1999         |
| Hg(II) | 1,3,4-thiadiazole-2,5-dithiol-organo-clay- carbon paste electrode                            | Pt wire       | Ag/AgCl (sat. KCl)                             | 0.05 M KNO <sub>3</sub>                            | DPASV                   | 0.40          | Hg(II) 0.15 $\mu\text{g L}^{-1}$ | Filho and Carmo, 2006      |
| Hg(II) | The calix[4]arene-modified GCE   | Pt wire       | Ag/Ag <sup>+</sup> (0.01 M AgNO <sub>3</sub> ) | 0.1 M H <sub>2</sub> SO <sub>4</sub> + 0.01 M NaCl | SWASV                   | -0.30         | Hg(II) 5 $\mu\text{g L}^{-1}$    | Lu et al., 2003            |

### 1.3. Centri-Voltammetry

Centri-voltammetry provides the combined benefit of centrifugation and voltammetry. The aforementioned technique offers an alternative to instrumental methods, due to a significant reduction in the required equipments costs and offers an inexpensive way of constructing analyzers. The method shows similarity with stripping voltammetric techniques. The significance difference and advantage of this method is that the preconcentrated analyte is not a small portion of the bulk solution as it is the usual case for ASV measurements (Monk, 2002), but a major portion of the analyte is collected onto the electrode surface by centrifugation.

Simple centrifuges are used in chemistry for isolating and separating solid particles from liquid. They vary widely in speed and capacity. They usually comprise a rotor containing two, four, six, or many more numbered wells within which the samples containing centrifuge tips may be placed.

A centrifuge is generally driven by an electric motor that puts an object in rotation around a fixed axis, applying a force perpendicular to the axis. The centrifuge works using the sedimentation principle, where the centripetal acceleration causes more dense substances to separate out along the radial direction (the bottom of the tube).

Since the motion is circular the acceleration can be calculated as the product of the radius and the square of the angular velocity. Traditionally named *relative centrifugal force* (RCF), it is the measurement of the acceleration applied to a sample within a centrifuge and it is measured in units of gravity. It is given by

$$\text{RCF} = \frac{r(2\pi N)^2}{g} \quad (1.16)$$

where  $g$  is earth's gravitational acceleration,  $r$  is the rotational radius,  $N$  is the rotational speed, measured in revolutions per unit of time. When the rotational speed is given in revolutions per minute (rpm) and the rotational radius is expressed in centimeters (cm) the above relationship becomes

$$\text{RCF} = 1.118 \times 10^{-5} r_{\text{cm}} N_{\text{rpm}}^2 \quad (1.17)$$

where  $r_{\text{cm}}$  is the rotational radius measured in centimeters (cm),  $N_{\text{RPM}}$  is rotational speed measured in revolutions per minute (rpm) (Wikipedia, 2010).

The centrifugation step carries out the bulk collection leading to a higher sensitivity. However, time consuming steps such as laborious decantation, filtration and dissolution are eliminated. For this purpose various carrier materials and reducing agents were employed to maintain the selectivity and the sensitivity. The detection limit of centri-voltammetric method under optimal conditions is comparable with those stripping techniques such as ASV. Carefully controlled and optimized experimental conditions were implemented to improve reproducibility of the analysis results.

Centri-voltammetric method was anticipated firstly by Hüseyin Tural. The procedure for the preconcentration via coprecipitation was described. The system was successfully tested using trace amounts of Pb(II) ions in aqueous solution preconcentrated with  $\text{Al}(\text{OH})_3$  as the carrier precipitate and resulting peak currents were found much higher than those without applying centrifugation. The detection limit was found as  $2.2 \times 10^{-9}$  M by Kirgöz et al, (2004).

In the second part of this study Amberlite XAD-7 resin was used as a carrier material for the purpose of preconcentration of Pb(II) ions. The sensitivity of the method was found comparable to that of stripping techniques and the detection limit for lead ions was calculated as  $5.2 \times 10^{-9}$  M with mercury coated gold sphere electrode. The precision of the method depends on the configuration of the working electrode and better reproducibility was obtained with mercury coated plate electrodes (RSD 3.3%,  $n = 6$ ) (Kirgöz, et al., 2005).

In another centri-voltammetric study, mercuric ion was reduced with borohydride to form metallic mercury droplets which were collected on a gold film electrode with the aid of centrifugal force without a carrier material. The calibration graph for mercury(II) has a regression coefficient of 0.9941; its linear

range is from 3.0 pM to 10.0 nM. Due to the effect of accumulation, the detection limit of mercury(II) is as low as 3 pM (Ürkmez 2004 and Ürkmez et al., 2009).

The simultaneous centri-voltammetric analysis of cadmium, lead, and copper ions was investigated in the presence of carrier precipitate,  $\text{Al}(\text{OH})_3$ , on mercury film electrode. The linear concentration ranges were obtained as  $7.0 \times 10^{-8}$  -  $2.0 \times 10^{-6}$  M for lead,  $5.0 \times 10^{-8}$  -  $2.0 \times 10^{-6}$  M for cadmium, and  $2.0 \times 10^{-7}$  -  $3.0 \times 10^{-6}$  M for copper ions (Vardar, 2008).

Cations which can be analyzed with ASV by using mercury electrodes are only those whose metallic forms are resolvable in mercury. Analysis of undetermined types, which can not be detected by ASV because of that they are insoluble in mercury, can be solved by centri-voltammetry as shown by Koçak et al. In this respect, Mo(VI) cation's, complexing ligand's (8-Hydroxyquinoline) presence and absence, calibration graph could be obtained concentration in the range of  $1 \times 10^{-7}$  -  $5 \times 10^{-6}$  M and with pyrogallol red lower detection limit of  $1.4 \times 10^{-8}$  M reached. In addition, the giant polyoxomolybdate (POM) molecule that formed on the electrode surface diffusing from the molybdenum ion and reducing at the electrode surface was observed in chloroacetic acid medium (Koçak et al, 2008, Koçak 2009).

Afterwards, in order to extend the field of application of centri-voltammetric method was studied with a biological molecule. For this purpose terbutaline [1-(3,5-dihydroxyphenyl)-2-(*tert*-butylamino) ethanol] was chosen as a test substance and was measured from  $8.0 \times 10^{-6}$  M to  $3.5 \times 10^{-5}$  M at GC and C-paste electrodes in acetate buffer (pH = 5.7) without using any carrier precipitate or resin (Erdugan et al., 2009).

Considering the previous studies with Centri-voltammetric method in general, analyte was reduced with the help of a reagent or by being absorbed in a carrier precipitate or by exchanging with an ion exchanger resin separated from the solution and with the help of centrifugal forces they were collected on the surface of the electrodes. In this thesis, for Hg(II) ions' more sensitive and reproducible analysis, it was intended that working with a reducing agent and a

carrier material which have never used in the centri-voltammetric method. Sorbents, synthetic ion exchangers, especially ion exchange resins were widely used in separation and enrichment of trace elements, and their analytical applications were researched. There are several monographs dealing with analytical application of ion exchangers (Mizuike, 1983).

#### **1.4. Material for Separation and Preconcentration**

Adsorption process with selected carrier material could be preceded by the following mechanisms:

- Ion-exchange reactions.
- Physical adsorption.
- Molecular sorption of electrolytes.
- Complex formation between the counter ion and functional group.
- Hydrate formation at the surface or in the pores of the adsorbent.

The most common methods for the removal of heavy metals are ion-exchange and chemical precipitation (Abo-Farha et al., 2009).

##### **1.4.1. Ion-Exchange Resins**

An ion exchange resin is an insoluble but permeable synthetic polymer containing ionizable functional groups. Table 1.5 tabulates three types of ion exchange resins most frequently used in inorganic trace analysis. All of these use cross-linked styrene divinylbenzene copolymer as resin base (Figure 1.13). As the degree of crosslinkage, i.e. percentage of divinylbenzene, increases, the wet volume capacity and the resistance to shrinking and swelling increase and the equilibrium rate and the permeability to large molecules decrease. Highly cross-linked resins with relatively small pores in the shape of spherical beads of 50 to 400 meshes (297 to 37  $\mu\text{m}$ ) are most commonly used (Mizuike, 1983).

**Table 1.5.** Most frequently used ion exchange resins (Mizuike, 1983).

| Resin  | Strong-acid cation exchange resin   | Strong-base anion exchange resin   | Chelating resin   |
|--|---|--|---|
| Functional group                                 | Sulfonic acid<br>$-\text{SO}_3^-$   | Quaternary ammonium<br>$-\text{CH}_2\text{N}^+(\text{CH}_3)_3$ or<br>$-\text{CH}_2\text{N}^+(\text{CH})_2(\text{C}_2\text{H}_4\text{OH})$                            | Iminodiacetate<br>$-\text{CH}_2\text{N} \begin{cases} \text{CH}_2\text{COO}^- \\ \text{CH}_2\text{COO}^- \end{cases}$   |
| Exchangeable pH range                            | 0-14  | 0-14   | 6-14  |
| Approximate specific capacity<br>meq/g dry resin | 5   | 3  |   |
| meq/mL resin                                     | 2   | 1  | 0.5   |
| Thermal stability                                | Up to 150°C   | Up to 50°C (OH <sup>-</sup> form) and 150°C (Cl <sup>-</sup> and other forms)  | Up to 75°C  |
| Approximate order of selectivity                 | $\text{Th}^{4+} > \text{Al}^{3+} > \text{Mg}^{2+} > \text{Na}^+$ ;<br>$\text{Ac}^{3+} > \text{La}^{3+} > \text{Y}^{3+} > \text{Sc}^{3+} > \text{Al}^{3+}$ ;<br>$\text{Ra}^{2+} > \text{Ba}^{2+} > \text{Pb}^{2+} > \text{Sr}^{2+} > \text{Ca}^{2+} > \text{Cd}^{2+} \geq \text{Zn}^{2+} \geq \text{Cu}^{2+} \geq \text{Ni}^{2+} \geq \text{Co}^{2+} \geq \text{Mg}^{2+} \geq \text{UO}_2^{2+} \geq \text{Be}^{2+}$ ;<br>$\text{Tl}^+ > \text{Ag}^+ > \text{Cs}^+ > \text{Rb}^+ > \text{NH}_4^+ \approx \text{K}^+ > \text{Na}^+ > \text{H}^+ > \text{Li}^+$ | $\text{I}^- > \text{HSO}_4^- > \text{ClO}_3^- > \text{NO}_3^- > \text{Br}^- > \text{CN}^- > \text{HSO}_3^- > \text{NO}_2^- > \text{Cl}^- > \text{OH}^- > \text{F}^-$ | $\text{Cu}^{2+} > \text{Pb}^{2+} > \text{Fe}^{3+} > \text{Al}^{3+} > \text{Cr}^{3+} > \text{Ni}^{2+} > \text{Zn}^{2+} > \text{Ag}^+ > \text{Co}^{2+} > \text{Cd}^{2+} > \text{Fe}^{2+} > \text{Mn}^{2+} > \text{Ba}^{2+} > \text{Ca}^{2+} > \text{Na}^+ > \text{K}^+$ |
| Inorganic impurities (µg/g in purified resins)   | Fe<1, Cu<0.8, Ni<0.05, Pb<0.2, Al<15, Total ash<500   | Fe<0.5, Cu<0.2, Ni<0.05, Pb<0.005, Al<5, Total ash<600   |   |
| Trade names                                      | Dowex 50 and 50W; AG 50 and 50W; Amberlite IR-120, CG-120; ZeoKarb 225; Diaion SK   | Dowex 1, Dowex 2; AG 1, AG 2; Amberlite IRA-400, CG-400, IRA-410; Diaion SA  | Dowex A-1; Chelex 100   |



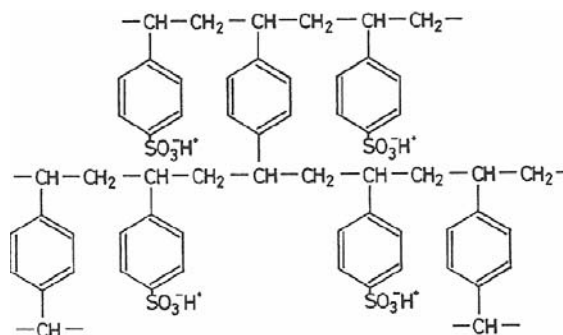


**Figure 1.13.** Strong acid cation exchange resin (Mizuike, 1983).

Careful washing (conditioning) of commercial resins (except for purified ones) before use, with acids, alkalies, complexing agents, water and organic solvents, is very important to remove inorganic and organic impurities resulting from the manufacturing process. Also, it must be kept in mind that, resins are sometimes decomposed in contact with solutions and cause contamination problems; for example, decomposition products from strong-base anion exchange resins interfere with the *polarographic determination* of trace metals.

There are other types of ion exchange resins having different resin bases and ionizable functional groups from those described above, though their analytical applications are limited. Those commercially available include moderately strong-acid cation exchange resins (cross-linked polystyrene with  $-\text{PO}(\text{OH})_2$  groups), weak-acid cation exchange resins (polymerized acrylic acid with  $-\text{COOH}$  groups), weak-base anion exchange resins (cross-linked polystyrene with  $-\text{CH}_2\text{NH}(\text{CH}_3)_2\text{OH}$  and  $-\text{CH}_2\text{NH}_2\text{CH}_3\text{OH}$  groups), and ion exchange resins having both acidic and basic groups (ion-retardation or snake-cage resin, linear polyacrylic acid with  $-\text{COOH}$  groups, trapped in cross-linked polystyrene with  $-\text{CH}_2\text{N}(\text{CH}_3)_3\text{Cl}$  groups). Resins with the various functional groups are useful in inorganic trace analysis and removal of some metal ions (Table 1.6).

Previously studies related to some selective resin for mercury were reviewed because the scope of this thesis is mercury analysis and application to spring waters. Table 1.7 lists some chelate resins that are reported to have a high selectivity for *mercury*; the table includes the order of selectivity. Some studies of ion exchange treatment for mercury in drinking water are presented in Table 1.8.

**Table 1.6.** Selected resins used for separation and/or preconcentration of metal ions.

| Resin  | Functional Groups                 | Metals   | Medium  | Sample                   | Detection Technique | Concentration Range ( $\mu\text{g L}^{-1}$ )               | Ref.                       |
|--|-----------------------------------|--|---|--------------------------|---------------------|--|----------------------------|
| Purolite C100, a cation exchange resin           | Sulfonic acid (-SO <sub>3</sub> ) | Ce <sup>4+</sup> , Fe <sup>3+</sup> , Pb <sup>2+</sup> | Water   | Aqueous systems          | Batch sorption      | 0.00265 - 0.265  | Abo-Farha et al., 2009     |
| Amberlite XAD-7, a chelating resin               |                                   | Pb <sup>2+</sup>                                       | 0.02 M NH <sub>4</sub> CH <sub>3</sub> COOH, pH 6.8 | -                        | Centri-voltammetry  | $5.0 \times 10^{-9}$ - $1.0 \times 10^{-9}$ M<br>1.0 - 0.2 | Kirgöz et al., 2005        |
| Amberlite IRA-400, an anion-exchange resin       | Chloride form                     | Hg <sup>2+</sup>                                       | HOAc/ NaOAc buffer, pH 6.5                          | Natural water            | CV-AAS              | 5 - 100  | Hernandez et al., 1991     |
| Dowex XZS-1, a cationic ion exchanger            | (-SO <sub>3</sub> H)              | Hg <sup>2+</sup>                                       | -   | Mine waste water streams | Ion exchange        | 0.005 - 0.1  | Monteagudo and Ortiz, 2000 |
| Glycidyl methacrylate-based cross-linked polymer | Amide                             | Hg <sup>2+</sup>                                       | Nonbuffered conditions                              | -                        | Batch sorption      | -  | Şenkal and Yavuz, 2006     |

**Table 1.6.** continued

| <b>Resin</b>  | <b>Functional Groups</b>   | <b>Metals</b>                       | <b>Medium</b>                       | <b>Sample</b> | <b>Detection Technique</b> | <b>Concentration Range</b> | <b>Ref.</b>              |
|---|--|-------------------------------------|-------------------------------------|---------------|----------------------------|----------------------------|--------------------------|
| Duolite GT-73,<br>a chelating resin   | Thiol (S-H)  | Hg <sup>2+</sup>                    | pH 7                                | -             | Batch sorption             | 0.010 – 0.28               | Chiarle et al., 2000     |
| Lewatit TP 207,<br>Lewatit TP 260,<br>Purolite S-930,<br>Purolite S-940,<br>Purolite S-950,<br>anion exchangers and<br>chelating ion exchangers | iminodiacetate for<br>Lewatit TP207,<br>Purolite S-930<br><br>aminomethyl-<br>phosphonate for<br>Lewatit TP260,<br>Purolite S-940,<br>Purolite S-950 | Cu <sup>2+</sup> , Zn <sup>2+</sup> | Baypure DS 100,<br>complexing agent | -             | Batch sorption             | -                          | Kołodzyńska et al., 2008 |
| Dithizone sulfonic acid,<br>Azothiopyrine-sulfonic<br>acid (ATPS), anion-<br>exchange resin   | ATPS: mercapto<br>and azo  | Hg <sup>2+</sup>                    | 0.5 M NaOH,                         | Waste water   | Ion exchange               | -                          | Tanaka et al., 1987      |

**Table 1.5.** Summary of mercury-selective chelate resins (EPA, 1997).

| Resin             | Order of Selectivity   |
|-------------------|--|
| Duolite ES-466    | Hg <sup>2+</sup> >Cu <sup>2+</sup> >Fe <sup>2+</sup> >Ni <sup>2+</sup> >Pb <sup>2+</sup> >Mn <sup>2+</sup> >Ca <sup>2+</sup> >Mg <sup>2+</sup> >Na <sup>+</sup>  |
| Dowex A-1         | Cu <sup>2+</sup> >Hg <sup>2+</sup> >Ni <sup>2+</sup> >Pb <sup>2+</sup> >Zn <sup>2+</sup> >Co <sup>2+</sup> >Cd <sup>2+</sup> >Fe <sup>2+</sup> >Mn <sup>2+</sup> >Ca <sup>2+</sup> >Na <sup>+</sup>  |
| Nisso Alm-525     | Hg <sup>2+</sup> >Cd <sup>2+</sup> >Zn <sup>2+</sup> >Pb <sup>2+</sup> >Cu <sup>2+</sup> >Ag <sup>+</sup> >Cr <sup>3+</sup> >Ni <sup>2+</sup>  |
| Diaion CR-10      | Hg <sup>2+</sup> >Cu <sup>2+</sup> >Pb <sup>2+</sup> >Ni <sup>2+</sup> >Cd <sup>2+</sup> >Zn <sup>2+</sup> >Co <sup>2+</sup> >Mn <sup>2+</sup> >Ca <sup>2+</sup> >Mg <sup>2+</sup> >Ba <sup>2+</sup> >Sr <sup>2+</sup> >>Na <sup>+</sup>   |
| Amberlite IRC-718 | Hg <sup>2+</sup> >Cu <sup>2+</sup> >Pb <sup>2+</sup> >Ni <sup>2+</sup> >Zn <sup>2+</sup> >Cd <sup>2+</sup> >Co <sup>2+</sup> >Fe <sup>2+</sup> >Mn <sup>2+</sup> >Ca <sup>2+</sup>   |
| Unicellex UR-10   | Hg <sup>2+</sup> >Cu <sup>2+</sup> >Fe <sup>3+</sup> >Al <sup>3+</sup> >Fe <sup>2+</sup> >Ni <sup>2+</sup> >Pb <sup>2+</sup> >Cr <sup>3+</sup> >Zn <sup>2+</sup> >Cd <sup>2+</sup> >Ag <sup>2+</sup> >Mn <sup>2+</sup> ><br>Ca <sup>2+</sup> >Mg <sup>2+</sup> >>Na <sup>+</sup> |
| Sirorez-Cu        | pH>5, Cu <sup>2+</sup> ; pH>0, Hg <sup>2+</sup>  |
| Sumichelate Q-10  | HgCl <sub>2</sub> >AuCl <sub>4</sub> <sup>-</sup> >Ag <sup>+</sup> >Cr <sub>2</sub> O <sub>7</sub> <sup>2-</sup>   |

**Table 1.6.** Ion exchange treatment for mercury in drinking water (EPA, 1997).

| Ion Exchange Resin | Resin Type                  | Mercury Concentration (µg L <sup>-1</sup> ) |        | Additional Treatment    | Other Conditions |
|--------------------|-----------------------------|---|--------|-------------------------|------------------|
|                    |                             | Initial                                     | Final  |                         |                  |
| Ionac SR-4         | Weak acid chelating resin   | 14.88                                       | 0.43   | Prefiltration           | GW, FS           |
| Purolite s-920     | Hg-specific chelating resin | 10.67                                       | 0.34   | Prefiltration           | GW, FS           |
| AFP-329            | Weak base anion             | 12.21                                       | 0.44   | Prefiltration           | GW, FS           |
| ASB-2              | Strong base anion resin     | 14.31                                       | 0.70   | Prefiltration           | GW, FS           |
| Duolite GT-73      | Weak acid cation thiol      | 200-70.000                                  | 1-5    | 0.2 µm prefilter        | DFW, FS          |
| Amberlite IRC 718  | Iminodiacetic acid resin    | 11,800                                      | 15-35  | None                    | SW, BS           |
| IRC 718 and GT 73  | (See above)                 | 14,000                                      | 15-200 | GT 73 used as polishing | SMW, BS          |

GW Ground water; FS Full scale; DFW Defense facility wastewater; SW Synthetic wastewater; BS Bench scale; SMW Smelter wastewater.

### 1.4.2. Purolite C100 as a Carrier Material

Purolite C100 is a high capacity, premium grade bead form conventional gel polystyrene sulphonate cation exchange resin designed to be used in industrial or household water conditioning equipment. The physical and chemical properties of Purolite C100 and the standard operating conditions are shown in Table 1.9. It removes the hardening ions, e.g. calcium and magnesium, and it replaces them with sodium ions. When the resin bed becomes exhausted and the hardening ions begin to break down, the capacity is restored by regeneration with common salt (Purolite Company, 2009).

The capacity depends largely on the amount of salt used in the regeneration. Purolite C100 is also capable of removing dissolved iron, manganese, and suspended matter by virtue of the filtering action of the bed.

**Table 1.7.** The physical and chemical properties of Purolite C100 and the standard operating conditions (Purolite Company, 2009).

| Typical Physical & Chemical Characteristics    |  |
|--|--|
| Polymer Matrix Structure                       | Crosslinked Polystyrene Divinylbenzene |
| Physical Form and Appearance                   | Clear spherical beads                  |
| Whole Bead Count                               | 90% min.                               |
| Functional Groups                              | R-SO <sub>3</sub> <sup>-</sup>         |
| Ionic Form, as shipped                         | Na <sup>+</sup>                        |
| Shipping Weight (approx.)                      | 850 g/l (53 lb/ft <sup>3</sup> )       |
| Screen Size Range:                             |  |
| - British Standard Screen                      | 14 - 52 mesh, wet                      |
| - U.S. Standard Screen                         | 16 - 50 mesh, wet                      |
| Particle Size Range                            | +1.2 mm <5%, -0.3 mm <1%               |
| Moisture Retention, Na <sup>+</sup> form       | 44 - 48%                               |
| Swelling                                       |  |
| Na <sup>+</sup> → H <sup>+</sup>               | 5% max.                                |
| Ca <sup>++</sup> → Na <sup>+</sup>             | 5% max.                                |
| Specific Gravity, moist Na <sup>+</sup> Form   | 1.29                                   |
| Total Exchange Capacity, Na <sup>+</sup> form, |  |
| wet, volumetric                                | 2.0 eq/l min.                          |
| dry, weight                                    | 4.5 eq/kg min.                         |
| Operating Temperature, Na <sup>+</sup> Form    | 150°C (300°F) max.                     |
| pH Range, Stability                            | 0 - 14                                 |
| pH Range Operating, Na <sup>+</sup> cycle      | 6 - 10                                 |

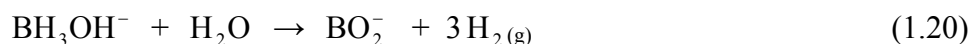
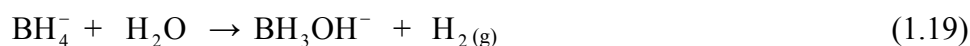
| Standard Operating Conditions<br>(Co-current Regeneration) |   |   |              |   |
|--|---|---|--------------|---|
| Operation  | Rate  | Solution                                    | Minutes      | Amount                                    |
| Service  | 8 - 40 BV/h<br>1.0 - 5.0 gpm/ft <sup>3</sup>  | Influent water                              | - per design | - per design                              |
| Backwash   | 7 - 12 m/h<br>3.0-5.0 gpm/ft <sup>2</sup>     | Influent water<br>5°- 30° C<br>(40° -80° F) | 5 - 20       | 1.5 - 4 BV<br>10 - 20 gal/ft <sup>3</sup> |
| Regeneration   | 2 - 7 BV/h<br>0.25 - 0.90 gpm/ft <sup>3</sup> | 8 - 20% NaCl                                | 15 - 60      | 60 - 320 g/l<br>4 -10 lb/ft <sup>3</sup>  |
| Rinse, (slow)  | 2 - 7 BV/h<br>0.25 - 0.90 gpm/ft <sup>3</sup> | Influent water                              | 30 approx.   | 2 - 4 BV<br>15 - 30 gal/ft <sup>3</sup>   |
| Rinse, (fast)  | 8 - 40 BV/h<br>1.0 - 5.0 gpm/ft <sup>3</sup>  | Influent water                              | 30 approx.   | 3 - 10 BV<br>24 - 45 gal/ft <sup>3</sup>  |
| Backwash Expansion 50% to 75%                              |   |   |              |   |
| Design Rising Space 100%                                   |   |   |              |   |
| "Gallons" refer to U.S. Gallon = 3.785 litres              |   |   |              |   |

Purolite C100 is insoluble in dilute or moderately concentrated acids, alkalines, and in all common solvents. However, exposure to significant amounts of free chlorine, hypochlorite ions, or other strong oxidizing agents over long periods of time will eventually break down the cross-linking. This will tend to increase the moisture retention of the resin, decreasing its mechanical strength, as well as generating small amounts of extractable breakdown products. The resin is thermally stable to 150°C in the sodium form and to 120°C in the hydrogen form.

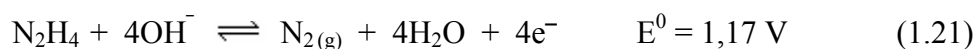
### 1.5. Aim and Scope of Thesis

In this PhD thesis, the main purpose is to develop a sensitive and selective analytical procedure which implied the enrichment and separation procedures for the determination of ultratrace amounts of inorganic mercury. Centri-voltammetric method that is consisted of the combination of voltammetric methods with separation techniques, such as coprecipitation, centrifugation, will be adapted to determination of mercury. For this purpose, by selecting a reducing agent and a carrier material which have not been used in a centri-voltammetric method before, developing methods are going to be validated and spring water samples have been applied. The studies with selected reducing agent (Chapter I) and carrier material (Chapter II) will be presented in two sections.

In Chapter I, the determination of Hg(II) ions was carried out via the aid of centri-voltammetric method. In the initial stage, mercury ions are first reduced to metallic mercury with a reducing agent *without any carrier material*. Then, they are collected by a centrifugal force on the gold film electrode surface. In these applications, reliable results are depended upon mainly on the performance of mercury reduction reaction and the reproducible preconcentration step. The reducing agents such as hydrazine (N<sub>2</sub>H<sub>4</sub>.H<sub>2</sub>O) are selected for reduction of mercury(II) ions. This reaction has known since 1930 (Willard and Boldyreff, 1930). Our previous experiments NaBH<sub>4</sub> reaction was considered (Ürkmez et al., 2009) (Eq. 1.18). It was used as solid due to the hydrolysis reactions of NaBH<sub>4</sub> in water (Eq. 1.19 and 1.20) (Chen and Lim, 2002).



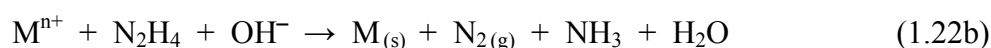
Hydrazine is also a powerful strong reductant widely used in various chemical reduction reactions of heavy metal ions to metallic form. An important half reaction involving hydrazine is:



It can effectively be employed in reduction of various metal cations (M<sup>m+</sup>) to the elemental state (M<sup>0</sup>) according to the following reaction:



Based on the discussion by Tobe and Burgess, metal ions can also be reduced:



Hydrazine can react with dissolved oxygen in water according to Audrieth and Ogg,



It can undergo self-oxidation and reduction in both alkaline and acidic solutions.



As one can see from the above reactions, most of metals can be easily reduced by using this powerful reductant. Since metal cations are immediately reduced to metallic state, there is very limited amount of metal ions present in the solution. Complexation between metal and ammonia (due to Eq. 1.22b and 1.24) therefore unlikely occurs. By using air stripping, ammonia molecules easily removed from the solution. In addition, unutilized hydrazine can be removed by aeration (Eq. 1.23). These properties of hydrazine make it attractive in the electrochemical studies (Chen and Lim, 2002).

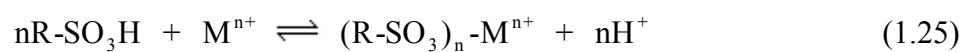
In this chapter, owing to the higher molecular weight of metallic mercury droplets was collected on GFE surface by a centrifugation without the aid of carrier materials. By this means, the particles that reach the surface, by creating amalgam with gold, were pre-concentrated.

Afterwards, we have anticipated achieving better results due to higher molecular weight of mercury ions coupled with the increased capacity of the preconcentration utilizing carrier material. It was aimed to apply and compare the centri-voltammetric method with others via interaction between the Hg(II) ions and the appropriate carrier material and without the reduction of the aforementioned ions in Chapter II. In this step of our study, Purolite C100 and Lewatit Monoplus TP 214 were selected as cation exchanger and chelating resin, respectively.

Purolite C100 of which properties and applications were explained in section 1.4.2 is a simple, fast and economic means for separating of heavy metals. Hydrogen ions in sulfonic group ( $\text{SO}_3\text{H}^-$ ) of the resin can serve as exchangeable



ions with metal cations. The sorption reactions were consistent with the following ion exchange process (Abo-Farha et al., 2009):



In this chapter centri-voltammetric method was applied with Lewatit Monoplus TP 214 that was specifically selective and Purolite C100 that was non selective as a carrier materials for mercury ions. In literature, any reported studies related to Hg(II) together with Purolite C100 could not be found so it was thought to be appropriate for the novelty.

## 2. MATERIALS AND METHODS

### 2.1. Apparatus

Voltammetric measurements in differential pulse (DP) mode were carried out with a Metrohm 693 Voltammetric Analyzer (VA) processor and a 694 VA Stand consisted of the three-electrode system (Figure 2.1). The auxiliary and reference electrodes were a platinum wire of large area and a miniature home made Ag/AgCl (saturated KCl) (Hassel et al, 1999), respectively. Gold film characteristics were investigated with cyclic voltammograms of gold film electrode (GFE) that were recorded by using a Palm Sens PSLite v1.7 model.



**Figure 2.1.** Metrohm 693 Voltammetric Analyzer (VA) processor and a 694 VA Stand with its own cell.

The working electrode was a bare glassy carbon (GCE) and a GFE which were prepared prior to each measurement of GCE support. In the studies of Chapter I and II of the thesis, a GCE supplied by Metrohm and a home made GCE, prepared from a glassy rod (diameter  $2.0 \pm 0.1$  mm), were used, respectively. This rod V10 Grade 10x2mm was supplied by SPI Supplies Division of Structure Probe, USA.

Suitable measuring cells for the purpose were used during voltammetric studies. In section I of study, the gold film electrode was prepared in Metrohm 693 VA system's own voltammetric cell (Figure 2.1). "A centrifugal cell" was used to reduce the mercury (II) ions and for collection of metallic mercury droplets on the electrode surface by a centrifugation process (Figure 2.2). Reoxidation of mercury in amalgam, following the aforementioned procedure,

was once again achieved in the voltammetric cell of the Metrohm 693 VA system. However in section II of study, the interaction of mercury (II) ions with the carrier material, collection of the carrier material enriched with mercury(II) ions, on the GCE surface via centrifugation and the voltammetric measurements were achieved in a single cell named the “centri-voltammetric cell” (Figure 2.3).

The “centrifugal cell”, made of Teflon and with an approximate volume of 5 mL, was also used as the reaction vessel. Its weight was about 75 g including the solution and the electrode (Figure 2.2). The working electrode was placed in the cell facing upward to collect the metallic mercury formed in the cell effectively.

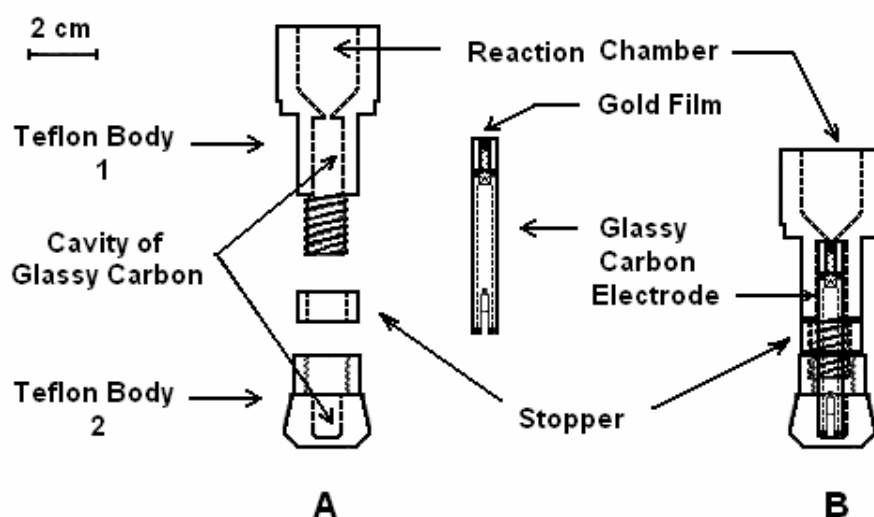


**Figure 2.2.** The designed centrifugal cell, A) centrifugal cell (dismounted)  
B) GCE placed and mounted in centrifugal cell facing upward.

New cell designed for Chapter II with a volume of approximately 50 mL was different from the “centrifugal cell”, used in Chapter I studies. This cell was made of Plexiglass with two separate parts: plexiglass body1 and plexiglass body2. Body 1, the solution section, was used by being mounted on to body 2, which contained the home made working electrode (Figure 2.3).

The large volume of cell was made possible to construct due to the small length of home made working electrode.

All of the procedures, preconcentration and voltammetric measurements, were able to be carried out in the same cell. Additionally, bare GCE was used as a working electrode, while eliminating the step of gold film formation. The sensitivity was thought to increase as a result of reduced number of processes.

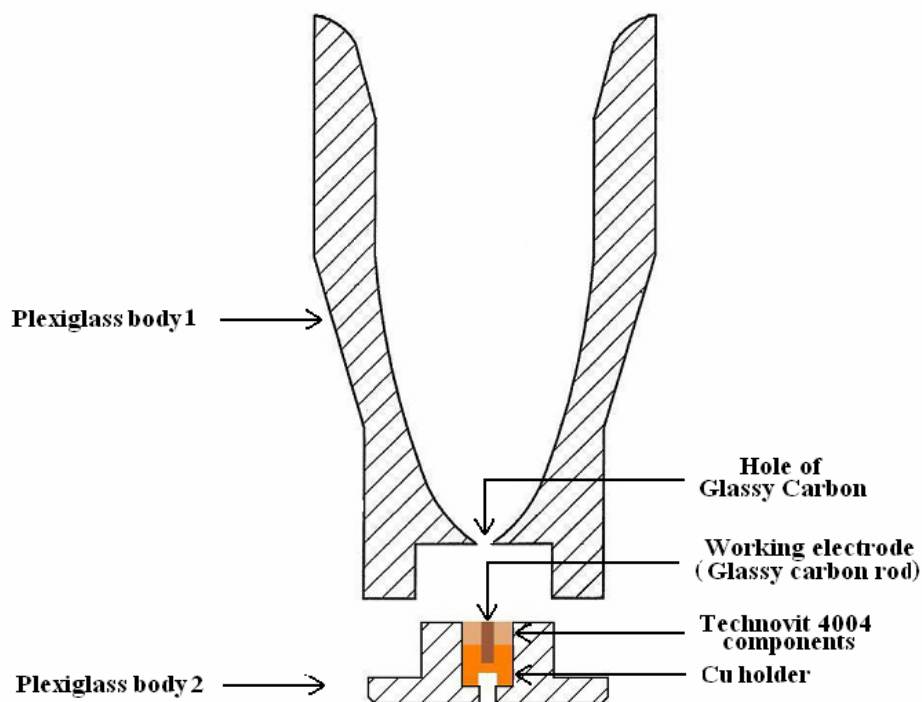


**Figure 2.3.** The designed centri-voltammetric cell and home-made working electrode.

pH values of solutions were measured by using Thermo Orion 3 Star with a combined glass electrode. Nüve NF 800 was used for centrifugation. An ELMA Transsonic 460/H ultrasonic bath was used for sonication.

The spectroscopic measurements of Hg(II), Pb(II), Cd(II) and Cu(II) cations were performed using the Perkin Elmer Optima 2100 DV Inductively Coupled Plasma Optical Emission Spectrometer (ICP-OES). For Hg(II) measurement ICP-OES was equipped with continuous flow hydride generator system (Perkin Elmer, Inc. Shelton, CT, USA). The Agilent Technologies 7700 Series Inductively Coupled Plasma Mass Spectrometer (ICP-MS) combined with ASX-500 was used for accuracy test (Figure 2.4).

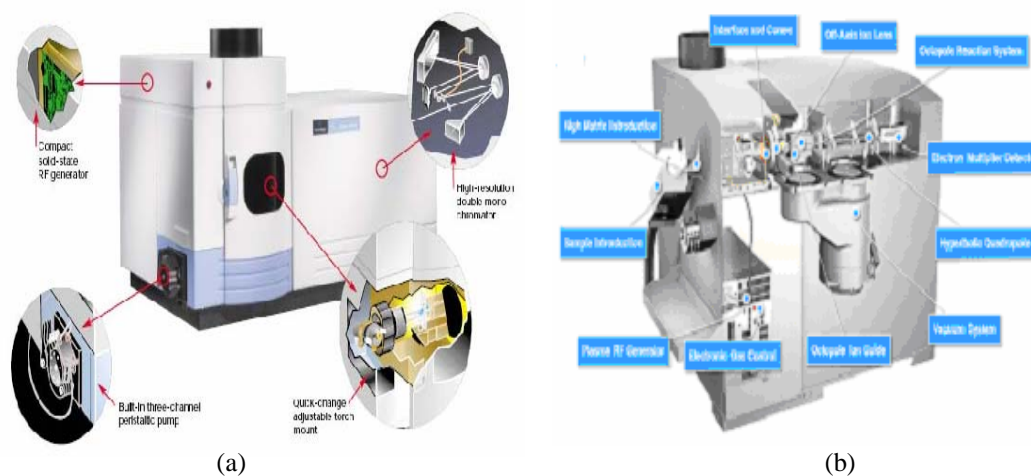


**Figure 2.4.** (a) Perkin Elmer Optima 2100 DV ICP-OES (New Mexico State University, 2010), (b) The Agilent Technologies 7700 Series ICP-MS (Agilent Technologies, 2010).

## 2.2. Chemicals and Solutions

Among the used chemicals;  $\text{HNO}_3$  (65%,  $1.39 \text{ g mL}^{-1}$ ),  $\text{HClO}_4$  (60%,  $1.53 \text{ g mL}^{-1}$ ),  $\text{NaOH}$  (99%),  $\text{KSCN}$  and  $\text{NaBH}_4$  (GR for analysis) were supplied from Germany (Merck).  $\text{N}_2\text{H}_4 \cdot \text{H}_2\text{O}$  was at 98% purity and supplied from Germany (Cat. 22,581-9, Aldrich).  $\text{HCl}$  (30%,  $1.15 \text{ g mL}^{-1}$ ) was suprapur grade (Merck). Metallic mercury (Cat. 26,101-7, Aldrich) was at 99.99% purity. High purity water obtained from Milli-Q (Millipure) apparatus was used throughout the study.

Purolite C100 was supplied by Purolite Company. Lewatit Monoplus TP 214 was obtained from the representative (ÖkoteK Company) of the Bayer Company, in Turkey.

A stock solution of  $\text{Hg}$  (II) was prepared by adding 1.50 mL concentrated (14.4 M)  $\text{HNO}_3$  solution into 1.3299 g pure metallic mercury to give the ratio of 1:4 for  $\text{Hg}/\text{H}^+$  in moles. The mixture was carefully heated until it was completely dry. Nitric oxide fumes were observed. The residue was dissolved gradually by adding 2.0 mL of  $\text{HClO}_4$  solution on a hot plate followed by the dilution of the mixture to 250.0 mL with ultra pure water. The concentration of this stock

solution (pH 1.96) was determined to be  $2.65 \times 10^{-2}$  M by potentiometric titration with a standard KSCN solution. Standard solutions of Hg (II) with lower concentrations were prepared daily by further dilution of the stock solution and the solutions were acidified by adding HClO<sub>4</sub> to achieve the previous acidic ratio.

A stock solution of Au(III) of 1000 ppm was prepared by dissolving 0.1 g pure metallic gold in 1.0 mL of the mixture of HNO<sub>3</sub> and HCl at ratio 1: 4 (v:v) and heating it until the nitric oxide gasses were removed from the mixture. The mixture was then diluted to 100 mL deionized with water.

The standard solutions of Cu(II), Cd(II) and Pb(II) ions of 1000 ppm were prepared as explaining in below and the working solutions with lower concentrations were prepared daily by further dilution of them via transfer with a digital adjustable Transferring pipette, (Brand 20-200  $\mu$ L, cat. No: 7041 78).

Stock solution of Cu(II) ions was prepared by dissolving 0.2500 g pure metallic copper (Merck, electrolytic powder) in 1.45 mL of HNO<sub>3</sub> solution (1:1) and by adding 0.40 mL concentrated HCl into this mixture. Then it was diluted to 0.25 L.

Stock solution of Cd(II) ions was prepared by dissolving 0,2500 g metallic cadmium into 1.20 mL mixture acid solution containing 5.0 mL of HCl solution (1:1) and 125  $\mu$ L concentrated HNO<sub>3</sub> solution. Then, it was diluted to 0.25 L.

Stock solution of Pb(II) ions was prepared by adding 175  $\mu$ L of concentrated HNO<sub>3</sub> solution into 0.3996 g Pb(NO<sub>3</sub>)<sub>2</sub> (Carlo Erba). This solution was diluted to 0.25 L.

Stock solutions of Fe(III) ion was prepared by dissolving FeCl<sub>3</sub>.6H<sub>2</sub>O salt (99%, Merck) in 2 M HCl as to be  $1.48 \times 10^{-3}$  M Fe(III) in  $10^{-2}$  M HCl.

Mercury Standard Solution of 1000  $\mu$ g L<sup>-1</sup> (water with the dilute nitric acid, HNO<sub>3</sub> 2%) with high purity standard grade (Lot: 0923220; Cat: 100033-1) were used for ICP-OES and ICP-MS measurements.

### 2.3. Procedure

All glassware was kept in a  $\text{HNO}_3$  solution bath (1/10 v/v) and rinsed with deionized water prior to use. Voltammetric measurements were performed at ambient conditions and voltammetric cell contents were kept under the nitrogen atmosphere during the measurements.

The steps of applied procedure were explained below. In order to see the effects of impurities, blank experiments were exercised through this study however their results were not included due to absence of significant levels of impurities.

The thesis study was conducted mainly in two parts in order to accomplish the objective, as described in the introduction section. In section I, the  $\text{Hg(II)}$  ions were reduced with hydrazine which was different from our previous study (Ürkmez et al, 2004, 2009). The formed metallic mercury, collected on the electrode surface with the help of centrifugal forces, was reoxidized via potential scanning and the voltammograms obtained during this process were evaluated. In section II of the study, the mercury ions were enriched directly on a carrier material without reduction reaction of the mercury ions. For that purpose, two different ion exchange resins, one of which was selective to mercury and other one was not were selected. The enriched resin was collected on the surface of the electrode with the aid of centrifugal forces, after interaction the resin and the mercury(II) ions, and then the voltammograms were recorded by potential scanning in suitable intervals.

In both sections, the impact of the effective parameters were investigated in intervals, as large as possible, in order to determine the optimum conditions and the calibration graphs were generated under such conditions. The content of  $\text{Hg(II)}$  was tried to be determined in natural water samples by examining the interfering effect of  $\text{Cu(II)}$ ,  $\text{Cd(II)}$ , and  $\text{Pb(II)}$  ions to the centri-voltammetric mercury analysis.

## **2.3.1. Procedure in Chapter I**

### **2.3.1.1. Preparation of Gold Film Electrode**

GFE was prepared by means of electrochemical deposition of Au(III) ions on the rotating bare GCE as a first step. The GCE surface was first polished with  $\text{Al}_2\text{O}_3$  on a polishing cloth and rinsed with water. Following the sonication step in water for 2 minutes, the electrode was placed in the voltammetric cell containing  $2.5 \times 10^{-5}$  M Au (III) ions and 0.5 M  $\text{HClO}_4$  (total volume 20mL). Then the electrochemical cleaning procedure was initiated by cycling the potential 100 times at the potential range of  $-600$  to  $800$  mV vs. Ag/AgCl. The gold film was prepared by depositing the metallic gold from Au (III) ions in the solution by three successive electrolysis steps at  $-500$  mV vs. Ag/AgCl for 300 s as total. A stirring rate of 1600 rpm was used in the deposition period. The conditioning step of 10 cycles was repeated between deposition periods to remove any deposited metallic impurities. Finally, the formed gold film was held at 0 V vs. Ag/AgCl for 120 s to ensure the stability of the film (Appendix 1). New gold film was plated before each measurement.

### **2.3.1.2. Reduction and Preconcentration of Mercury(II) Ions**

Electrochemically prepared GFE was tightly placed in the Teflon body 1 of the centrifugal cell (Figure 2.4). Then the stopper was placed between body 1 and body 2. Finally, body 1, the stopper and body 2 were screwed together. Here, the stopper serves to adjust the length of the cavity to the height of the electrode in the centrifugal cell. If not stated otherwise, an aliquot (5 mL) of the “reaction mixture” containing  $1.0 \times 10^{-9}$  M Hg(II) and 1.0 M  $\text{HClO}_4$  was placed in the reaction chamber of the cell. Then concentrated reducing agent (hydrazine,  $\text{N}_2\text{H}_4 \cdot \text{H}_2\text{O}$ ) was finally added into the reaction chamber (Figure 2.4). This mixture was stirred for 30 s and centrifuged to collect the formed metallic mercury on the surface of GFE. Hereby, the preconcentration step was achieved by means of centrifugal forces and was produced an amalgam at electrode surface. The high solubility of mercury in gold also helps to increase the preconcentration effect.



Since the reaction between hydrazine and Hg(II) is fast, it was considered to have no issues in terms of reaction kinetics (Chen and Lim, 2002).

### **2.3.1.3. Anodic Stripping of Mercury in the Amalgam**

The GFE was then transferred into the voltammetric cell of VA stand containing the “stripping solution” of 1.0 M HClO<sub>4</sub> and 0.35 M HCl (unless otherwise was noted). This solution was deaerated with nitrogen for 300 s prior to the measurement. The potential was scanned in positive direction in the range of 200 to 750 mV vs. Ag/AgCl in quiescent solution. The anodic stripping peaks resulting from the re-oxidation of mercury were recorded by differential-pulse voltammetry with pulse amplitude of 50 mV, pulse duration of 0.6 s and scan rate of 10 mVs<sup>-1</sup>. These resulting peak currents were utilized for analytical purposes.

## **2.3.2. Procedure in Chapter II**

### **2.3.2.1. Pretreatment Applied to Purolite C100 Resin**

Purolite C100 was dried for 12 hours at 50°C. It was then homogenized by grounding and mixing with a mixer. Ground resin particles were sieved by using a 45 µm sieve. Particles of 45 µm or smaller in size were used to preconcentrate Hg(II) ions as sorbent and carrier material.

It's known that resins need to hold in water for a whole day to allow them to expand in volume (to swell) to improve the productivity of ion transfer mechanisms in classical application of resins. But, in centri-voltammetric use, reduction of density due to swelling has reduced the effectiveness of centrifugal forces significantly, thus the resulting peak currents related to mercury ions were not obtained. Therefore, Purolite C100 was not allowed to swell, but it was studied by holding it at the selected adsorption durations.

### 2.3.2.2. Preparation of Home-made Working Electrode

A copper holder was built to house the glassy carbon rod tightly. This holder was placed in its Plexiglass cavity body 2, as shown in Figure 2.3, following the placement of GC rod in it. Thereafter, the entire electrode with the exception of its copper holder was filled with a mixture that was prepared with Technovit 4004 components supplied from the company named Kulzer. The surface of this mixture was sanded upon freezing and it was polished along with the electrolyte surface. In addition, GCE surface was first polished with  $\text{Al}_2\text{O}_3$  on a piece of velvet and rinsed with water. Following the sonication step in water for 2 minutes, the electrode was placed in the centri-voltammetric cell and it was conditioned by holding it at 650 mV vs. Ag/AgCl for 600 seconds.

### 2.3.2.3. Sorption and Centri-voltammetric Procedure for Mercury(II) Ions

The solution containing Hg(II) was placed in a beaker and the pH was adjusted to the study level with 0.1 M NaOH and 0.1 M  $\text{HClO}_4$  to be total volume 20 mL. 6.0 mg of resin was added to the mixture and it was deaerated with nitrogen gasses while it was stirred for 20 minutes.

The mixture was transferred to a centri-voltammetric cell at the end of 20 minutes and it was centrifuged for 10 minutes at 3000 rpm (unless indicated otherwise). The cell was carefully placed in the voltammetric stand and the reference and auxiliary electrodes were immersed into the mixture solution. After adding 1 mL of concentrated  $\text{HClO}_4$  to this solution, potential was scanned from -1000 mV to 800 mV vs. Ag/AgCl with a rate of  $10 \text{ mVs}^{-1}$  DP mode. Pulse amplitude and duration were 50 mV and 40 ms, respectively (Appendix 2). The resulting peak currents related to the mercury ions were recorded.

### **3. RESULTS AND DISCUSSION**

It was obvious that voltammograms which would be obtained from planned studies of this thesis, would be related to the type of used working electrode, its position, applied pretreatment process, surface property during the experiment, and the features of the solution which it was dip into. Because of this, used GCE and GFE in various medium and by applying different pretreatment procedures to them were examined in terms of their responses. Afterwards, the studies which were intended to be developed ultratrace Hg(II) analysis methods have been started. Investigation of the effective parameters in these methods and determination of the optimal experimental conditions were presented in Chapter I and II. Finally, the preferred method's; that is to say, in terms of sensitivity, selectivity, and ease of application being more advantageous method's, application to natural water samples and comparison with a current method were carried out.

#### **3.1. Preliminary Investigations for Working Electrodes**

##### **3.1.1. Activation of Glassy Carbon Electrode**

Different pretreatments for preparing and activating the glassy carbon electrode surface for electrochemical measurements have been widely discussed in literature (Engstrom, 1982, Dai and Shui, 1996). In the light of this discussion procedure described below has been applied.

Firstly, GCE was polished with  $\text{Al}_2\text{O}_3$  for 5 minutes and rinsed with water and cleaned ultrasonically in mixture (1:1) of ethanol and water for 3 minutes. The cleaned electrode was placed in voltammetric stand and the +1.5 V positive potential (DC mode) was applied for 10 minutes in 0.1 M  $\text{HClO}_4$  electrolyte solution. Then, the negative potential of -2.0 V (DC mode) was applied to the electrode for 30 seconds in the same solution and electrode was scanned in the potential range of -2.0 V to +1.0 V in CV mode 5 cycles at 50 mV/s. The obtained voltammograms (CVs) were shown in Figure 3.1. Besides that surface alteration was shown clearly that there had been problems about deposition of gold film on

the surface of GCE which were activated by this way. Although the parameters like Au(III) concentration, deposition potential and deposition time were same, gold film surfaces which had been obtained from the previous studies could not be formed. This situation could be detected even with the naked eye. Therefore, the activation method which we had used on our previous studies had not create problems, was applied (Ürkmez et al., 2009). Before its first use as a support to gold film (Chapter I) and a bare electrode (Chapter II) +0.65 V positive potential was applied to this electrode for 5 minutes. In addition, after each gold film formation, this film was held at 0 V for 120 s in the same Au(III) solution to ensure the stability of the film (Ürkmez et al., 2009 ).

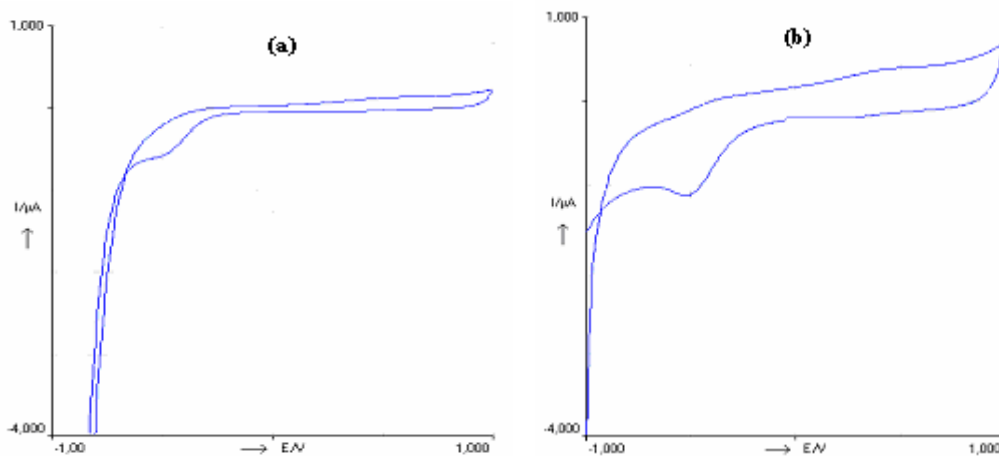


**Figure 3.1.** CVs for the GCE (a) before and (b) after activation procedure in 0.1 M HClO<sub>4</sub> solution at 50 mV/s.

### 3.1.2. Behavior of Gold Film Electrode

The main disadvantage of gold electrodes is the well known phenomenon of structural changes of their surface, caused by amalgam formation, and the time-consuming cleaning treatments that are needed to achieve reproducibility (Bonfil, et al, 2000). For these reasons, investigation of GFE behavior is necessary and important.

After pretreatment which was applied to GCE, formed and conditioned GFE's voltammetric behavior depend on film thickness was investigated by changing only the concentration of Au(III) solution. In mentioned centri-

voltammetric study, Hg(II) ions was reduced with borohydride and formed metallic mercury droplets were determined by preconcentrating with centrifugal forces on electrode surface. It was observed that peak related to mercury at thicker gold film had split and observed peak current had been decreased (Ürkmez, 2004). In present studies depositing potential ( $E_{\text{dep}}$ ) and time ( $t_{\text{dep}}$ ) parameters which have affects on film thickness and morphology were investigated with the use of borohydride, with the aim of completing the deficiency.

The effect of deposition time on the gold film surface deposited at -400 mV was investigated and the obtained voltammograms were given Figure 3.2. The same effects were evaluated for the Hg(II) peak current (Figure 3.3). The highest peak current at this deposition potential (Figure 3.3b) was obtained with a deposition time of 150 s (3 times), but this deposition time caused an increase on the baseline (Figure 3.4 and 3.2). In that in terms of sensitivity lower surface current would be preferred for 100 second (3 times) deposition would be more proper.

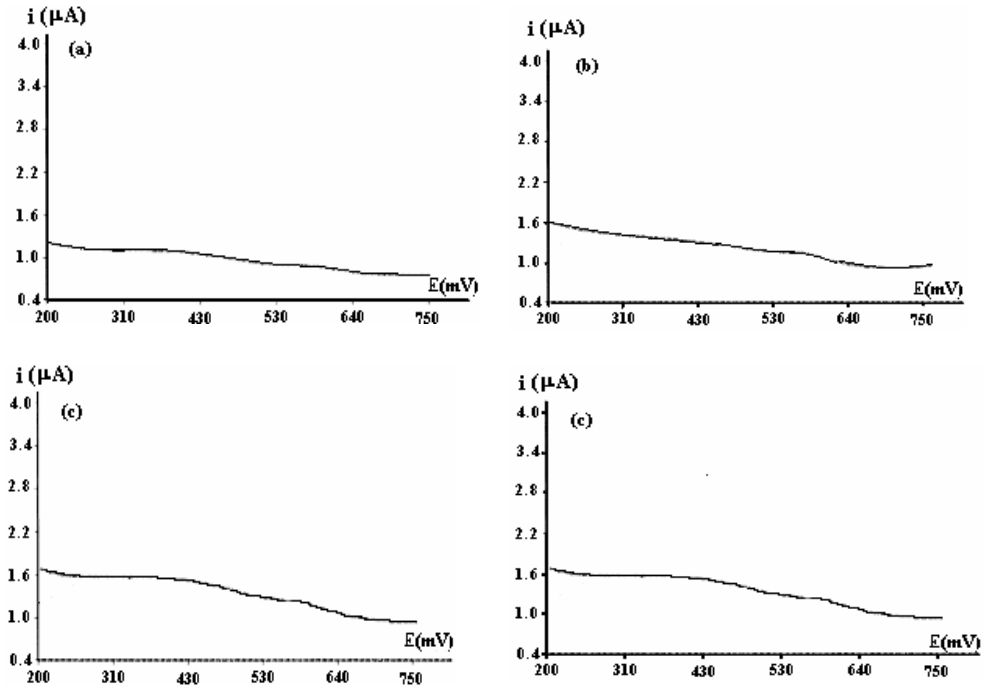


**Figure 3.2.** DP voltammograms of GFE in 1.0 M HClO<sub>4</sub> stripping solution in different deposition times. Conditions of formation GFE:  $2.5 \times 10^{-5}$  M Au<sup>3+</sup>, 0.5 M HClO<sub>4</sub>,  $E_{\text{dep}}$ : -400 mV and  $t_{\text{dep}}$  (a) 100, (b) 150, (c) 200, and (d) 300 s.

However, it was concluded that in order to film thickness could be reached the level which they had on the 150th minute; deposition potential should be shifted towards negative values such as -500 mV (Figure 3.5). Peaks related to Hg(II) (Figure 3.8) which was obtained with formed GFE in this conditions giving lower surface were formed almost at the same size. These results were shown that formed films in both conditions were identical. GFE was prepared by depositing Au(III) ions at -500 mV during 100 s three times in further studies (Appendix 1).

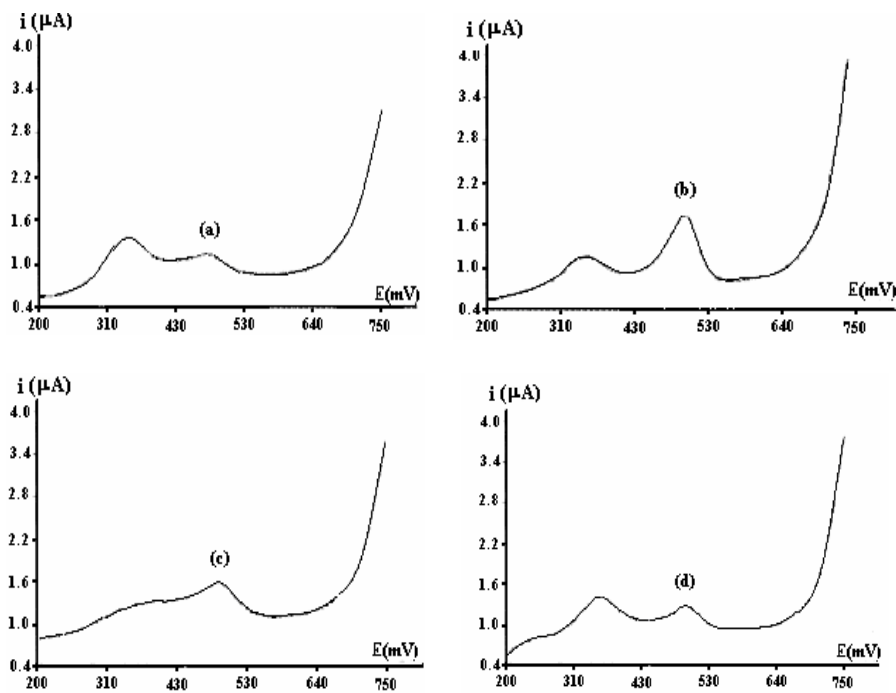


**Figure 3.3.** Effect of deposition time of GFE on mercury peak current. Hg(II) concentration:  $1.0 \times 10^{-9}$  M, Experimental conditions;  $m_{BH}$ : 90 mg,  $t_{cent}$ : 5 min,  $v_{cent}$ : 3000 rpm, stripping solution content: 1.0 M HClO<sub>4</sub> and 0.35 M HCl. Conditions of formation GFE:  $2.5 \times 10^{-5}$  M Au<sup>3+</sup>, 0.5 M HClO<sub>4</sub>,  $E_{dep}$ : -400 mV and  $t_{dep}$  (a) 100, (b) 150, (c) 200, and (d) 300 s.

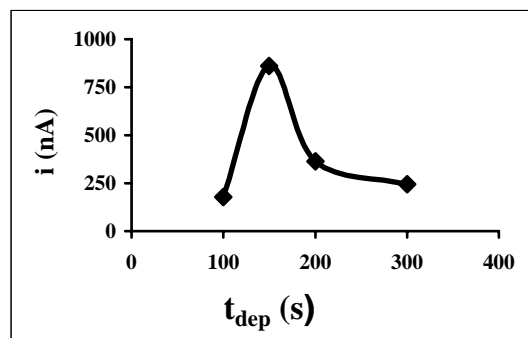


**Figure 3.4.** Effect of deposition time of GFE ( $E_{dep}$ : -400 mV) on mercury peak current which are observed at about 0.5 V.

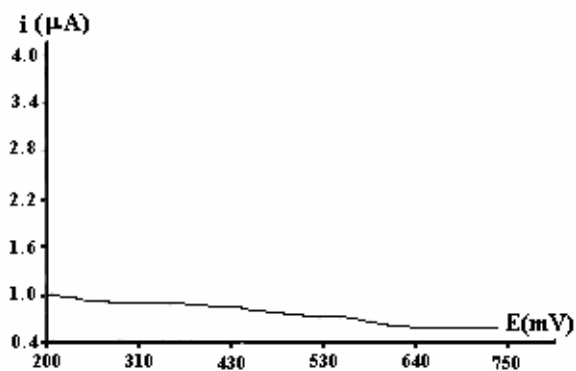


**Figure 3.5.** DP voltammogram of GFE in 1.0 M HClO<sub>4</sub> stripping solution. Conditions of formation GFE:  $2.5 \times 10^{-5}$  M Au<sup>3+</sup>, 0.5 M HClO<sub>4</sub>,  $E_{\text{dep}}$  and  $t_{\text{dep}}$  -500 mV and 100 s, respectively.

Behavior of GFE was tested in different supporting electrolytes at freshly prepared electrode. In this context, some halides which can complex with Hg(II) and some acids were selected and, studied in the solution of the following combinations;

- a) 0.1 M HClO<sub>4</sub> + 0.05M KI
- b) 0.1 M HClO<sub>4</sub> + 0.05 M KSCN
- c) 1.0 M HClO<sub>4</sub> + 0.35 M HCl
- d) 1.0 M HClO<sub>4</sub>
- e) 0.01 M HNO<sub>3</sub>
- f) 0.1M HCl

The composition of the stripping solution was effected baseline signal of GFE (Figure 3.6). In the presence of iodide and thiocyanate, signals shown on the voltammograms (Figure 3.6a and b) had prohibitive property (interfering effect) about measurement of the mercury. In the presence of chloride GFE's potential range of work has narrowed (Figure 3.6c and f). However, this narrowing was not at the level to prohibit the observation of the mercury signals. As stripping of gold, the stripping peak of mercury was also shifted to less positive potentials (Okçu et al., 2005). It was seen that baseline was appropriate on the recorded voltammograms in other stripping solutions (d, e) (Figure 3.6d and e). However, in the presence of chloride ions, which can create complex but can not interfere with Hg(II) ions, reoxidation of the mercury from amalgam which on the

electrode surface occurred easily. Based on this results being appropriate with the literatures (Okçu et al., 2005; Giacomino et al., 2007), supporting electrolytes including 1.0 M HClO<sub>4</sub> and 0.35 M HCl were decided to be used.

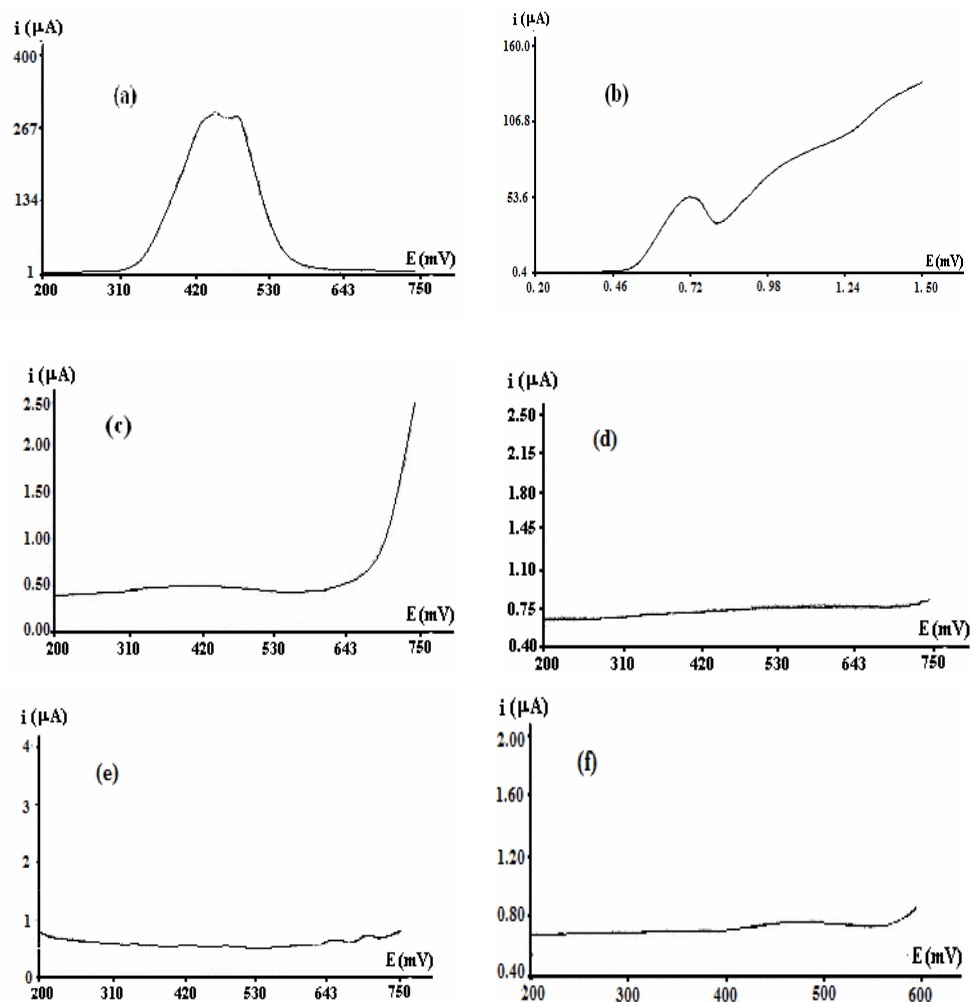


**Figure 3.6.** DP voltammograms of GFE in (a) 0.1 M HClO<sub>4</sub> + 0.05 M KI, (b) 0.1 M HClO<sub>4</sub> + 0.05 M KSCN, (c) 1.0 M HClO<sub>4</sub> + 0.35 M HCl, (d) 1.0 M HClO<sub>4</sub>, (e) 0.01 M HNO<sub>3</sub>, (f) 0.1 M HCl, stripping solution.

Behavior of the films formed by oxygen containing Au(III) solutions or not were compared. In the presence of oxygen film formation led to a slight rise on the surface. To carry out the slipping operation in the presence of oxygen or absence of oxygen has not changed the results. This result being appropriate with the literature, Korolczuk and Rutyna had worked with undeaerated solutions for anodic stripping voltammetry and methyl mercury determination (Korolczuk and Rutyna, 2008).



The high sensitivity determination of the gold thin film electrode can be ascribed to that the surface of the electrode was covered with nanometer sized gold particles. This result in the increase of the surface area thus increases the redox active sites on the surface of the electrode. The CV voltammogram and the SEM images of the gold thin film electrode were shown in Figure 3.7. The results indicate that the surface of the electrode was covered with gold nanoparticles. These particles have dimensions ranging from 20-50 nm.

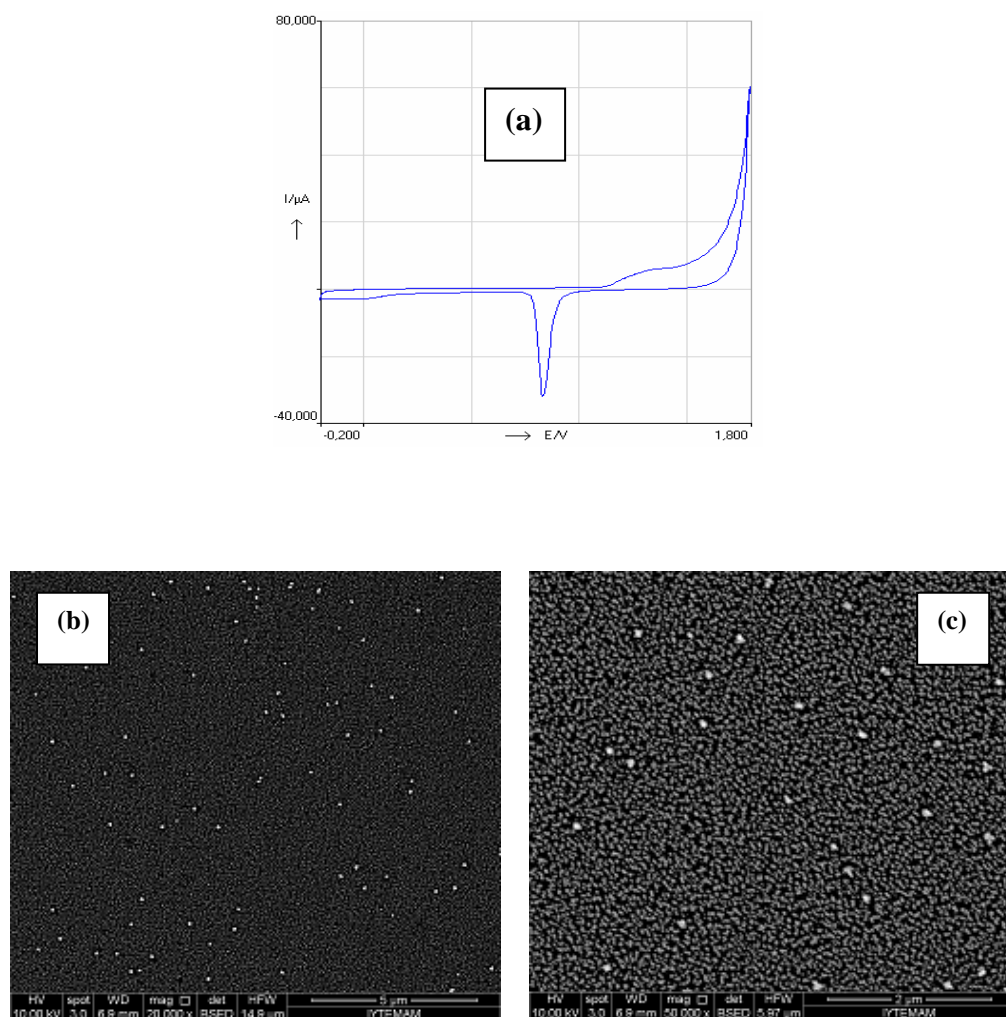


**Figure 3.7.** (a) Cyclic voltammogram for the gold film electrode in 0.1 M HClO<sub>4</sub> solution at 50 mV/s and SEM images of GFE electrochemically deposited on a GCE magnified by (b) 20000 and (c) 50000 times.

## 3.2. CHAPTER I

### **Centri-Voltammetric Determination of Mercury(II) Using Hydrazine as a Reducing Agent**

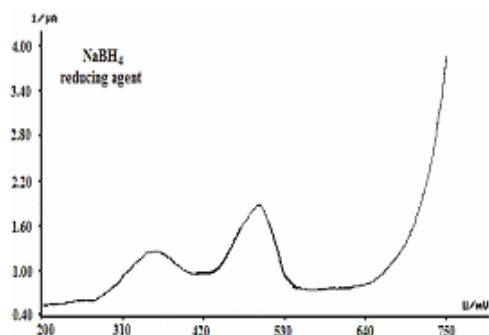
In order to obtain at the optimum conditions for mercury determination, two aspects should be considered: the electrode preparation and the detection. As to the electrode aspect, principle factors consist of the performance of deposition of gold on glassy carbon surface in terms of uniformity and reproducibility of electrode surface (Section 3.1). As to the detection aspect, the governing factors consist of the parameters preconcentration and stripping steps such as, kinds and amounts of reducing agent, pH of reduction reaction medium, centrifugation speed and time, kinds of stripping solution.

#### **3.2.1. Effect of Reducing Agent on Centri-voltammetric Mercury Determination**

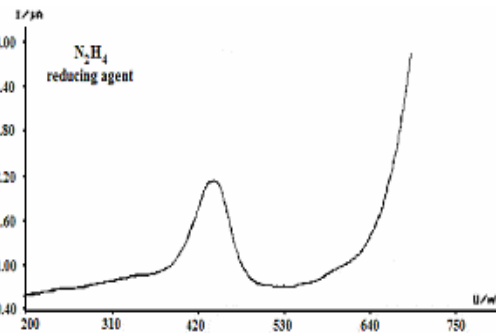
In this section of the study the performance of hydrazine as a reducing agent for mercury reduction reaction was investigated and the obtained results were compared with that of  $\text{NaBH}_4$  that was used as a reducing agent in the previously reported method (Ürkmez et al., 2009). For a healthy comparison of both methods, they were applied in their optimum conditions in solutions containing the same amount of  $\text{Hg(II)}$ .

The voltammograms obtained for  $1.0 \times 10^{-9}$  M  $\text{Hg(II)}$  solutions were presented on the Figure 3.8 and Figure 3.9. Experimental conditions (pH, amount of  $\text{NaBH}_4$  ( $m_{\text{BH}}$ ),  $\text{N}_2\text{H}_4$  concentration ( $C_{\text{hyd}}$ ), centrifugation time ( $t_{\text{cent}}$ ), centrifugation speed ( $v_{\text{cent}}$ ), stripping solution content) were specified on the Figure. On Figure 3.8, the peaks of reoxidation of the metallic mercury after the reduction with  $\text{NaBH}_4$  were observed at the potential of 335 mV (395 nA) and 494 mV (824 nA). On Figure 3.9, the single peak, after the reduction with hydrazine, was observed at 487 mV (963 nA). When  $\text{NaBH}_4$  was used, signal related to mercury was split, and the use of hydrazine has highly removed this splitting. The considered peak for

determination of Hg(II) was nearby +0.5 V. When the reduction reaction of mercury(II) was occurred with hydrazine the obtained reoxidation peak current increased according to reduction with NaBH<sub>4</sub>.

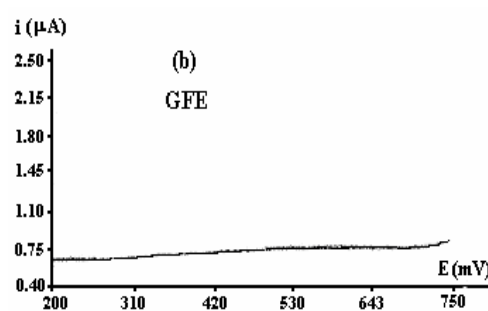
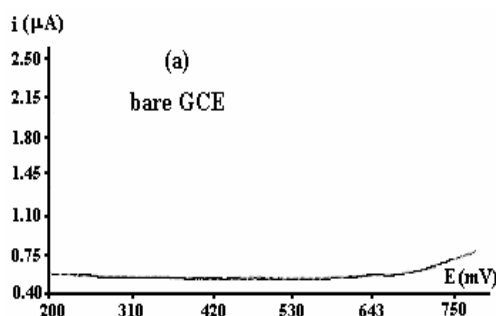


**Figure 3.8.** The obtained voltammogram for  $1.0 \times 10^{-9}$  M Hg(II) by using NaBH<sub>4</sub>. Experimental conditions: **pH<1**, **m<sub>BH</sub>**: 90 mg, **t<sub>cent</sub>**: 5 min, **v<sub>cent</sub>**: 3000 rpm, stripping solution content: 1.0 M HClO<sub>4</sub> and 0.35 M HCl.



**Figure 3.9.** The obtained voltammogram for  $1.0 \times 10^{-9}$  M Hg(II) by using N<sub>2</sub>H<sub>4</sub>. Experimental conditions: **pH<1**, **C<sub>hyd</sub>**: 0.07 M, **t<sub>cent</sub>**: 7 min, **v<sub>cent</sub>**: 3000 rpm, stripping solution content: 1.0 M HClO<sub>4</sub> and 0.35 M HCl

In order to be sure about that during the reduction of Hg(II) ions with hydrazine if there has an effect on gold film or not, blank studies were carried out and the obtained voltammograms were given in Figure 3.10. As shown from Figure 3.10, when hydrazine concentration was 0.1 M, background current was quite high at pH 5, however background current was decreased at pH<1 in the same hydrazine concentration. While the concentration of hydrazine was decreasing, baseline current continued to reduce. These results clearly show that baseline current value changes related to pH value of the reaction medium and, hydrazine concentration and also these parameters should be optimized for Hg(II) analysis. In addition, when c and d voltammograms, which were obtained for the same hydrazine concentration, was compared on Figure 3.10, it was understood that pH is a more effective factor.



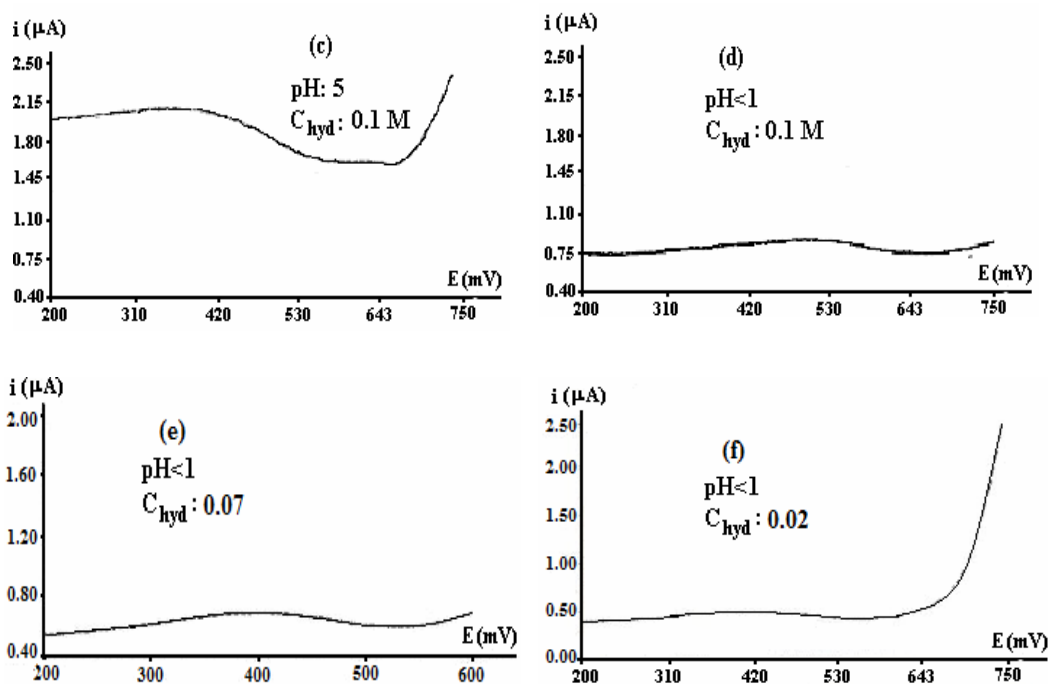


**Figure 3.10.** Voltammograms for **a**) bare GCE, **b**) GFE (Conditions of its formation:  $2.5 \times 10^{-5}$  M  $\text{Au}^{3+}$ , 0.5 M  $\text{HClO}_4$ ) background current in 0.1 M  $\text{HClO}_4$  + 0.35 M  $\text{HCl}$ , **(c, d, e, f)** The voltammograms of the blank study for hydrazine in different concentration and pH of reaction medium. Experimental conditions:  $v_{\text{cent}}$ : 3000 rpm,  $t_{\text{cent}}$ : 7 min, stripping solution content: 1.0 M  $\text{HClO}_4$ , 0.35 M  $\text{HCl}$ .

### 3.2.2. Effect of pH on Mercury Reduction with Hydrazine

In order to increase the mercury reoxidation peak current, the pH effect on the reduction reaction of mercury ions with hydrazine should be evaluated. The dependence of the peak currents at initial pH of the reduction medium was studied. When the initial pH was changed from 2.0 to 9.0 by using 0.01 M  $\text{NaOH}$  and 0.01 M  $\text{HClO}_4$  solutions two peaks (peak 1 and peak 2) were observed in the all recorded voltammograms (not shown). Their potentials were at about 0.35 V (peak 1) and 0.50 V (peak 2). The peak currents at about 0.35 V and 0.50 V were reached maximum values at about pH 4 and 5, respectively (Table 3.1). However, regular increasing or decreasing could not be monitored at the interchange of the first and second peak currents at this pH range.

**Table 3.1.** The effect of pH on mercury reduction reaction with hydrazine.  $\text{Hg(II)}$  concentration:  $5.0 \times 10^{-9}$  M,  $C_{\text{hdy}}$ : 0.1M,  $v_{\text{cent}}$ : 3000 rpm,  $t_{\text{cent}}$ : 7 min, stripping solution content: 1.0 M  $\text{HClO}_4$  and 0.35 M  $\text{HCl}$ .

| pH  | Peak 1       |                | Peak 2       |               |
|-----|--------------|----------------|--------------|---------------|
|     | Current (nA) | Potential (mV) | Current (nA) | Potential(mV) |
| 2.0 | 374          | 381            | 106          | 462           |
| 3.0 | -            | -              | 788          | 497           |
| 4.2 | <b>1470</b>  | 346            | 506          | 490           |
| 5.1 | 803          | 352            | <b>1300</b>  | 483           |
| 6.0 | 384          | 347            | 303          | 472           |
| 7.2 | 111          | 335            | 259          | 453           |
| 9.0 | 100          | 355            | 256          | 494           |

The presence of double peaks are not well suited for analysis and taking into account that results of blank studies done for hydrazine, it was decided that studies should be done at lower pH values. When the same procedure was repeated with the use of  $1.0 \times 10^{-9}$  M Hg(II) solution, peak about 0.35 V on 1 and lower than 1 pH values converted to an indistinct shoulder and it extremely decreased. It was shown on Figure 3.11, Table 3.2 that even it can not be measured. Another point as important as single peak formation is that when  $\text{pH} < 1$  peak current around 0.5 V was not high enough for even  $1.0 \times 10^{-9}$  M Hg(II) solution. Moreover potential of this peak was appropriate with peak 2 potential which were shown on higher pH values. Further studies were carried out at  $\text{pH} < 1$ .

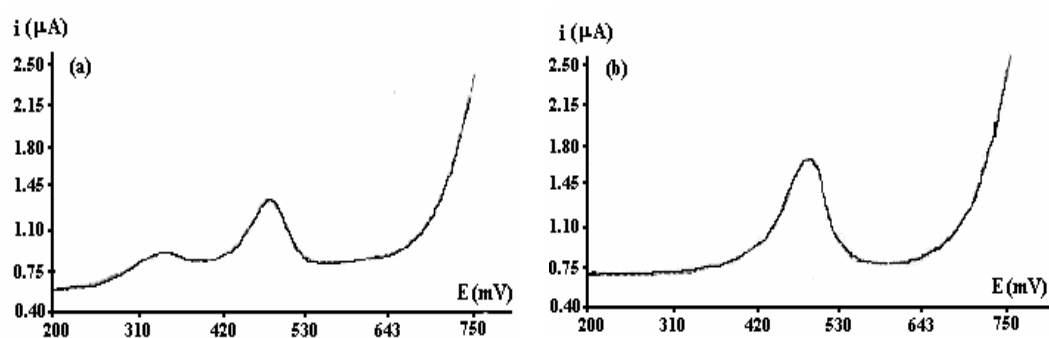


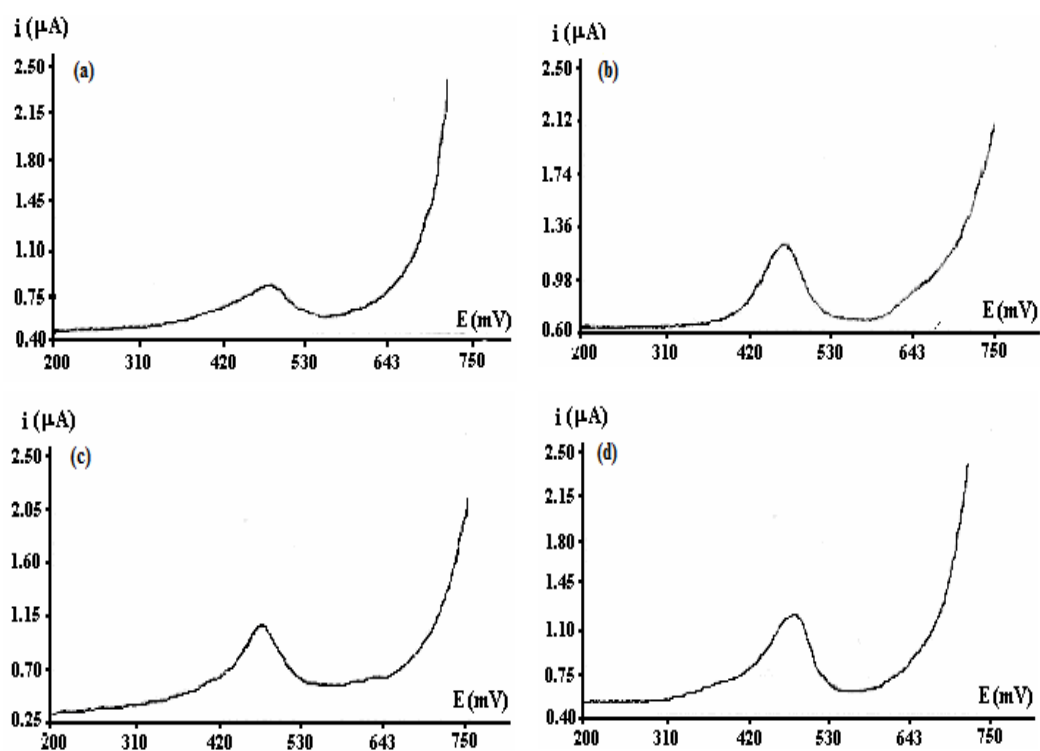
**Figure 3.11.** The voltammograms at lower initial pH values: (a) pH: 1.0, (b) pH < 1. Experimental conditions: Hg(II) concentration:  $1.0 \times 10^{-9}$  M,  $C_{\text{hdy}}$ : 0.07 M,  $v_{\text{cent}}$ : 3000 rpm,  $t_{\text{cent}}$ : 7 min.

**Table 3.2.** The currents of mercury reoxidation peak at lower initial pH values. Hg(II) concentration:  $1.0 \times 10^{-9}$  M.

| pH | Peak current<br>(nA) | Peak Potential<br>(mV) |
|----|----------------------|------------------------|
| 1  | 540                  | 477                    |
| <1 | 963                  | 484                    |

### 3.2.3. Effect of Hydrazine Concentration on Mercury Reduction Reaction

The influence of concentration of hydrazine on resulting reoxidation peak currents of mercury was investigated at a large scale. In order to be sure about the quantitative of the reduction reaction, hydrazine was used in an excessive supply when compared with the concentration of the Hg(II). The obtained voltammograms were given on Figure 3.12 and the data obtained from these voltammograms were presented on Table 3.3.



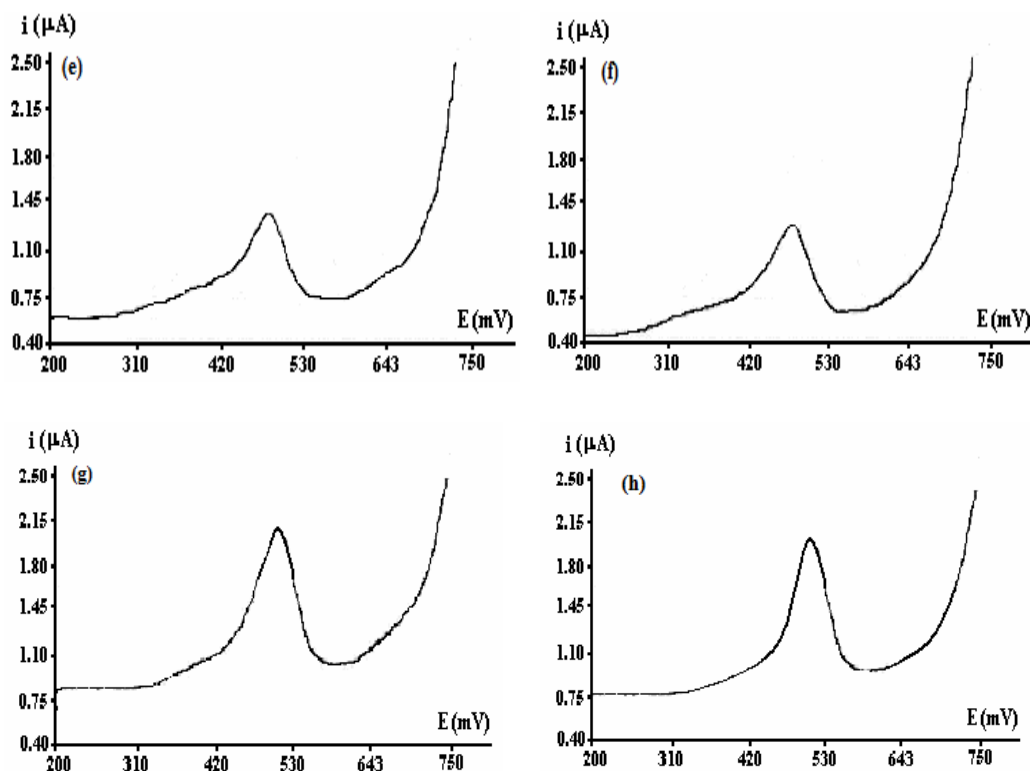


**Figure 3.12.** The influence of concentration of hydrazine on resulting reoxidation peak currents of mercury. Experimental conditions: Hg(II) concentration:  $1.0 \times 10^{-9}$  M, pH < 1,  $v_{\text{cent}}$ : 3000 rpm,  $t_{\text{cent}}$ : 2 min, stripping solution content: 1.0 M HClO<sub>4</sub> and 0.35 M HCl.  $C_{\text{hdy}}$ : (a)  $1.0 \times 10^{-8}$ , (b)  $1.0 \times 10^{-5}$ , (c)  $5.0 \times 10^{-3}$ , (d)  $2.0 \times 10^{-2}$ , (e)  $3.0 \times 10^{-2}$ , (f)  $5.0 \times 10^{-2}$ , (g)  $7.0 \times 10^{-2}$ , (h)  $1.0 \times 10^{-1}$  M.

**Table 3.3.** Effect of hydrazine concentration on the resulting peak currents of  $1.0 \times 10^{-9}$  M Hg(II)

| $\text{N}_2\text{H}_4$ Concentration (M) | Peak current (nA) | Peak Potential (mV) |
|--|-------------------|---------------------|
| $1.0 \times 10^{-8}$                     | 249               | 487                 |
| $1.0 \times 10^{-5}$                     | 503               | 485                 |
| $5.0 \times 10^{-3}$                     | 520               | 487                 |
| $2.0 \times 10^{-2}$                     | 534               | 485                 |
| $3.0 \times 10^{-2}$                     | 586               | 488                 |
| $5.0 \times 10^{-2}$                     | 623               | 478                 |
| $7.0 \times 10^{-2}$                     | 723               | 488                 |
| $1.0 \times 10^{-1}$                     | 790               | 483                 |

As can be followed from the Table 3.3 the added concentration of hydrazine affected on the resulting peak current. The peak current increases with the increasing  $\text{N}_2\text{H}_4$  concentration while the peak potential remains almost the same.

However, when the concentration of hydrazine was ten times higher than Hg(II), the subjected peak current values were decreases. In these circumstances, even if the reaction is quantitative, metallic mercury droplets with provided centrifuge forces can not be collected on the electrode surface significantly. On plotting the results against the concentration of reducing agent, it was shown that the reduction reaction goes to complete (Figure 3.13A and B). Hydrazine concentration of  $7 \times 10^{-2}$  M was selected in further studies to avoid excess amount hydrazine.

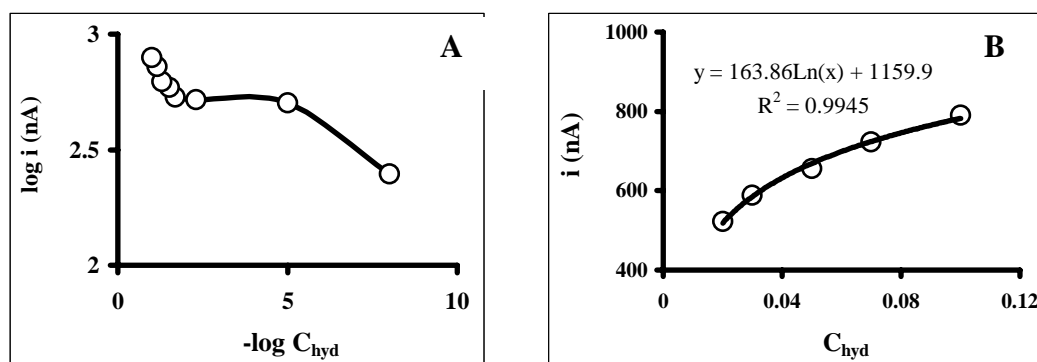


**Figure 3.13.** Effect of hydrazine concentration on the resulting peak currents of  $1.0 \times 10^{-9}$  M Hg(II): (A) Logarithmically graph included all data; (B) Linear graph of selected  $C_{\text{hyd}}$

### 3.2.4. Effect of Centrifugation Time (with reducing agent)

Centrifugation plays a major role in centri-voltammetry and enables the effectiveness of pre-concentration process. Reduction of mercuric ions to metallic mercury produces small mercury droplets distributed through the reaction solution and effective centrifugal force is required to collect these droplets onto the electrode surface. Therefore, the centrifugation parameters, namely time and speed, were optimized in this study.

First time of centrifugation was optimized by exercising the range of time from 2 to 12 minutes at 3000 rpm. The obtained voltammograms were given on Figure 3.14 and the data obtained from these voltammograms were presented on Table 3.4. The maximum peak current value was observed in 7 minutes so the optimum time was considered as 7 minutes (Figure 3.15).



Although the peak current was anticipated to increase up to a limit (to a point where maximum amount of mercury is collected) with the increase in duration due to an increase in the amount reaching the electrode surface, it has declined after 7 minutes despite a centrifugal rotation speed of 3000 rpm (Figure 3.15). At the same centrifugal cell, Hg(II) ions' being reduced with borohydride peak current values showed similar changes with the centrifugation time (Ürkmez et al, 2009). The decrease in the peak heights after 7 min of centrifugation was attributed to the warming up of the cell due to long duration of centrifugation. Although the GFE was tightly placed in the cavity of Teflon cell, longer duration of centrifugation might have resulted in disconnection between the electrode body and the walls of cell cavity and therefore mercury droplets can start to leak into the holes.

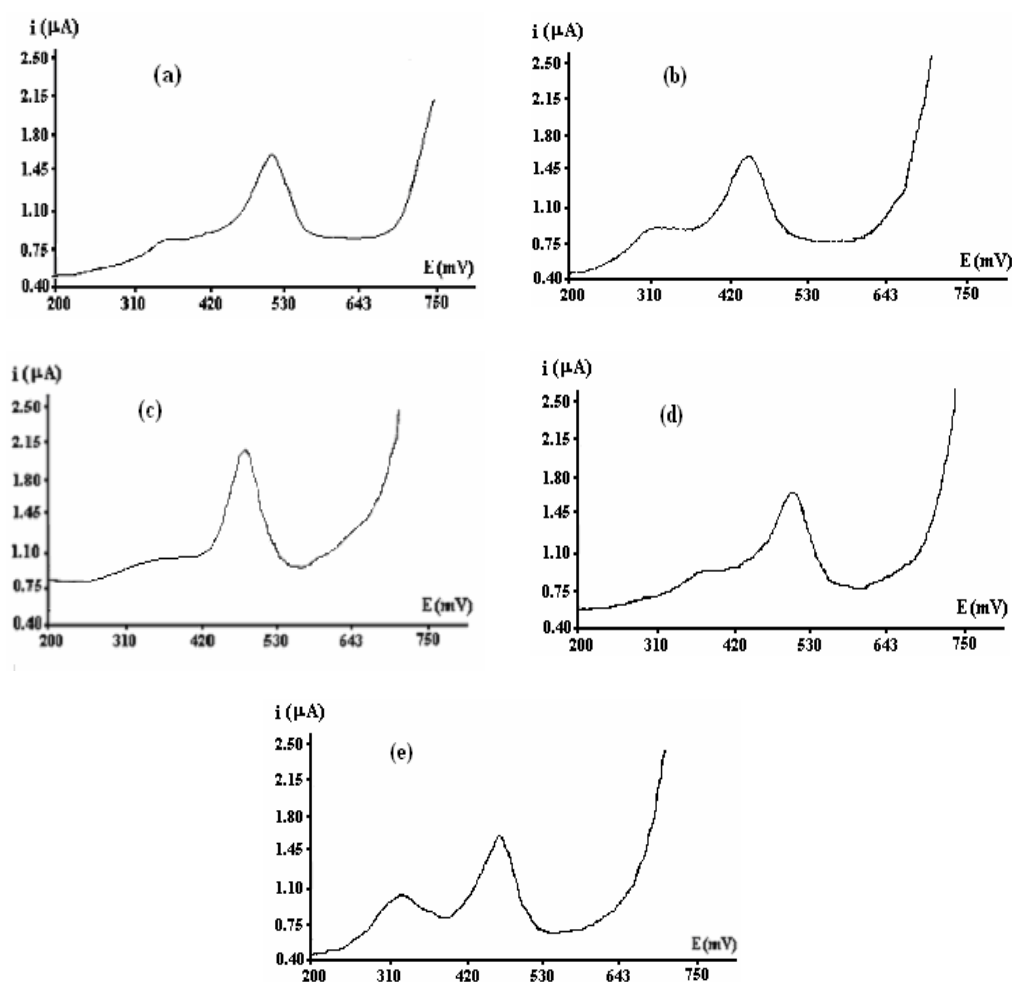


**Figure 3.14.** The influence of the centrifugation time on resulting reoxidation peak currents of mercury. Hg(II) concentration:  $1.0 \times 10^{-9}$  M. Experimental conditions; **pH** < **1**,  $C_{\text{hdy}}$ : 0.07 M,  $v_{\text{cent}}$ : 3000 rpm, stripping solution content: 1.0 M HClO<sub>4</sub> and 0.35 M HCl.  $t_{\text{cent}}$ : (a) 2, (b) 5, c) 7, (d) 9, (e) 12 min.

**Table 3.4.** The influence of centrifugation time on the resulting peak currents of  $1.0 \times 10^{-9}$  M Hg(II).

| Centrifugation Time (min) | Peak current (nA) | Peak Potential (mV) |
|---------------------------|-------------------|---------------------|
| 2                         | 723               | 466                 |
| 5                         | 788               | 467                 |
| 7                         | 963               | 465                 |
| 9                         | 781               | 468                 |
| 12                        | 801               | 487                 |

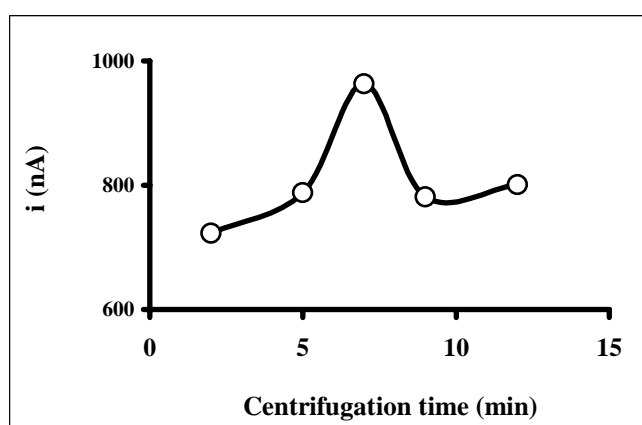


**Figure 3.15.** The influence of centrifugation time on the resulting peak currents of  $1.0 \times 10^{-9}$  M (II)

### 3.2.5. Effect of Centrifugation Speed (with reducing agent)

The relationship between centrifugal force and particle size is very important from the point of view of sensitivity and reproducibility of centri-voltammetric measurements. In order to clarify this relationship, studies were carried out in the range of 500 – 3500 rpm. The obtained voltammograms were given on Figure 3.16 and the data obtained from these voltammograms were presented on Table 3.5.

It is obvious that as the speed of centrifugation is increased, accumulation of mercury will increase. Although the centrifuge device used in the study has a speed range up to 4000 rpm, in order to avoid distorting the cell and the

centrifuge device as well, speed of centrifugation was raised until 3500 rpm. Since the relatively high current values for the process were obtained at 3000 rpm, following studies were carried out this speed value (Figure 3.17).

When Figure 3.15 and 3.17 were compared, in the range of work alteration of peak current has seemed to be quite different. It was understood from here that centrifugation speed was a more effective parameter than centrifugation time.

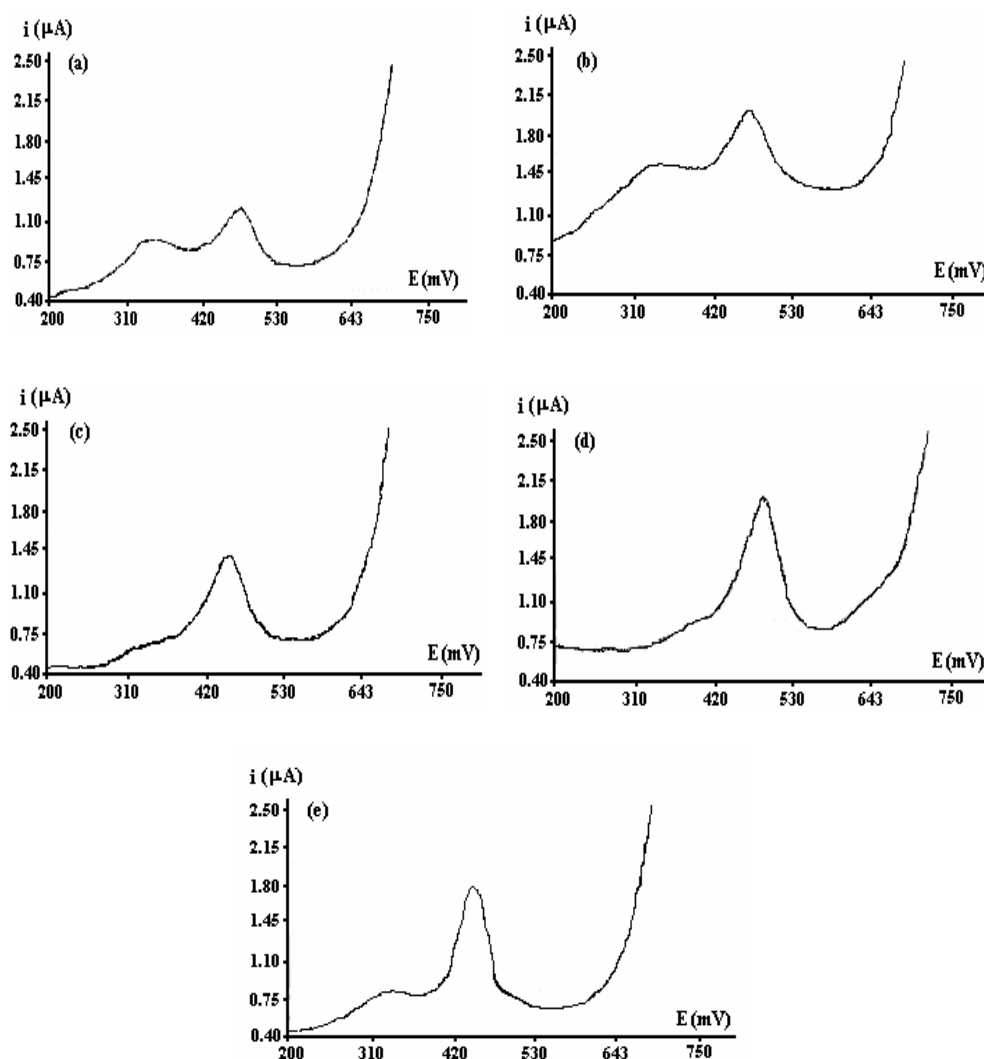


**Figure 3.16.** The influence of the centrifugation speed on resulting reoxidation peak currents of mercury. Hg(II) concentration:  $1.0 \times 10^{-9}$  M. Experimental conditions; pH < 1,  $C_{\text{hdy}}$ : 0.07 M,  $t_{\text{cent}}$ : 7 min., stripping solution content: 1.0 M HClO<sub>4</sub> and 0.35 M HCl.  $v_{\text{cent}}$ : (a) 500 (b) 1000, (c) 2000, (d) 3000, (e) 3500 rpm.

**Table 3.5.** The influence of centrifugation speed on the resulting peak currents of  $1.0 \times 10^{-9}$  M Hg(II)

| Centrifugation speed(rpm) | Peak current (nA) | Peak Potential (mV) |
|---------------------------|-------------------|---------------------|
| 500                       | 426               | 460                 |
| 1000                      | 590               | 463                 |
| 2000                      | 694               | 462                 |
| 3000                      | 963               | 468                 |
| 3500                      | 1100              | 460                 |

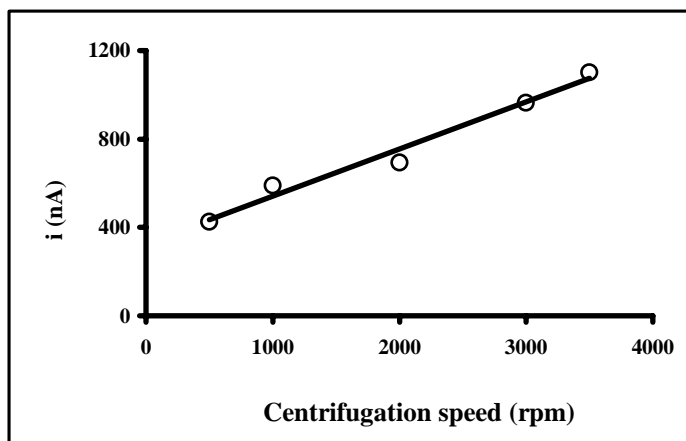


**Figure 3.17.** The influence of centrifugation time on resulting reoxidation peak currents of  $1.0 \times 10^{-9}$  M Hg(II).

### 3.2.6. Effect of Stripping Solution Content on Mercury Peak Current

In general, there are three mass-transfer processes by which a reacting species may be brought to an electrode surface. These are: diffusion, migration and convection. In voltammetry the effect of migration is usually eliminated by adding a 50 or 100 fold excess of an inert “supporting electrolyte”. It not only eliminates the effects of migration, but also greatly increases the conductivity and diminishes the potential drop  $iR$  of solution. In order to obtain true current-potential curves the electrical conductivity of the solution must be maintained. Perchlorates, chlorates, sulphates and chlorides of alkali and alkaline earth metals

that enable the voltammetric investigations over a wide range of potentials are particularly suitable as supporting electrolytes (Willard et al, 1981).

The anions of supporting electrolyte often form complexes with metal cations under investigation, and buffer mixtures may control the pH, and thereby affect the electrochemical behavior of the electroactive species. For this reason, effect of supporting electrolyte solution (stripping solution) at anodic stripping step was investigated as behavior of GFE was tested in different supporting electrolytes at freshly prepared electrode (Section 3.1.2).

Single or binary component stripping solutions was selected such as 0.1 M HNO<sub>3</sub>, 0.1 M HCl, 1.0 M HClO<sub>4</sub> plus 0.35 M HCl, 0.1 M HCl plus 0.1 M HNO<sub>3</sub>. The obtained voltammograms with these solution for 1×10<sup>-9</sup> M Hg(II) were given in Figure 3.18. The best background current, the best peak shape, the highest current and the farthest peak potential from the oxidation of gold were observed when the stripping solution were contained 1.0 M HClO<sub>4</sub> and 0.35 M HCl.

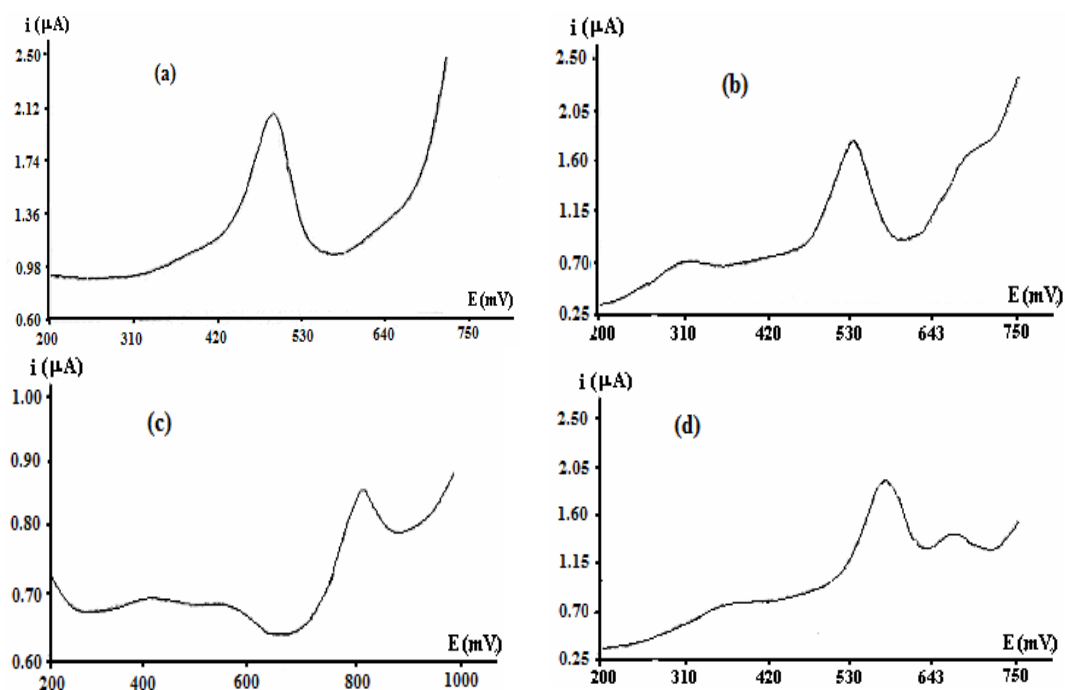


**Figure 3.18.** The effect of stripping solution content on resulting reoxidation peak currents, Hg(II) concentration  $1 \times 10^{-9}$  M. Experimental conditions:  $\text{pH} < 1$ ,  $C_{\text{hdy}}$ : 0.07 M,  $v_{\text{cent}}$ : 3000 rpm,  $t_{\text{cent}}$ : 7 min, stripping solution content: (a) 1.0 M HClO<sub>4</sub> + 0.35 M HCl, (b) 0.1 M HCl + 0.1 M HNO<sub>3</sub>, (c) 0.1 M HNO<sub>3</sub>, (d) 0.1 M HCl.

Chloride ions are known to have a particular effect on reoxidation peaks of mercury. Previous studies revealed that a certain amount of chloride increases the anodic peak current of mercury and shifts the peak potential to negative potential. This effect was attributed to be a complexing reaction between Hg(II) and Cl<sup>-</sup> ions in the solution to form the anionic forms of mercury(II) (Zen and Chung, 1995; Okçu et al., 2005). Therefore the effect of HCl concentration in 1.0 M HClO<sub>4</sub> stripping solution on mercury reoxidation peak current was also examined in this study. For this purpose HCl concentration was changed from 0.05 M to 0.45 M and voltammograms were recorded (Figure 3.19).

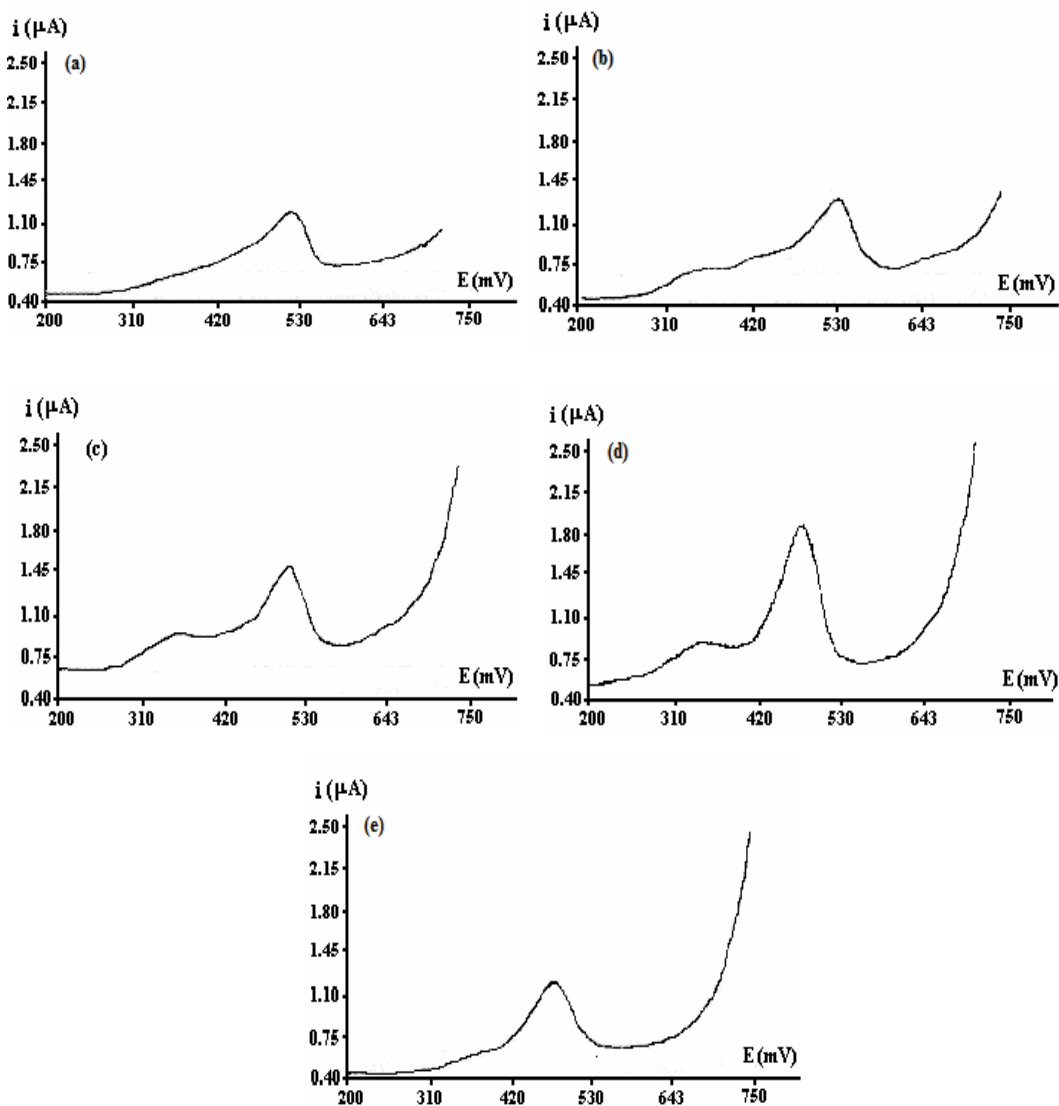


**Figure 3.19.** The effect of HCl concentration in 1.0 M HClO<sub>4</sub> stripping solution on mercury reoxidation peak current, Hg(II) concentration  $1 \times 10^{-9}$  M,  $\text{pH} < 1$ ,  $C_{\text{hdy}}: 0.07$  M,  $t_{\text{cent}}: 7$  min.,  $v_{\text{cent}}: 3000$  rpm; HCl concentration: (a) 0.05, (b) 0.10, (c) 0.20, (d) 0.35, (e) 0.45 M.

When Table 3.6 and Figure 3.20 were considered, it was understood that the peak potentials related to the reoxidation of mercury shifted in a more negative potential values, the peak currents were increased and then shown a decline for higher chloride contents (0.45 M) as the chloride content increased. The peak current was gave a maximum at 0.35 M HCl similarly our previously studies which Hg(II) was reduced with NaBH<sub>4</sub> (Ürkmez et al, 2004, 2009). Zen and Chung reported that higher concentrations of HCl can cause a depression of the peak current, which indicates a competitive effect chloride ions and mercurate(II) anions. Lower concentrations of HCl can be also unfavourable, due to the need of a reasonable excess of chloride ions for converting HgCl<sub>2</sub> into its anionic forms (Zen and Chung, 1995). A 0.35 M concentration of HCl was therefore used in the subsequent experiments.

**Table 3.6.** Effect of HCl concentration on resulting peak currents values of  $1.0 \times 10^{-9}$  M Hg(II).

| HCl Concentration (M) | Peak current (nA) | Peak Potential (mV) |
|-----------------------|-------------------|---------------------|
| 0.05                  | 418               | 566                 |
| 0.10                  | 520               | 540                 |
| 0.20                  | 607               | 515                 |
| 0.35                  | 965               | 488                 |
| 0.45                  | 576               | 480                 |

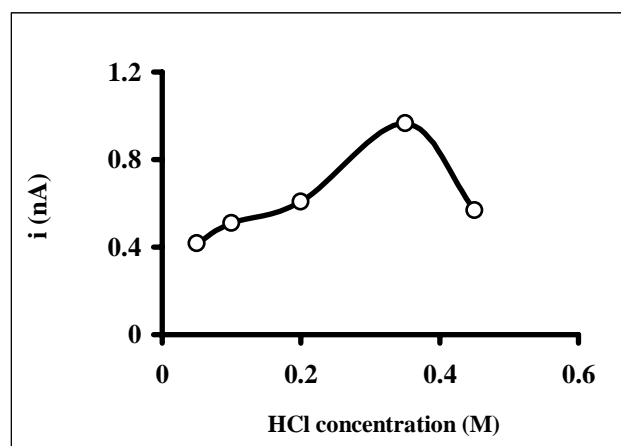


**Figure 3.20.** The influence of chloride ion concentration in the stripping solution on anodic stripping peaks current values of  $1.0 \times 10^{-9}$  M Hg(II).

### 3.2.7. Resulting Peak Currents of Hg(II) in Optimum Conditions

The conditions were determined to obtain the highest levels of current related to mercury(II) ion with hydrazine by studying the largest possible intervals to investigate the effect of various parameters. The optimal parameters of the method were summarized in Table 3.7 and the obtained voltammograms under these conditions were given in Figure 3.21.

**Table 3.7.** The list of optimal working conditions for the procedure with reducing agent (Hydrazine).

| Experimental Parameters | Optimal conditions |
|-------------------------|--------------------|
| pH                      | <1                 |
| Hydrazine concentration | 0.07 M             |
| Centrifugation time     | 7 min              |
| Centrifugation speed    | 3000 rpm           |
| Mode                    | DP                 |
| Sweep rate / U.step     | 10 mV/s / 6 mV     |
| Pulse amplitude         | 50 mV              |

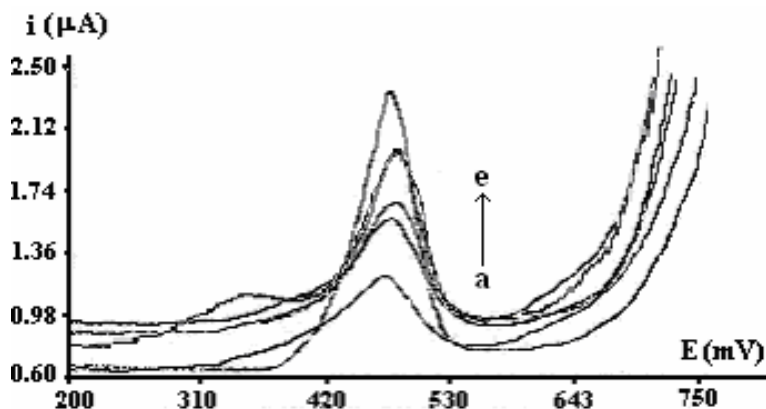


**Figure 3.21.** The voltammograms obtained under optimum experimental conditions ( $C_{\text{hdy}}$ : 0.07 M,  $\text{pH} < 1$  (0.5 M  $\text{HClO}_4$ ),  $t_{\text{cent}}$ : 7 min,  $v_{\text{cent}}$ : 3000 rpm, stripping solution content: 1.0 M  $\text{HClO}_4$  and 0.35 M  $\text{HCl}$ ). Hg(II) concentration: (a)  $1.0 \times 10^{-10}$ , (b)  $1.5 \times 10^{-10}$ , (c)  $5.0 \times 10^{-10}$ , (d)  $1.0 \times 10^{-9}$ , (e)  $5.0 \times 10^{-9}$  M.



Calibration curve of Hg(II) concentrations ranging from  $1.0 \times 10^{-8}$  M to  $1.0 \times 10^{-10}$  M was found in a logarithmically linear fashion with the equation as follows:  $\text{Log}i_p = -0.3467\text{Log}C_{\text{Hg(II)}} + 6.0912$ . Its regression coefficient was ( $R^2$ ) 0.9869 (Table 3.8, Figure 3.22).

**Table 3.8.** The effect of mercury (II) concentration on current values obtained with hydrazine under the optimized conditions.

| Concentration of Hg(II) (M) | Peak current (nA) | Peak Potential (mV) |
|-----------------------------|-------------------|---------------------|
| $1.0 \times 10^{-10}$       | 402               | 484                 |
| $1.5 \times 10^{-10}$       | 560               | 485                 |
| $5.0 \times 10^{-10}$       | 693               | 483                 |
| $1.0 \times 10^{-9}$        | 963               | 487                 |
| $5.0 \times 10^{-9}$        | 1610              | 484                 |
| $1.0 \times 10^{-8}$        | 2060              | 490                 |

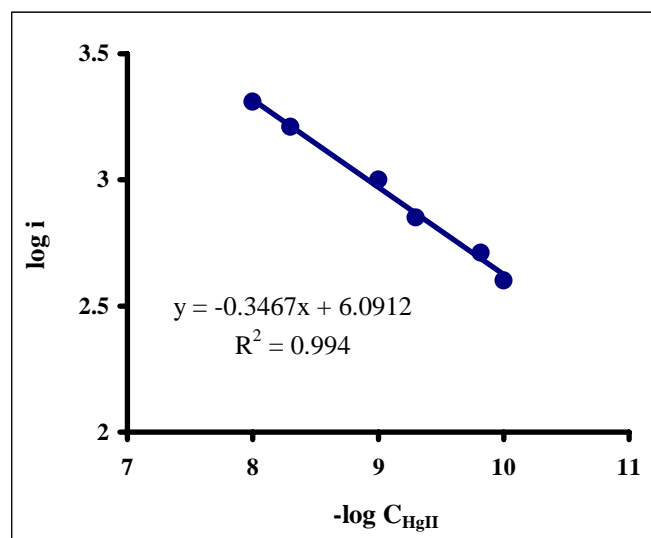


**Figure 3.22.** The calibration graph for Hg(II) ions obtained with hydrazine under the optimal conditions.

### 3.3. CHAPTER II

#### **Centri-Voltammetric Determination of Mercury(II) Using Purolite C100 as a Carrier Material**

In order to see the effects of impurities, blank experiments were exercised through this study but significant levels of impurities were not observed (Figure 3.23a).

6 mg of Purolite C100 was added to the solution of  $1 \times 10^{-7}$  M Hg(II) and pH was adjusted at 7.5 and all procedures with the exception of centrifugation were applied to observe the impact of centrifugal forces on peak currents related to the mercury (Figure 3.23b). The entire of voltammetric procedures were repeated in the absence of Purolite C100 to observe the adsorber and carrier effect of Purolite C100 (Figure 3.23c). Additionally, the voltammogram of  $1 \times 10^{-7}$  M Hg(II) adjusted pH to 7.50 was taken in the absence of Purolite C100 and a centrifugation process for the purposes of comparison (Figure 3.23d). It was concluded that the centrifugal forces and the carrier material were not effective alone since there was no evidence of any signal related to Hg(II) in these voltammograms (Figure 3.23).

Following studies were conducted to see the influence of experimental parameters such as pH, preconcentration (adsorption) time ( $t_{\text{ads}}$ ), resin amount ( $m_r$ ), centrifugation time ( $t_{\text{cent}}$ ) and speed ( $v_{\text{cent}}$ ).

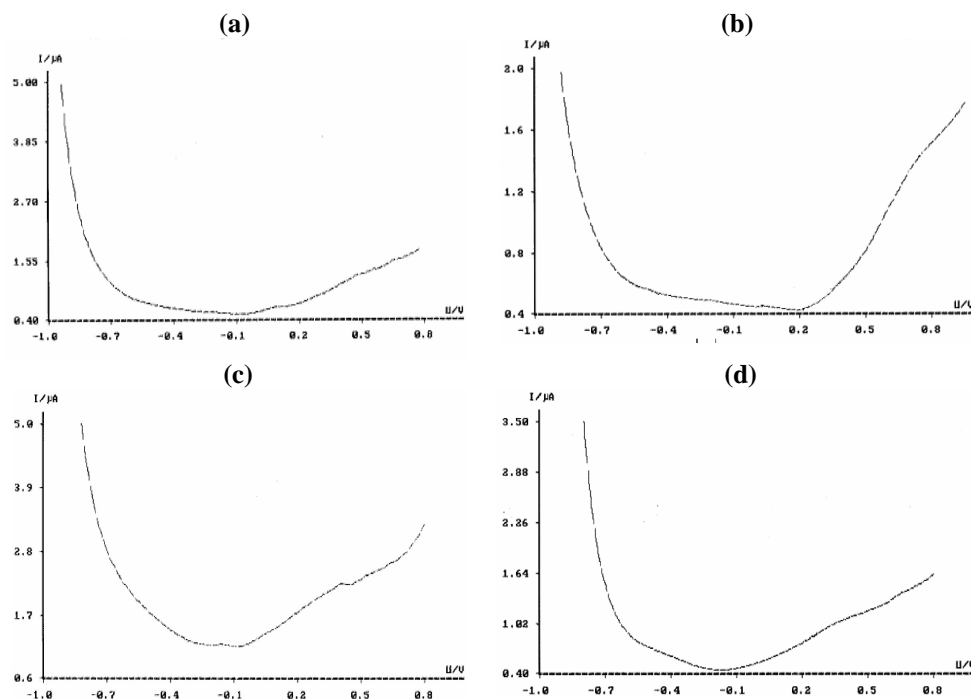


**Figure 3.23.** The voltammograms obtained for (a) blank solution, (b) without centrifugation with Purolite C100 for  $1 \times 10^{-7}$  M  $\text{Hg}^{2+}$ , (c) without Purolite C100 with centrifugation for  $1 \times 10^{-7}$  M  $\text{Hg}^{2+}$ , (d) without Purolite C100 and centrifugation for  $1 \times 10^{-7}$  M  $\text{Hg}^{2+}$ . Related experimental parameters: **pH:** 7.50,  **$m_r$ :** 6.0 mg,  **$t_{\text{ads}}$ :** 15 min,  **$v_{\text{cent}}$ :** 3000 rpm,  **$t_{\text{cent}}$ :** 10 min.

### 3.3.1. Effect of pH

The effect of pH on the resulting peak currents related to the mercury ions was investigated at the range of 1.0 - 9.0. Additional studies were also carried out at  $\text{pH} < 1$  for comparison purposes to the studies of hydrazine (Figure 3.24). The peak current and peak potential values obtained from voltammograms were given at Table 3.9.

As the pH of medium was increased, the peak currents related to the mercury ions have been elevated at the beginning (until 7.50). There hasn't been a significant change in levels greater than pH 7.50 (Figure 3.25). The proton and mercury(II) ions pit one against another for bonding to the studied resin. Although ionic valance of Hg(II) ion was greater than that of proton ion, since the concentration of proton in solution was lower than that of mercury(II) ion ( $1 \times 10^{-7}$  M), at higher pH levels, the displacement of protons in Purolite C100 resin has

become easier. Therefore, the peak current has been reached its maximum value which was related to the concentration of mercury ions. At lower pH levels as the concentration of protons increased, the enrichment of Hg(II) ions on the resin has become harder and the peak current values have decreased.

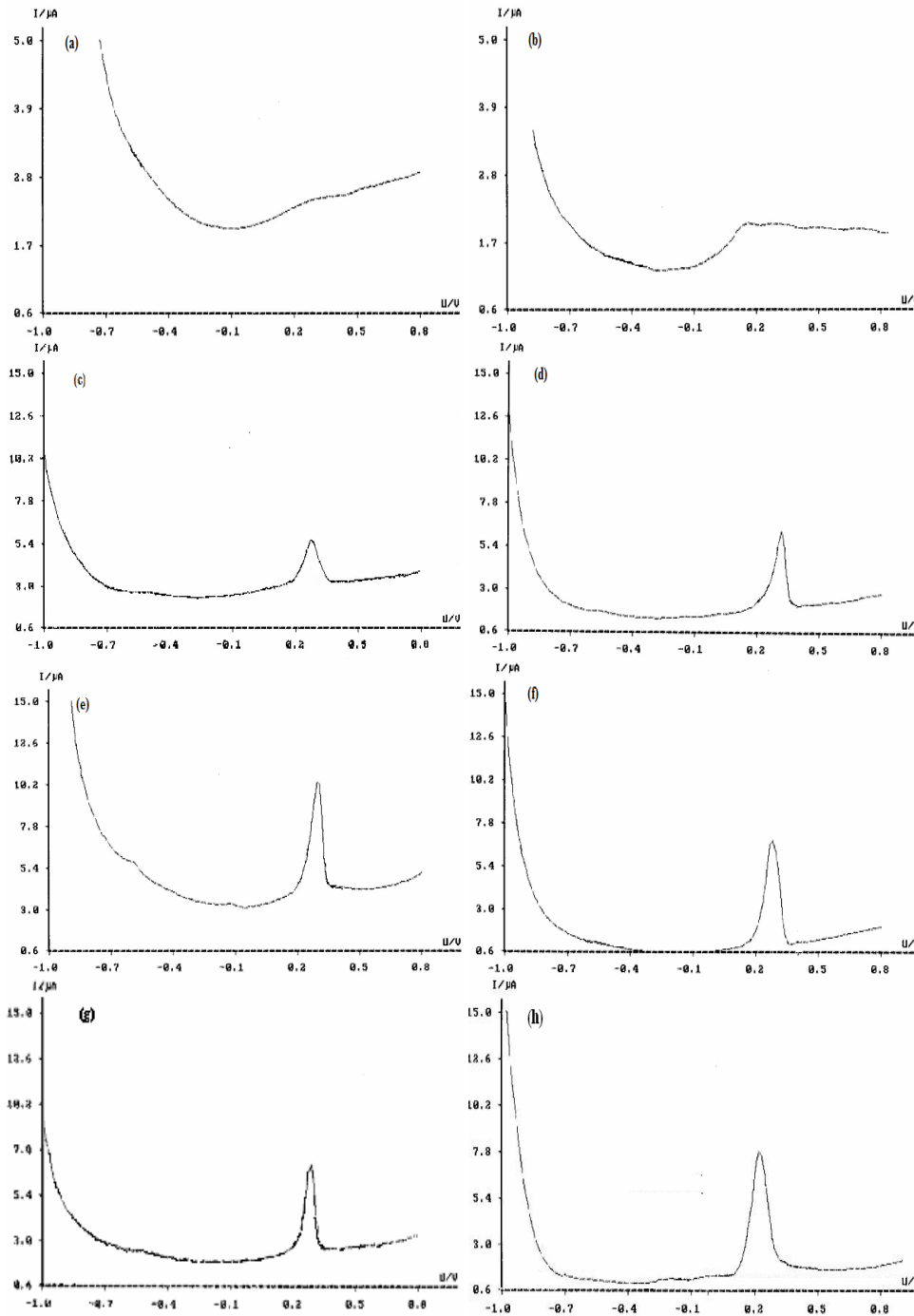


**Figure 3.24.** The influence of pH on the peak currents of solution containing  $1 \times 10^{-7}$  M  $\text{Hg}^{2+}$  in 0.5 M  $\text{HClO}_4$  ( $m_r$ : 6.0 mg,  $t_{\text{ads}}$ : 20 min,  $v_{\text{cent}}$ : 3000 rpm,  $t_{\text{cent}}$ : 10 min). pH values: (a) <math><1</math>, (b) 1.00, (c) 2.50, (d) 4.00, (e) 6.00, (f) 7.50, (g) 9.00, (h) 9.50.

**Table 3.9.** The influence of pH on the peak currents of solution containing  $1 \times 10^{-7}$  M  $\text{Hg}^{2+}$  in 0.5 M  $\text{HClO}_4$ .

| pH   | Peak current ( $\mu\text{A}$ ) | Peak Potential (mV) |
|------|--------------------------------|---------------------|
| <1.0 | -                              | -                   |
| 1.0  | -                              | -                   |
| 2.5  | 2.32                           | 278                 |
| 4.0  | 3.53                           | 325                 |
| 6.0  | 4.37                           | 294                 |
| 7.5  | 5.80                           | 302                 |
| 9.0  | 5.66                           | 281                 |
| 9.5  | 6.07                           | 293                 |

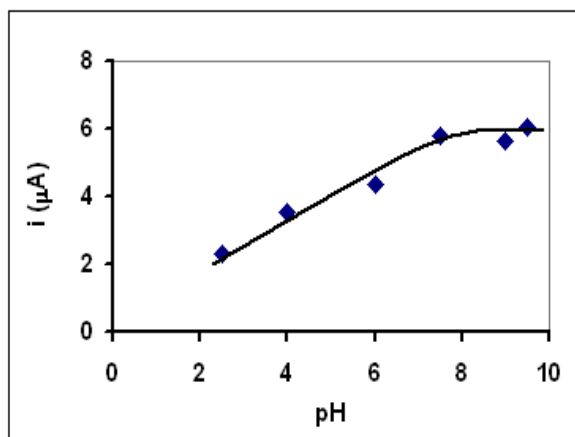


**Figure 3.25.** The influence of pH on the peak currents of solution containing  $1 \times 10^{-7}$  M  $\text{Hg}^{2+}$  in 0.5 M  $\text{HClO}_4$ .

The following studies were carried out at  $\text{pH} = 7.50$  since the peak related to  $\text{Hg(II)}$  has also reached its sufficiently high value in this pH medium. As the voltammograms in Figure 3.24 was compared in terms of base currents, it was observed that the base current decreases generally as the pH increases and has reached its minimum value when  $\text{pH} = 7.50$ . In addition, it was stated that Purolite C100 resin was stable in the interval of 0-14 pH and the 6-10 pH interval was appropriate for the regeneration cycle (Table 1.9). Therefore, the determined optimal pH value was also in agreement with this interval.

### 3.3.2. Effect of Adsorption Duration

The adsorption efficiency of Hg(II) ions by Purolite C100 resin depends both on the amount of resin and the duration of contact. First, the influence of duration of contact was studied.

The duration of contact must be long enough for the preconcentration (adsorption, ion exchange) process to be completed. It is evident that more mercury is absorbed by the resin as duration of adsorption increased and the peak current levels increase. Because mercury(II) enriched resin will collect at the electrode surface by the aid of centrifugal forces.

For that reason, 5, 10, 15, 20, 25 and 30 min waiting periods were applied to the solution system including 6 mg Purolite C100 before centrifugation for measuring  $1 \times 10^{-7}$  M Hg(II) ions in 0.5 M HClO<sub>4</sub>. Voltammograms were recorded for these various durations (Figure 3.26).

As shown in Table 3.10 and Figure 3.27, the current levels decline after 20<sup>th</sup> minute on the contrary to what's anticipated. The reason of this situation might be to form stronger bound between mercury ion and the functional groups of resin as duration of adsorption increased and desorption of mercury is not probable the same ratio. It should be noted that the peak currents were plotted against the adsorption duration and this parameter excludes the time passed during centrifugation step. In this case; 10 minutes of centrifugation duration must be considered as the time elapsed.

Additionally, it was worked with Lewatit Monoplus TP 214 that was specifically selective with mercury ions. Unfortunately, the study failed to remove absorbed mercury ions to the Lewatit from this resin and it was not possible to take place the electrochemical reduction reaction of Hg(II) ions via potential scanning in a supporting electrolyte of 1.0 M HCl and 0.5 M HClO<sub>4</sub>. The reason might be that Hg(II) ions produce a stable chemical form with Lewatit.

Thus, it wasn't possible to obtain a peak related to mercury during studies with Lewatit 214 for the very same reason.

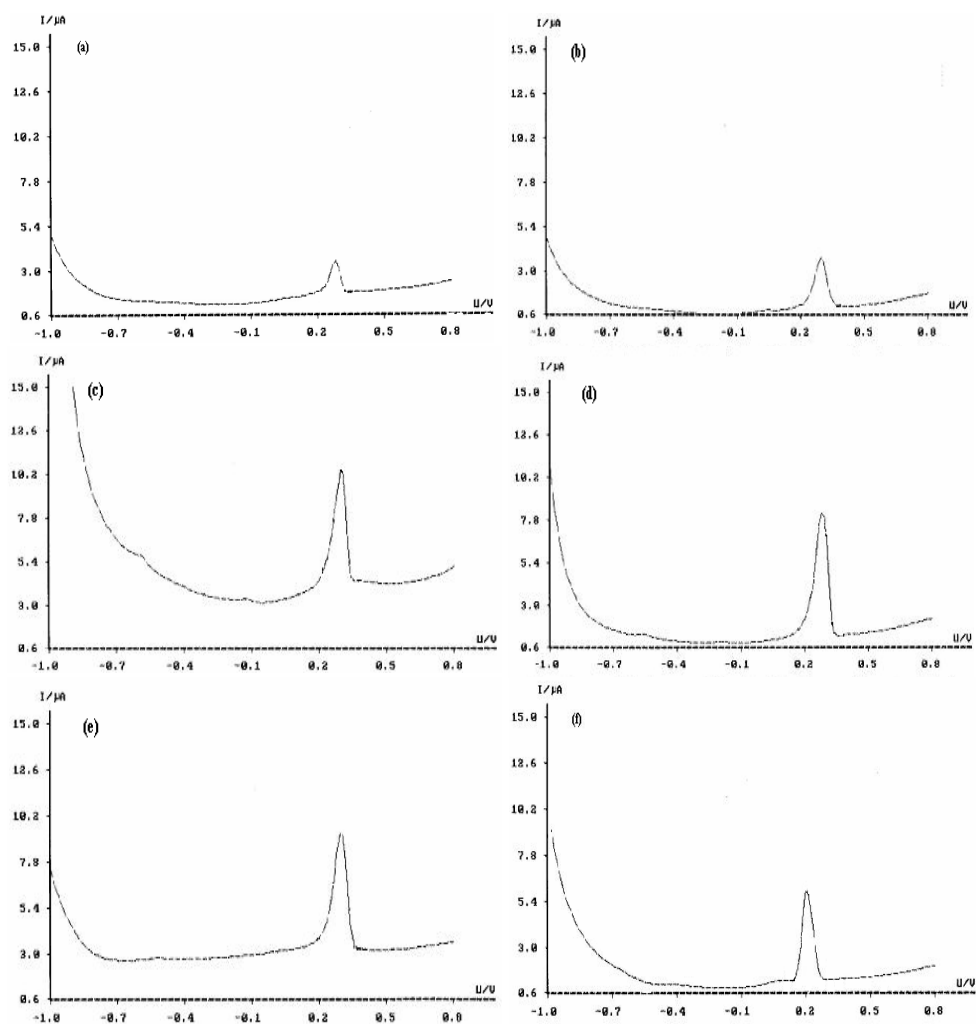


**Figure 3.26.** The influence of adsorption duration on the peak currents of solution containing  $1 \times 10^{-7}$  M  $\text{Hg}^{2+}$  in 0.5 M  $\text{HClO}_4$  (pH: 7.50,  $m_r$ : 6.0 mg,  $v_{\text{cent}}$ : 3000 rpm,  $t_{\text{cent}}$ : 10 min).  $t_{\text{ads}}$ : (a) 5, (b) 10, (c) 15, (d) 20, (e) 25, (f) 30 min.

**Table 3.10.** The influence of adsorption duration on the peak currents of solution containing  $1 \times 10^{-7}$  M  $\text{Hg}^{2+}$  in 0.5 M  $\text{HClO}_4$ .

| Adsorption duration (min) | Peak current ( $\mu\text{A}$ ) | Peak Potential (mV) |
|---------------------------|--------------------------------|---------------------|
| 5                         | 1.68                           | 282                 |
| 10                        | 2.67                           | 298                 |
| 15                        | 5.80                           | 302                 |
| 20                        | 6.64                           | 289                 |
| 25                        | 5.75                           | 303                 |
| 30                        | 4.76                           | 266                 |

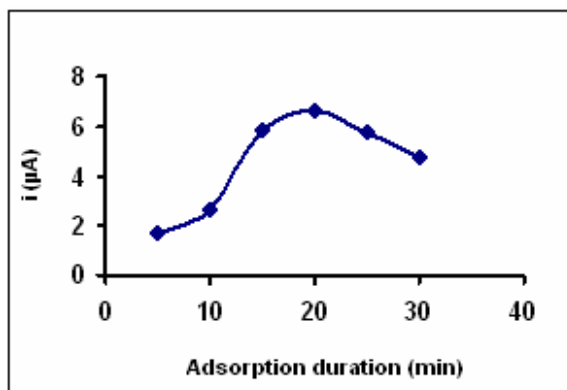


**Figure 3.27.** The influence of adsorption duration on the peak currents of solution containing  $1 \times 10^{-7}$  M  $\text{Hg}^{2+}$  in 0.5 M  $\text{HClO}_4$  (pH: 7.50,  $m_r$ : 6.0 mg,  $v_{\text{cent}}$ : 3000 rpm,  $t_{\text{cent}}$ : 10 min).

### 3.3.3. Effect of Amount of Purolite C100

The main purpose of this part of the study is to find the optimum resin amount that will yield the maximum peak current. For this reason, Purolite C100 was added to  $1 \times 10^{-7}$  M  $\text{Hg}(\text{II})$  solution at changing amount from 1.5 mg to 12.0 mg. The obtained voltammograms and peak current values are shown in Figure 3.28 and Table 3.11, respectively.

It's obvious that the mercury ions will continue to be absorbed by the resin until almost all mercury ions in solution are exhausted when an resin as ion exchanger or an absorbent, which is compatible with  $\text{Hg}(\text{II})$  ion is sufficiently added. Therefore, it can easily and safely be predicted that the peak currents, which are obtained following the measurement process, will first increase and then reach a limit when the amount of resin is gradually increased.

But, as shown in Figure 3.29, the peak current increased at the beginning with the amount of resin as anticipated, and started to decline after 6 mg. It could be stated that the Purolite C100 layer, that is formed at the electrolyte surface, following the centrifuge process was became thicker and the peak current levels declined by the resistance caused by this layer when large levels of Purolite C100 is used. The peak current levels were relatively high and almost constant in 3-6



mg Purolite C100 interval (Figure 3.29). But, further experiments were carried out by using 6 mg of resin since a smaller amount Hg(II) enriched of Purolite C100 was harder collected at the electrode surface with the assistance of centrifugal forces.

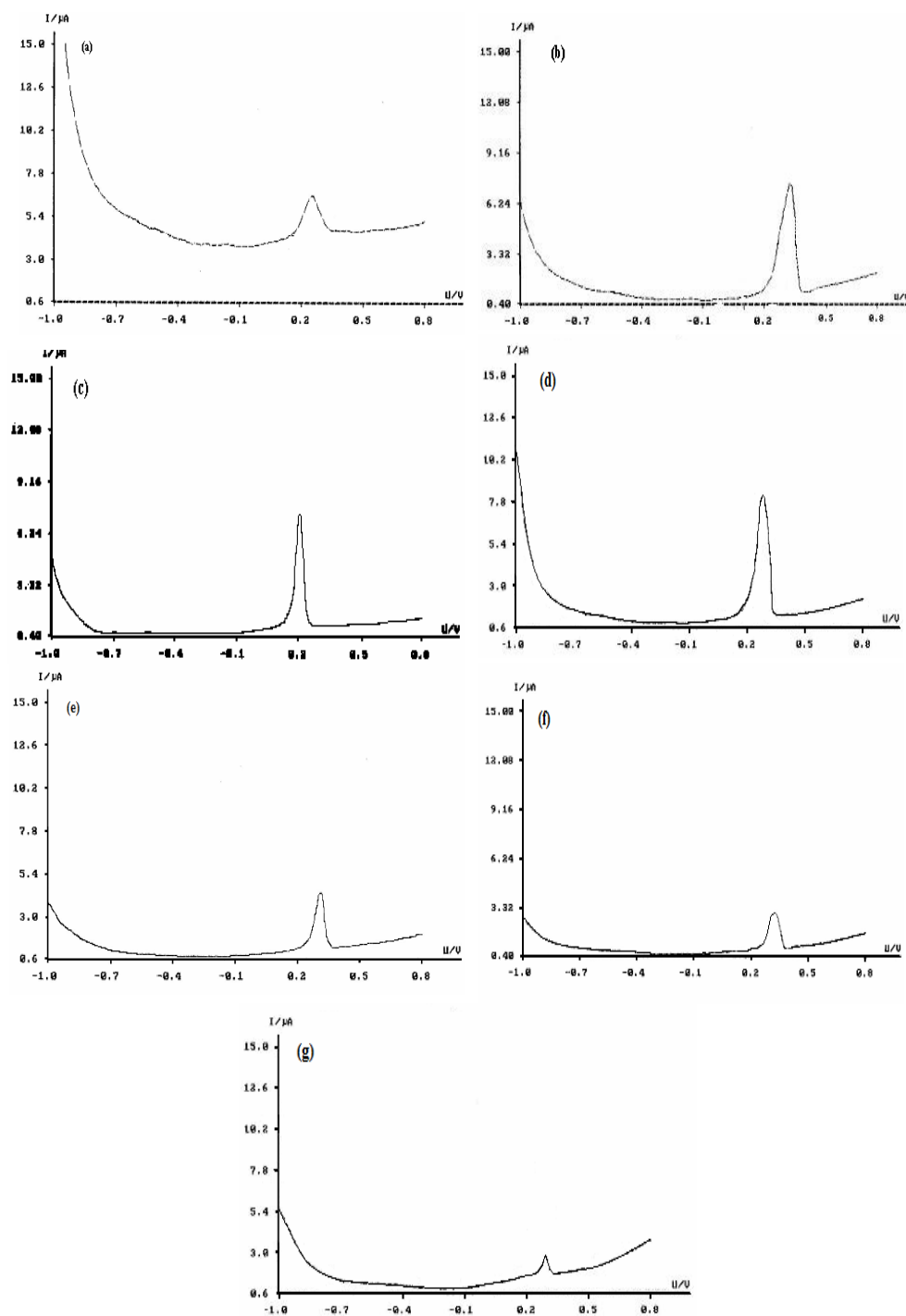


**Figure 3.28.** Dependence of the peak currents on the resin amount for the solution containing  $1 \times 10^{-7}$  M  $\text{Hg}^{2+}$  in 0.5 M  $\text{HClO}_4$  (pH : 7.50,  $t_{\text{ads}}$  : 20 min,  $v_{\text{cent}}$  : 3000 rpm,  $t_{\text{cent}}$  : 10 min).  $m_r$  : (a)1.5, (b) 3.0, (c) 5.0 (d) 6.0, (e)7.0, (f) 8.0, (g) 12.0 mg.

**Table 3.11.** Dependence of the peak currents on the resin amount for the solution containing  $1 \times 10^{-7}$  M in 0.5 M HClO<sub>4</sub>.

| Amount of resin (mg) | Peak current ( $\mu$ A) | Peak Potential (mV) |
|----------------------|-------------------------|---------------------|
| 1.5                  | 2.11                    | 263                 |
| 3.0                  | 6.37                    | 328                 |
| 5.0                  | 6.25                    | 275                 |
| 6.0                  | 6.54                    | 302                 |
| 7.0                  | 3.07                    | 314                 |
| 8.0                  | 2.16                    | 330                 |
| 12.0                 | 0.828                   | 287                 |

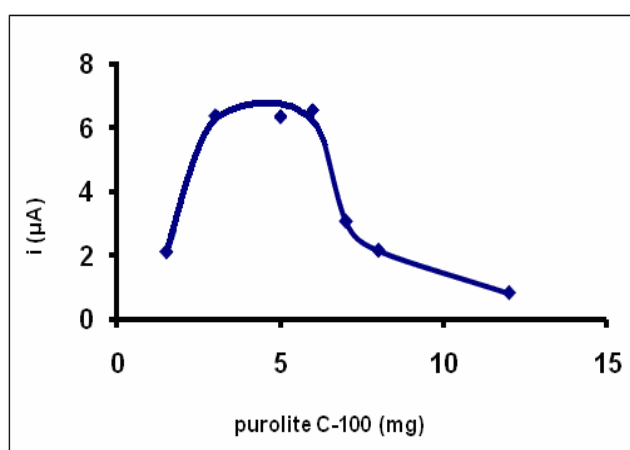


**Figure 3.29.** Dependence of the peak currents on the resin amount for the solution containing  $1 \times 10^{-7}$  M Hg<sup>2+</sup> in 0.5 M HClO<sub>4</sub> (pH: 7.50,  $t_{\text{ads}}$ : 20 min,  $v_{\text{cent}}$ : 3000 rpm,  $t_{\text{cent}}$ : 10 min).

### 3.3.4. Effect of Centrifugation Time (with carrier material)

Centrifugation plays a major role in centri-voltammetry and enhances the effectiveness of preconcentration process. Therefore the centrifugation parameters, namely time and speed, should be optimized.

Firstly, time of centrifugation was optimized by varying the time intervals from 3 to 12 min at 3000 rpm (Figure 3.30). The maximum peak current value was obtained at centrifugation time of 10 min (Table 3.12 and Figure 3.31). This duration represents the point of time where the maximum amounts of selected

Purolite C100 particles ( $\leq 45 \mu\text{m}$ ) collected at the electrode surface upon enrichment with mercury. This time interval may change with the rotation speed of centrifuge, type of resin, and with the size of particles.

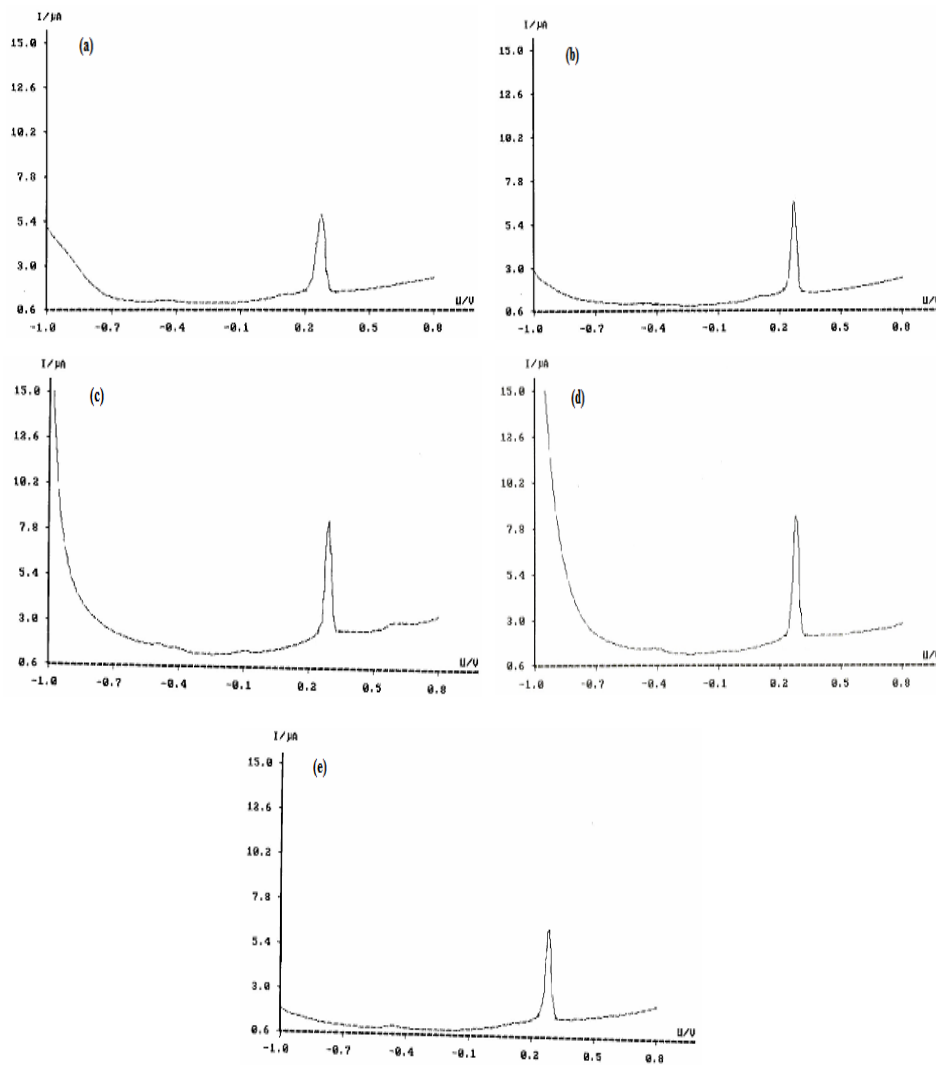


**Figure 3.30.** The influence of the centrifugation time on the peak currents for the solution containing  $1 \times 10^{-7} \text{ M Hg}^{2+}$  in  $0.5 \text{ M HClO}_4$  (**pH:** 7.50,  **$m_r$ :** 6.0 mg,  **$t_{\text{ads}}$ :** 20 min,  **$v_{\text{cent}}$ :** 3000 rpm).  **$t_{\text{cent}}$ :** (a) 3, (b) 5, (c) 8, (d) 10, (e) 12 min.

Although the peak current was anticipated to increase up to a limit (to a point where maximum amount of mercury is collected) with the increase in duration due to an increase in the amount reaching the electrode surface, it has declined after 10 minutes despite a centrifugal rotation speed of 3000 rpm.

**Table 3.12.** The influence of the centrifugation time on the peak currents for the solution containing  $1 \times 10^{-7}$  M  $\text{Hg}^{2+}$  in 0.5 M  $\text{HClO}_4$ .

| Time of centrifugation (min) | Peak current ( $\mu\text{A}$ ) | Peak Potential (mV) |
|------------------------------|--------------------------------|---------------------|
| 3                            | 4.20                           | 280                 |
| 5                            | 5.13                           | 274                 |
| 8                            | 5.69                           | 292                 |
| 10                           | 6.25                           | 283                 |
| 12                           | 4.74                           | 285                 |

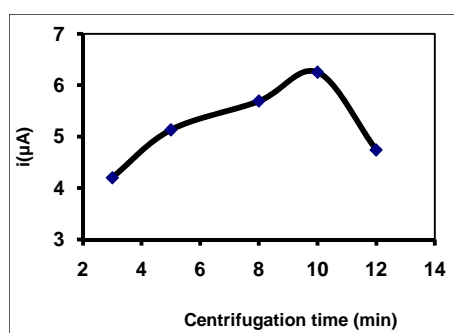


**Figure 3.31.** The influence of the centrifugation time on the peak currents for the solution containing  $1 \times 10^{-7}$  M  $\text{Hg}^{2+}$  in 0.5 M  $\text{HClO}_4$  (pH: 7.50,  $m_r$ : 6.0 mg,  $t_{\text{ads}}$ : 20 min,  $v_{\text{cent}}$ : 3000 rpm).

But, the change in the peak current level, in the time interval when this parameter was studied, was relatively smaller when compared to changes in the current levels when other parameters were examined (Figure 3.25, 3.27, 3.29 and 3.31). In other words, it was concluded that the duration of centrifugation was not a significant factor and the duration of 10 minute centrifuge time intervals were applied to subsequent experiments.

### 3.3.5. Effect of Centrifugation Speed (with carrier material)

It's expected that the resulting peak currents related to mercury ions will increase since the probability of smaller particles reaching the electrode surface will be high with the increasing speed of centrifugation and with the use of

Purolite C100 of 45  $\mu\text{m}$  or smaller, used in the studies. In this study, the effect of centrifugation speed in the range of 500 – 3000 rpm was investigated (Figure 3.32) and the increase in the peak current was observed, as anticipated (Table 3.13 and Figure 3.33). Despite that, the centrifugation speed was not increased to a higher level in order to prevent a possible damage to the centrifuge device.

The increase in the obtained peak current levels, at the studied centrifugation speeds, is especially significant when compared to the duration of centrifugation process. This situation shows that the speed of centrifugation is a more significant parameter than the duration.

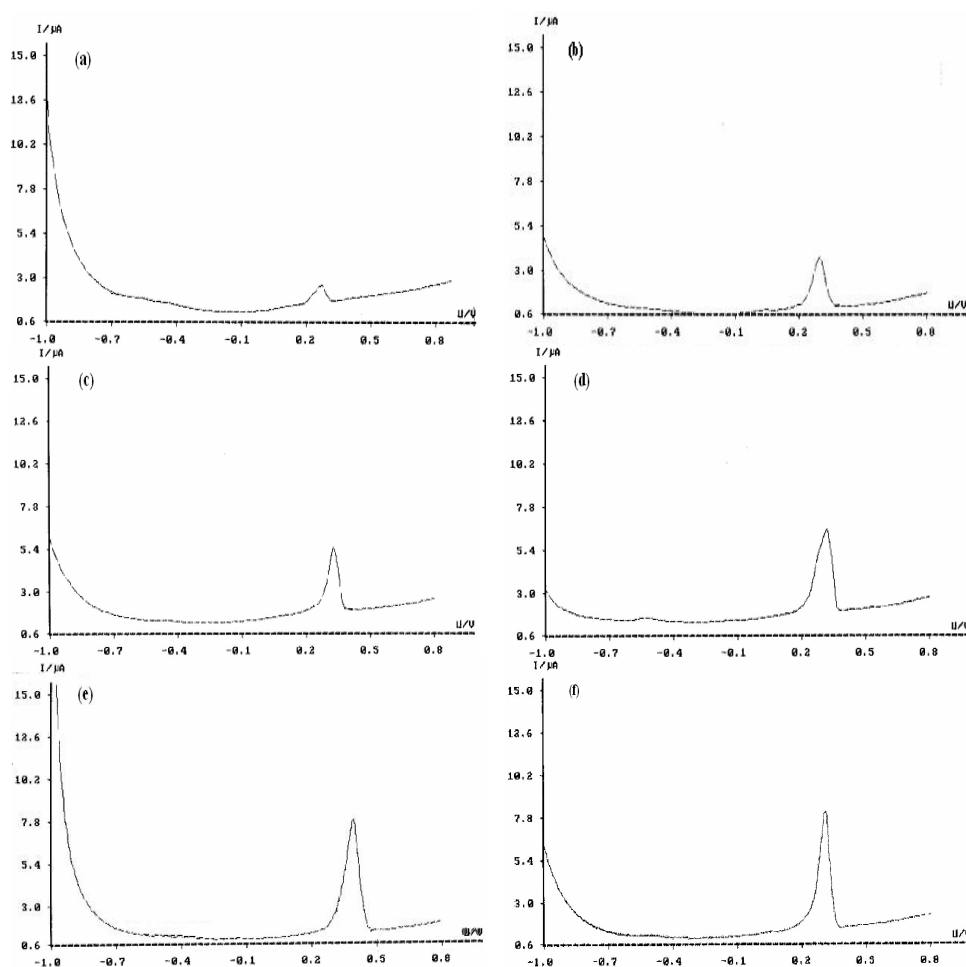


**Figure 3.32.** The effect of centrifugation speed on the peak currents for the solution containing  $1 \times 10^{-7}$  M  $\text{Hg}^{2+}$  in 0.5 M  $\text{HClO}_4$  (pH: 7.50,  $m_r$ : 6.0 mg,  $t_{\text{ads}}$ : 20 min,  $t_{\text{cent}}$ : 10 min).  $v_{\text{cent}}$ : (a) 500, (b) 1000, (c) 1500, (d) 2000, (e) 2350, (f) 3000 rpm.

**Table 3.13.** The effect of centrifugation speed on the peak currents for the solution containing  $1 \times 10^{-7}$  M  $\text{Hg}^{2+}$  in 0.5 M  $\text{HClO}_4$ .

| Speed of centrifugation (rpm) | Peak current ( $\mu\text{A}$ ) | Peak Potential (mV) |
|-------------------------------|--------------------------------|---------------------|
| 500                           | 0.99                           | 280                 |
| 1000                          | 2.67                           | 295                 |
| 1500                          | 3.42                           | 333                 |
| 2000                          | 4.48                           | 324                 |
| 2350                          | 5.80                           | 335                 |
| 3000                          | 6.64                           | 314                 |

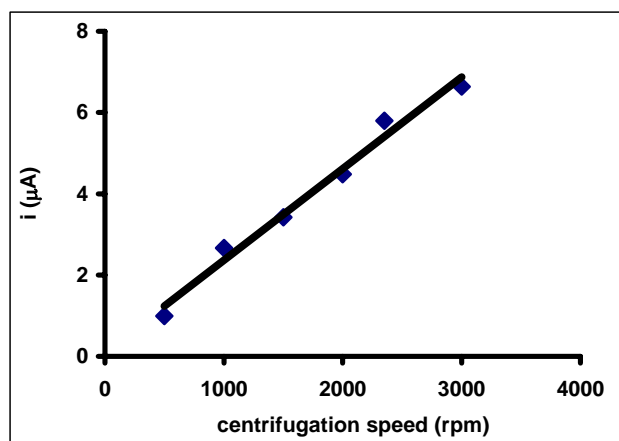


**Figure 3.33.** The effect of centrifugation speed on the peak currents for the solution containing  $1 \times 10^{-7}$  M  $\text{Hg}^{2+}$  in 0.5 M  $\text{HClO}_4$  (pH: 7.50,  $m_r$ : 6.0 mg,  $t_{\text{ads}}$ : 20 min,  $t_{\text{cent}}$ : 10 min)

### 3.3.6. Effect of Sweep Rate of Potential (with carrier material)

The effect of the sweep rate of potential was examined at the rates of 10, 20, 30 and 40  $\text{mVs}^{-1}$ . The obtained voltammograms in this range were shown in Figure 3.34 for  $1 \times 10^{-9}$  M  $\text{Hg}(\text{II})$  solution.

The peak currents values obtained from voltammograms in Figure 3.34 were demonstrated in Table 3.14 and Figure 3.35. As can be seen clearly, the sweep rate of potential has an important impact on the peak currents. The values of peak currents were significantly decreased when the sweep got faster. This can be attributed to the insufficiently mass transfer to the electrode surface from the resin. The highest peak currents values were obtained at 10  $\text{mVs}^{-1}$  and the further experiments were carried out at this rate.

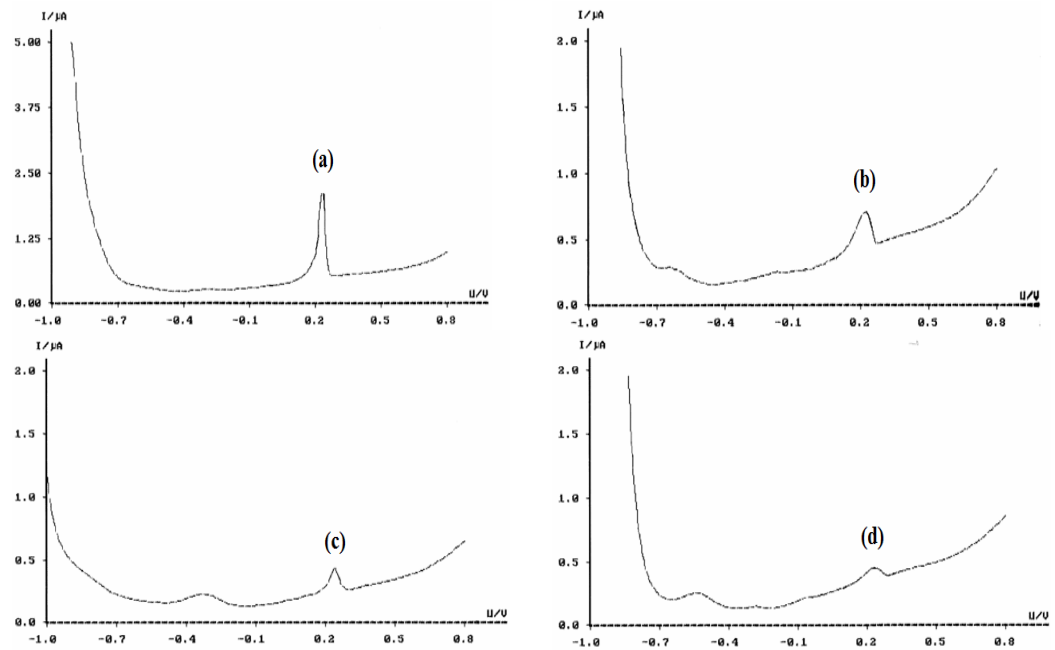


**Figure 3.34** The influence of sweep rate centri-voltammetric results for the solution containing  $1 \times 10^{-9}$  M  $\text{Hg}^{2+}$  in 0.5 M  $\text{HClO}_4$  (pH: 7.50,  $m_r$ : 6.0 mg,  $t_{\text{ads}}$ : 20 min,  $t_{\text{cent}}$ : 10 min,  $v_{\text{cent}}$ : 3000 rpm), sweep rate: (a) 10, (b) 20, (c) 30, (d)  $40 \text{ mVs}^{-1}$ .

**Table 3.14.** The influence of sweep rate centri-voltammetric results for the solution containing  $1 \times 10^{-9}$  M  $\text{Hg}^{2+}$  in 0.5 M  $\text{HClO}_4$

| Sweep rate ( $\text{mVs}^{-1}$ ) | Peak current (nA) | Peak Potential (mV) |
|----------------------------------|-------------------|---------------------|
| 10                               | 1580              | 276                 |
| 20                               | 267               | 276                 |
| 30                               | 167               | 282                 |
| 40                               | 92                | 268                 |

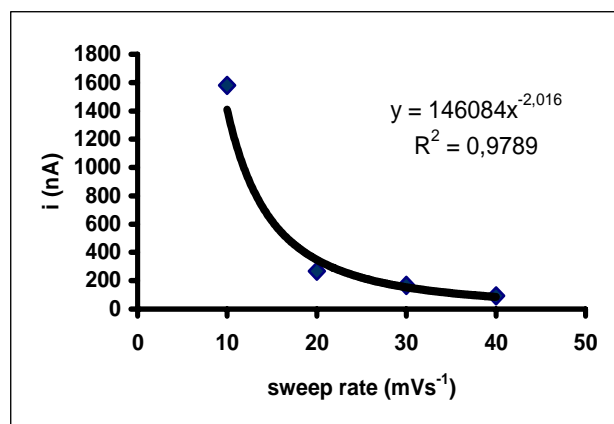


**Figure 3.35.** The influence of sweep rate centri-voltammetric results for the solution containing  $1 \times 10^{-9}$  M  $\text{Hg}^{2+}$  in 0.5 M  $\text{HClO}_4$  (pH: 7.50,  $m_r$ : 6.0 mg,  $t_{\text{ads}}$ : 20 min,  $t_{\text{cent}}$ : 10 min,  $v_{\text{cent}}$ : 3000 rpm).

### 3.3.7. Effect of Sweep Range of Potential (with carrier material)

In order to see the effects of sweep range of potential was exercised by narrowing the potential range for  $1 \times 10^{-9}$  M Hg(II) solution. The obtained voltammograms for these ranges were shown in Figure 3.36 for  $1 \times 10^{-9}$  M Hg(II) solution.

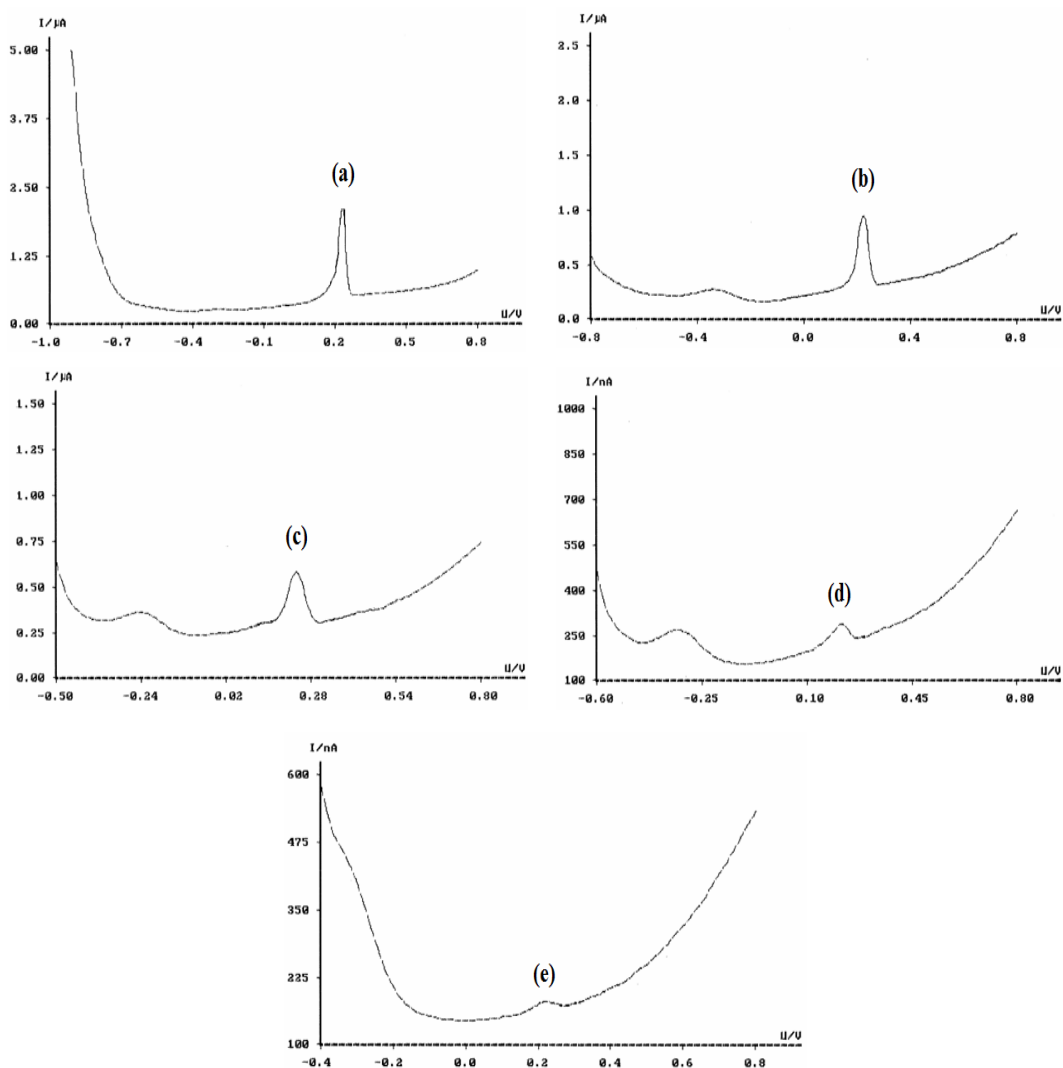


**Figure 3.36.** The effect of sweep range on the peak currents for the solution containing  $1 \times 10^{-9}$  M  $\text{Hg}^{2+}$  in 0.5 M  $\text{HClO}_4$  (pH: 7.50,  $m_r$ : 6.0 mg,  $t_{\text{ads}}$ : 20 min,  $t_{\text{cent}}$ : 10 min,  $v_{\text{cent}}$ : 3000 rpm), sweep range: (a) -1000 --+800, (b) -800 - +800, (c) -600 - +800, (d) -400 - +800, (e) -200 - +800 mV.

As seen on Figure 3.37 and Table 3.15, when the starting of potential sweep was less few negative than -1.0 V, the resulting peak current values were proportionally decreased. The graph which was drawn with obtained current



values versus initial potential values has exponential variations (Figure 3.37). This result can be attributed that Hg(II) ions in solution were firstly reduced, then formed metallic Hg at the electrode surface was reoxidized during potential sweep. Yet, the initial potential was shifted toward to less negative values, reduced Hg(II) amount was decreased. As a result of those observing peak current values becomes smaller. Increasing of the sweep rate, peak currents became smaller which is convenient with previous result.

The highest peak current value was reached between -1000 mV and +800 mV range of sweep on the positive direction and following studies were presented at this range.

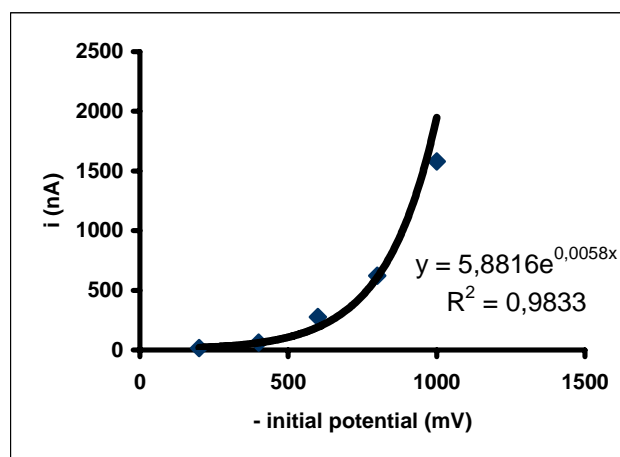


**Figure 3.37.** The effect of sweep range on the peak currents for the solution containing  $1 \times 10^{-9}$  M  $\text{Hg}^{2+}$  in 0.5 M  $\text{HClO}_4$ .

**Table 3.15.** The effect of sweep range on the peak currents for the solution containing  $1 \times 10^{-9}$  M  $\text{Hg}^{2+}$  in 0.5 M  $\text{HClO}_4$ .

| Sweep range (mV) | Peak current (nA) | Peak Potential (mV) |
|------------------|-------------------|---------------------|
| -200 - +800      | 15                | 275                 |
| -400 - +800      | 63                | 265                 |
| -600 - +800      | 275               | 277                 |
| -800 - +800      | 623               | 266                 |
| -1000 - +800     | 1580              | 278                 |

### 3.3.8. Resulting Peak Currents of Hg(II) in Optimum Conditions

The conditions were determined to obtain with Purolite C100 the highest levels of current related to mercury(II) ion by studying the largest possible intervals to investigate the effect of various parameters. The optimal parameters of the method were summarized in Table 3.16 and the obtained voltammograms under these conditions were given in Figure 3.38.

**Table 3.16.** The list of optimal working conditions for the procedure with a carrier material (Purolite C100).

| Experimental Parameters    | Optimal conditions |
|----------------------------|--------------------|
| pH                         | 7.50               |
| Adsorption duration        | 20 min             |
| Purolite C100 resin amount | 6.0 mg             |
| Centrifugation time        | 10 min             |
| Centrifugation speed       | 3000 rpm           |
| Mode                       | DP                 |
| Sweep rate ; U.step        | 10 mV/s ; 6 mV     |
| Pulse amplitude            | 50 mV              |
| Sweep range                | -1000 - + 800mV    |

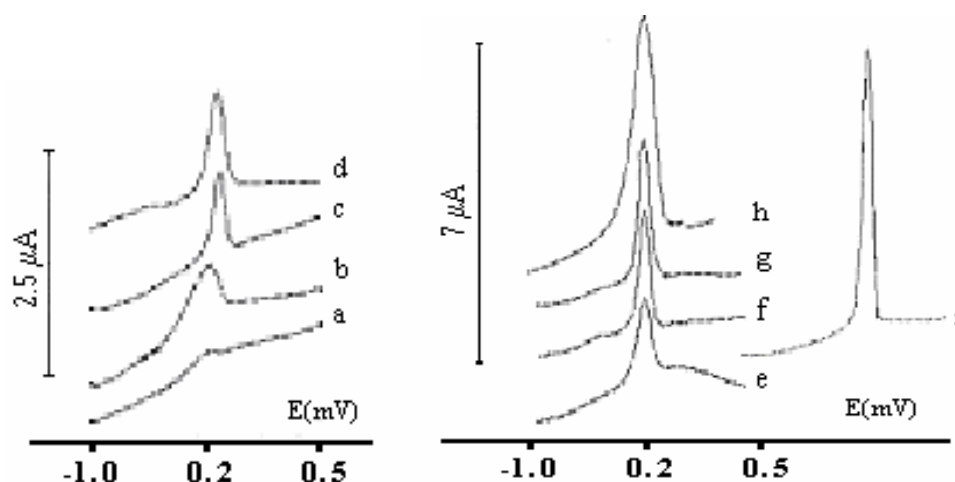


**Figure 3.38.** The effect of Hg(II) concentration on current values obtained with Purolite C100 under the optimized conditions (pH: 7.50,  $m_r$ : 6.0 mg,  $t_{ads}$ : 20 min,  $v_{cent}$ : 3000 rpm,  $t_{cent}$ : 10 min). Hg(II) concentrations: (a)  $1 \times 10^{-11}$ , (b)  $5 \times 10^{-11}$ , (c)  $1 \times 10^{-10}$ , (d)  $5 \times 10^{-10}$ , (e)  $1 \times 10^{-9}$ , (f)  $5 \times 10^{-9}$ , (g)  $1 \times 10^{-8}$ , (h)  $5 \times 10^{-8}$ , (i)  $1 \times 10^{-7}$  M.

Calibration curve of Hg(II) concentrations ranging from  $1.0 \times 10^{-7}$  M to  $5.0 \times 10^{-11}$  M was found in a logarithmically linear fashion with the equation as follows:  $\text{Log}i_p = -0.3047\text{Log}C_{\text{Hg(II)}} + 5.9119$ . Its regression coefficient was ( $R^2$ ) 0.9937 (Table 3.17, Figure 3.39).

**Table 3.17.** The effect of Hg(II) concentration on current values obtained with Purolite C100 under the optimized conditions.

| Concentration of Hg(II) (M) | Peak current (nA) |
|-----------------------------|-------------------|
| $1 \times 10^{-11}$         | 198               |
| $5 \times 10^{-11}$         | 551               |
| $1 \times 10^{-10}$         | 794               |
| $5 \times 10^{-10}$         | 1120              |
| $1 \times 10^{-9}$          | 1610              |
| $5 \times 10^{-9}$          | 2380              |
| $1 \times 10^{-8}$          | 3060              |
| $5 \times 10^{-8}$          | 4510              |
| $1 \times 10^{-7}$          | 6250              |

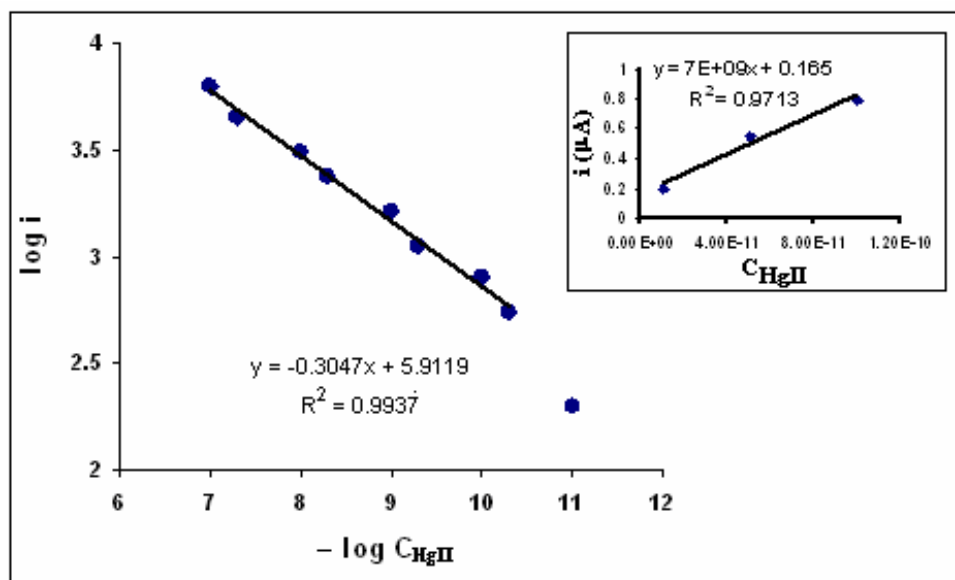


**Figure 3.39.** The calibration graph for Hg(II) ions in 0.5 M HClO<sub>4</sub> obtained with Purolite C100 under the optimal conditions.

### 3.4. Validation of Centri-voltammetric Methods

Method validation is one of the measures universally recognized as a necessary part of a comprehensive system of quality assurance in analytical chemistry.

A reference method can in principle be used to test for bias in another method under validation. This is a useful option when checking an alternative to, or modification of, an established standard method already validated and in use in the laboratory. Both methods are used to analyze a typical test material, preferably covering a useful range of concentration fairly evenly. Comparison of the results over the range by a suitable statistical would demonstrate any bias between the methods (IUPAC, 2002).

Validation parameters such as linear range, limit of detection, accuracy, precision and selectivity were investigated.

#### 3.4.1. Linearity and Limit of Detection

Calibration data and graphs related to centri-voltammetric method by using hydrazine and Purolite C100 were given in the section 3.2.7 and 3.3.6 respectively. Calibration curves of hydrazine and Purolite C100 show a *logarithmically* linear behaviour with regression coefficients of 0.9869 and 0.9937, respectively. In addition, the linear ranges were  $1.0 \times 10^{-8}$  M to  $1.0 \times 10^{-10}$  M and  $1.0 \times 10^{-7}$  M to  $5.0 \times 10^{-11}$  M for hydrazine and Purolite C100, respectively. These results were compared with previously work which was achieved centri-voltammetric mercury analysis by using borohydride (Ürkmez et al., 2009) and the combined graphs were given in Figure 3.40.

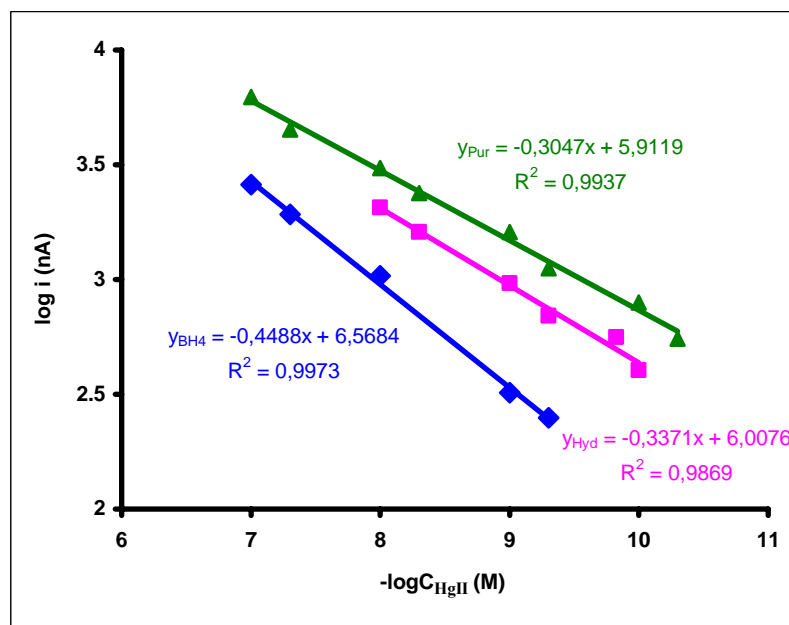


**Figure 3.40.** The comparison of calibration graphs. Without carrier material: (  $\blacklozenge$  ) borohydride and (  $\blacksquare$  ) hydrazine as a reducing agent, with carrier material: (  $\blacktriangle$  ) Purolite C100.

As can be seen from the calibration graph, along with the slopes are not very different the widest concentration range is reached when Purolite C100 was used.

The minimum Hg(II) concentrations, measured by developed centri-voltammetric method are  $5.0 \times 10^{-10}$ ,  $1.0 \times 10^{-10}$  and  $5.0 \times 10^{-11}$  M, by using borohydride, hydrazine and Purolite C100, respectively (Figure 3.40). First and second of these concentrations values that are achieved by both reducing agents and by utilization of “*centrifuge cell*”, which was designed in the previous work period are close to each other. But, the splitting of peak in small Hg(II) concentrations, when borohydride is used, creates a problem and restricts limit of detection. Such an issue is non-existent when hydrazine is used, as well as, the study with hydrazine is more practical. But in both applications, the preparation step of gold film electrode prolongs the process time.

It has been possible to reach Hg(II) levels of as low as  $5 \times 10^{-11}$  M, in studies, when Purolite C100 resin was used as a carrier material and without a reduction reaction. The sensitivity has been improved even further on studies that utilized

“the centri-voltammetric cell” that was newly introduced (Figure 2.3). The use of a bare GCE in studies with Purolite C100 has shortened the procedure. Aside from those, the method is more economical based on chemicals, and the sensitivity can be improved since greater current levels are obtained in the solutions with the same concentration levels (Figure 3.40).

Additionally, the obtained results for  $1 \times 10^{-9}$  M Hg(II) with centri-voltammetry was compared with ASV which was carried out given below procedure, at the same  $\text{Hg}^{2+}$  concentration (Table 3.18).

The ASV procedure consisted of the following steps: (a) The analysis was performed without oxygen for this reason solutions were deaerated with nitrogen for 300 s before the measurement, (b) glassy carbon electrode was scanned at potential range of +200 to +750 mV in stripping solution (1.0 M  $\text{HClO}_4$  + 0.35 M HCl), (c) formed gold film electrode on GC electrode surface ( $2.5 \times 10^{-5}$  M  $\text{Au}^{3+}$ , deposition time 300 s and deposition potential -800 mV), (d) adding  $1 \times 10^{-9}$  M  $\text{Hg}^{2+}$  and 0.1 M  $\text{HClO}_4$  supporting electrolyte, (e)  $E_{\text{dep}}$ : -800 mV,  $t_{\text{dep}}$ : 300 s for mercury at stirring solution, (f) The stripping step was performed with differential puls mode potential scanned at +200 to +750 mV in stripping solution (1.0 M  $\text{HClO}_4$  + 0.35 M HCl).

**Table 3.18.** Comparison of Centri-Voltammetric method with ASV for  $1 \times 10^{-9}$  M  $\text{Hg}^{2+}$

| Method   | Electrode | Peak current (nA) | Peak Potential (mV) |
|--|-----------|-------------------|---------------------|
| ASV  | GFE       | 146               | 504                 |
| Centri-Voltammetry with hydrazine without carrier material   | GFE       | 963               | 497                 |
| Centri-Voltammetry with Purolite C 100 as a carrier material | GCE       | 1610              | 263                 |

In Table 3.18, for first and second of these methods although on voltammograms there is not much difference between the peaks potential values, centri-voltammetric peak current value (obtained with hydrazine) was much more

(~6.5 times) than the current values obtained by ASV. In the both of them, since GFE was used, the stripping of metallic mercury from formed amalgam at electrode surface was also carried out at about same potential. The reason of increasing of peak current in second method was the preconcentration procedure carried out via centrifugation.

On the other hand, in the third method, not only the current value was bigger than current value obtained by other methods but also its peak potential value was more negative than that of other methods. In this method working electrode was GCE and mercury ions came close to electrode surface as sorbed to Purolite C100. Therefore, during the potential scanning these ions were first reduced metallic form and then they were reoxidized from electrode surface. It was thought that because of that Hg(II) ions which bonded to Purolite C100 were brought closer to electrode surface by centrifugation, mass transfer (on diffusion conditions) to the electrode was increased. Due to the efficiency of this preconcentration procedure current has increased 11 times than ASV.

**Table 3.19.** Successive current values for  $5.0 \times 10^{-11}$  M mercuric ions solution under the optimized conditions for Purolite C100. s: standard deviation.

| n          | 1   | 2   | 3   | 4   | 5   | 6   | 7   | s          | RSD% |
|------------|-----|-----|-----|-----|-----|-----|-----|------------|------|
| $i_p$ (nA) | 551 | 487 | 535 | 550 | 484 | 499 | 548 | $\pm 30.7$ | 5.9  |

Limit of detection (LOD) of centri-voltammetric analysis using Purolite C100 was determined according to the signal of minimum measurable concentration for Hg(II) due to no signal in blank experiment. By this purpose, seven ( $n$ ) successive replicates were carried out using a solution of the minimum concentration at calibration graph ( $5.0 \times 10^{-11}$  M Hg(II) ) under optimized conditions (Table 3.19 ). LOD was calculated as  $1 \times 10^{-13}$  M from the standard deviation (3s) of peak current values and  $\log i_p = -0.3047 \log C_{\text{Hg(II)}} + 5.9119$ . Limit of quantification (LOQ) was similarly calculated as  $5.8 \times 10^{-12}$  M from the standard deviation (10s).

### 3.4.2. Accuracy

To test the accuracy, ICP-MS measurement was used in this study. Although ICP-OES and CV-AAS are the most used techniques in the determination of traces of mercury, the low concentration level of mercury in water is not compatible with the detection limit of these techniques. In order to achieve accurate, reliable and sensitive results, preconcentration and separations are needed when the concentrations of analytes in the sample are too low to be determined directly by ICP-OES, even with mercury vapor generation or ICP-MS.

A standard sample containing a Hg(II) concentration of  $5.0 \times 10^{-9}$  M ( $1.0 \mu\text{g L}^{-1}$ ) was used to test the accuracy of the centri-voltammetric analysis method using Purolite C100 and hydrazine. The obtained results were compared with ICP-MS measurements and given Table 3.20. Relative percentage errors of the proposed methods were 6.3% and 10.3%, respectively while that of ICP-MS was 2.8%. This accuracy level is quite good.

**Table 3.20.** Comparison of the result of accuracy testing

| Method                   | $C_{\text{Std}} (\mu\text{g L}^{-1})$ | $C_{\text{found}} (\mu\text{g L}^{-1})$ | $e_{\text{rel}}\%$ |
|--------------------------|---------------------------------------|---|--------------------|
| With ICP-MS (201 Hg)     | 1.0                                   | 1.028                                   | +2.8               |
| With hydrazine (n=3)     | 1.0                                   | 0.894                                   | -10.6              |
| With Purolite C100 (n=3) | 1.0                                   | 0.937                                   | -6.3%              |

$C_{\text{Std}}$ : standard concentration;  $C_{\text{found}}$ : experimentally found standard concentration  
 $e_{\text{rel}}\%$ : relative percentage error.

### 3.4.3. Precision

To examine the repeatability, six ( $n$ ) successive replicates were carried out in a solution of  $1.0 \times 10^{-9}$  M Hg(II) under optimized conditions (Table 3.21). The relative standard deviations (RSD) for the centri-voltammetric method using hydrazine and Purolite C100 were calculated as 1.39% and 1.78%, respectively. As anticipated, these RSD values are smaller than our previous study (13.2%,



Ürkmez et al., 2009). As the hydrazine is liquid the measurement are applied easily, after the reaction there are no missing and neither hydrazine nor oxidation products are left in the medium, the results are reproducible.

**Table 3.21.** Successive current values for  $1.0 \times 10^{-9}$  M mercuric ions solution under the optimized conditions for hydrazine and Purolite C100, s: standard deviation.

| Method        | n             | 1    | 2    | 3    | 4    | 5    | 6    | s          | RSD% |
|---------------|---------------|------|------|------|------|------|------|------------|------|
| Hydrazine     | $i_p$<br>(nA) | 963  | 992  | 957  | 960  | 958  | 960  | $\pm 13.4$ | 1.39 |
| Purolite C100 |               | 1610 | 1600 | 1640 | 1660 | 1580 | 1610 | $\pm 28.8$ | 1.78 |

However, the centri-voltammetric mercury analysis with Purolite C100 is preferred since the linear concentration range of calibration graph is larger and the procedure is shortened due to a smaller number of step than other applications.

#### 3.4.4. Selectivity

Many times, in the commonly used supporting electrolytes, the reduction peak potentials of each metal are very close, and thus the simultaneous voltammetric determination of neighboring elements would be hindered. However, as well known, the voltammetric interference problems are fundamentally linked to the concentration ratios between the two neighboring elements (Locatelli and Melucci, 2010; Locatelli and Torsi, 2003). In the case of Hg(II) voltammetric determination, the more important interfering, qualitatively investigated already by Hatle (1987), seems to be Cu(II). In this study, the interference is strictly linked to the Hg(II) - foreign ions (Cu(II), Pb(II), Cd(II), Fe(III)) concentration ratios.

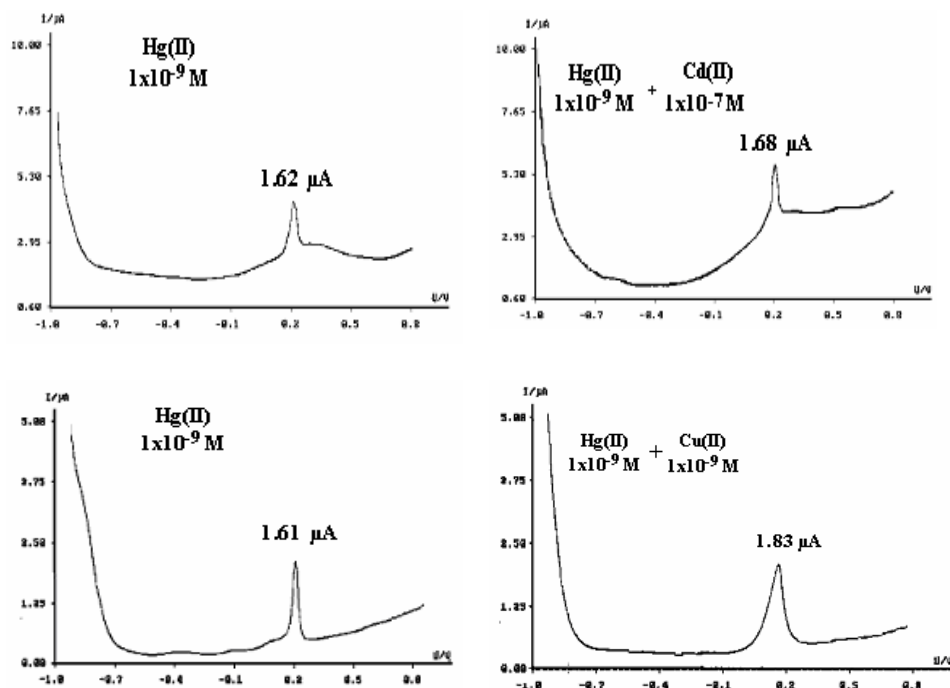
The possible interference of Cd(II), Pb(II), Cu(II) and Fe(III) on the mercury signals was evaluated and the results were given in Table 3.22.

**Table 3.22.** The effects of some foreign ions to the signal of  $1 \times 10^{-9}$  M Hg(II).

| Concentration (M)     | Cations          |                  |                  |                  |
|-----------------------|------------------|------------------|------------------|------------------|
|                       | Cd <sup>2+</sup> | Pb <sup>2+</sup> | Cu <sup>2+</sup> | Fe <sup>3+</sup> |
| $1.0 \times 10^{-6}$  |                  |                  | +                | +                |
| $1.0 \times 10^{-7}$  | -                | +                | +                | -                |
| $1.0 \times 10^{-9}$  | -                | +                | +                |                  |
| $5.0 \times 10^{-10}$ |                  | -                | -                |                  |
| $1.0 \times 10^{-10}$ |                  | -                | -                |                  |

+ : interference effect was observed; - : interference effect was not observed

When these ions concentration is more dilute than  $1 \times 10^{-9}$  M, it was not observed any interference effect. For example, as these ions concentration is  $1 \times 10^{-7}$  M in the cell, although Pb(II) and Cu(II) interferences were observed Fe(III) and Cd(II) interferences were not observed. However, in the presence of  $1 \times 10^{-6}$  M Fe(III) ions, the peak of Fe(III) was also observed (Figure 3.41).



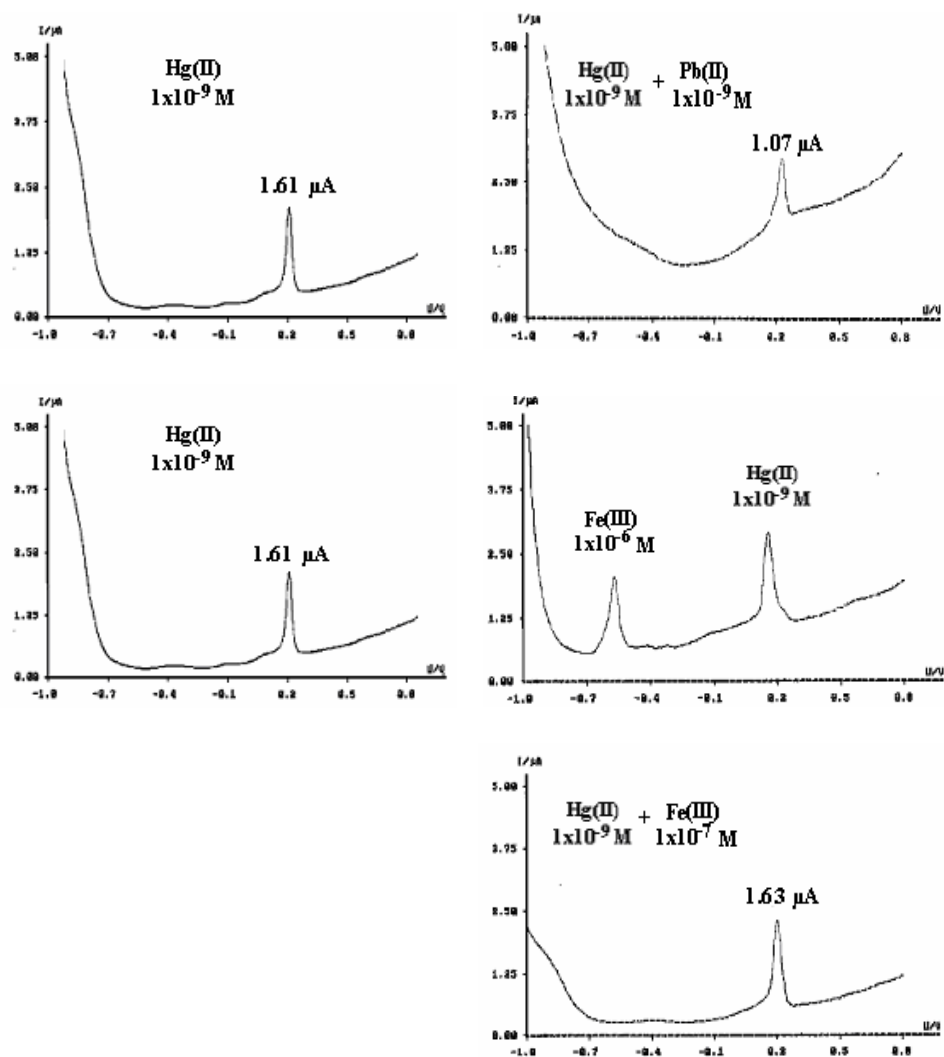


**Figure 3.41.** Investigation of interfering effect of some foreign ions for  $1 \times 10^{-9}$  M Hg(II).

### 3.5. Analytical Applications

This method was applied to mercury(II) analysis in two different spring water samples which were collected from Saip and Ambarseki villages (Karaburun, İzmir) and they were stored by acidified with  $\text{HClO}_4$ .

Standard additions were applied to these water samples diluted 100 fold with centri-voltammetry using Purolite C100 in optimum experimental conditions. Obtained voltammograms were given in Figure 3.42.

The data obtained from these voltammograms and plotted standard addition graph were given in Table 3.23 and Figure 3.43.

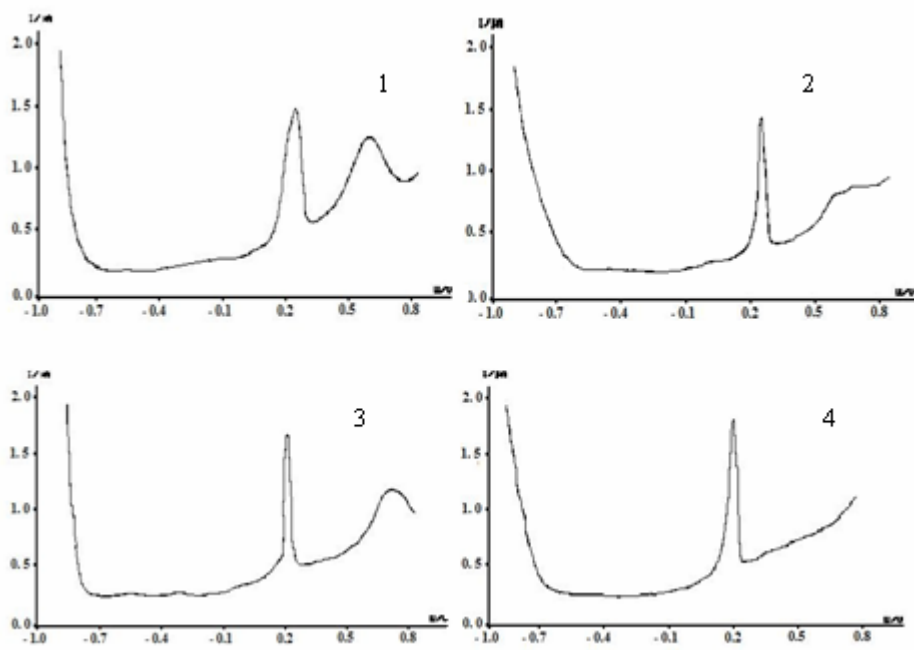


**Figure 3.42.** Voltammograms of standard addition experiments for (1) Sample I, (2) Sample I +  $1.5 \times 10^{-11}$  M, (3) Sample I +  $3.0 \times 10^{-11}$  M, (4) Sample I +  $5.0 \times 10^{-11}$  M Hg(II) in the cell.

**Table 3.23.** The results of standard addition to Sample I.

| Sample I | $C_{\text{standard}}$ (M) | $I_{\text{peak}}$ (nA) | E (mV) | Recovery % |
|----------|---------------------------|------------------------|--------|------------|
|          | 0                         | 950                    | 230    |            |
|          | $1.5 \times 10^{-11}$     | 1040                   | 233    | 76.1       |
|          | $3.0 \times 10^{-11}$     | 1150                   | 239    | 82.9       |
|          | $5.0 \times 10^{-11}$     | 1210                   | 227    | 80.6       |

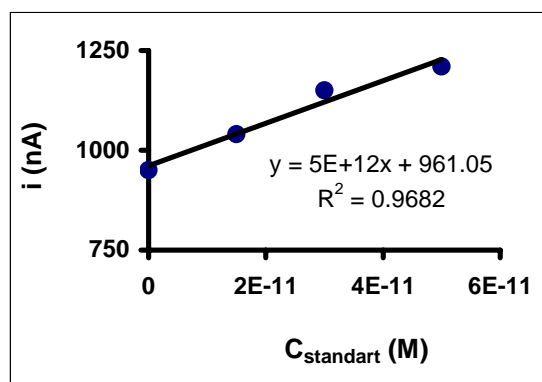


**Figure 3.43.** Standard addition graph for Sample I.

Similar procedures were also applied to the Sample II. Obtained voltammograms, data and plotted standard addition graph were shown in Figure 3.44, Table 3.24 and Figure 3.45, respectively.

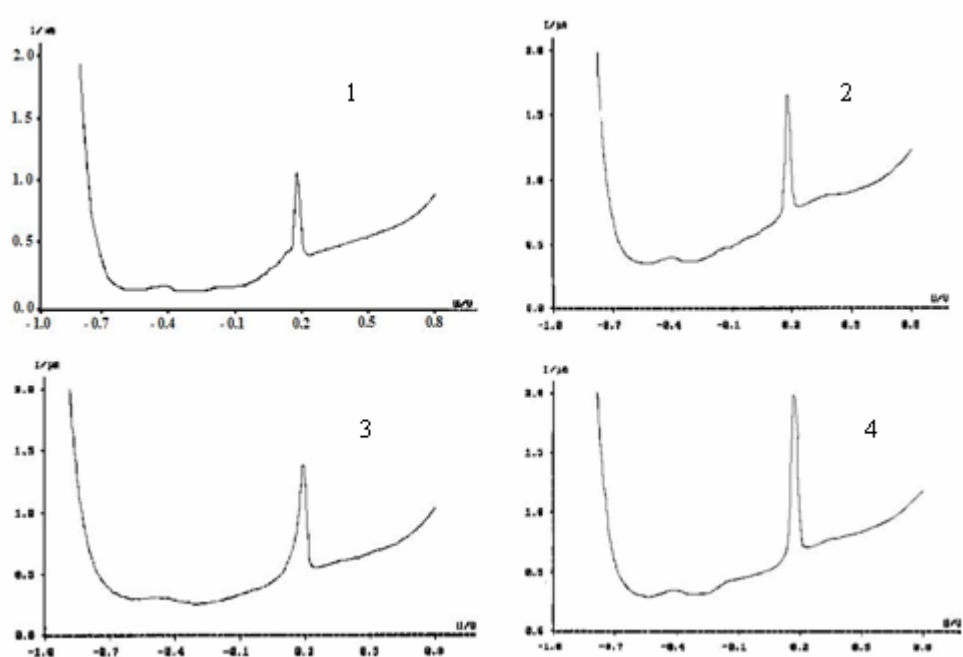


**Figure 3.44.** Voltammograms of standard addition experiments for (1) Sample II, (2) Sample II +  $1.5 \times 10^{-11}$  M, (3) Sample II +  $3.0 \times 10^{-11}$  M, (4) Sample II +  $5.0 \times 10^{-11}$  M Hg(II) in the cell.

**Table 3.24.** The results of standard addition to Sample II.

|           | $C_{\text{standard}}$ (M) | $I_{\text{peak}}$ (nA) | E (mV) | Recovery % |
|-----------|---------------------------|------------------------|--------|------------|
| Sample II | 0                         | 567                    | 189    |            |
|           | $1.5 \times 10^{-11}$     | 770                    | 195    | 78.3       |
|           | $3.0 \times 10^{-11}$     | 925                    | 185    | 92.1       |
|           | $5.0 \times 10^{-11}$     | 1330                   | 173    | 118.9      |

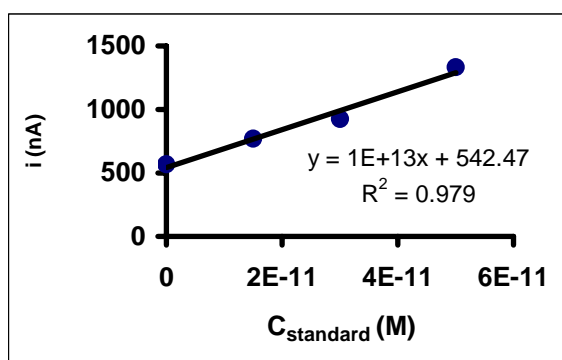


**Figure 3.45.** Standard addition graph for Sample II.

To prove the accuracy of mercury analysis with the developed centri-voltammetric method it should be compare with a valid method such as ICP-OES

combined on-line hydride generation kit. For that reason, firstly, Cu(II), Pb(II), Cd(II) and Hg(II) contents of spring water samples non diluted were also measured with ICP-OES to evaluate their interfering effects. The results were given in Table 3.25 and obtained values of Hg(II) were also shown as comparative centri-voltammetric results in Table 3.26.

**Table 3.25.** ICP-OES results of the determination of Cu(II), Pb(II) and Cd(II) in spring water samples.

|                  | <b>Cd<sup>2+</sup> (M)</b> | <b>Cu<sup>2+</sup> (M)</b> | <b>Pb<sup>2+</sup> (M)</b> |
|------------------|----------------------------|----------------------------|----------------------------|
| <b>Sample I</b>  | $7.49 \times 10^{-9}$      | $3.20 \times 10^{-8}$      | $1.13 \times 10^{-8}$      |
| <b>Sample II</b> | $2.60 \times 10^{-9}$      | $3.20 \times 10^{-8}$      | $6.17 \times 10^{-9}$      |

**Table 3.26.** Comparison of the obtained mercury(II) concentrations with centri-voltammetry using Purolite C100 and ICP-OES in spring water samples.

|                  | <b>Centri-Voltammetry</b> | <b>ICP-OES</b>          | <b>Absolute Difference</b> | <b>Difference%</b> |
|------------------|---------------------------|-------------------------|----------------------------|--------------------|
| <b>Sample I</b>  | $5.42 \times 10^{-9}$ M   | $4.87 \times 10^{-9}$ M | $0.55 \times 10^{-9}$ M    | 11                 |
| <b>Sample II</b> | $1.92 \times 10^{-8}$ M   | $1.88 \times 10^{-8}$ M | $0.04 \times 10^{-8}$ M    | 2                  |

It was shown that difference percent was higher on the Sample I. Its reason was that Pb(II) ions of this sample had a higher concentration. As to concentration of Cd(II) ions there was not an interference affect. Possible interference effects were removed by diluted 100 fold of spring water samples before centri-voltammetric analysis. Because the concentrations of Cu(II), Pb(II) and Cd(II) cations in spring water samples are more concentrated than  $1 \times 10^{-9}$  M according to ICP-OES measurement. This dilute ratio was not hindered mercury(II) centri-voltammetric analysis and vicinity of obtained results is advantage of developed method in terms of sensitivity. The determined mercury concentration for Sample I and II is in drinking water tolerance level. Regarding to drinking water the maximum contamination levels for inorganic mercury are set to 6 µg/L according to World Health Organization (WHO, 2008)

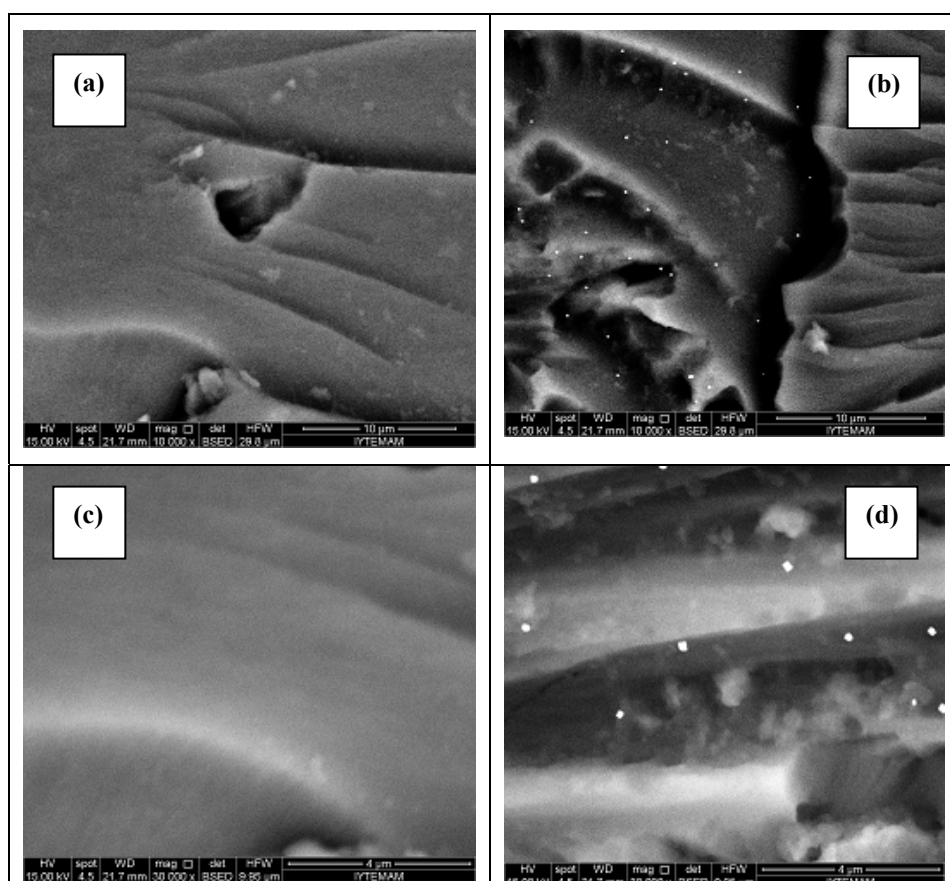
Average recovery values for Sample I and II was calculated as 79.9% and 96.5 %, respectively. These values were proved that the developed centri-voltammetric method by using Purolite C100 was reliable.

### 3.6. Investigation of Surface of Electrodes and Purolite C100 Resin

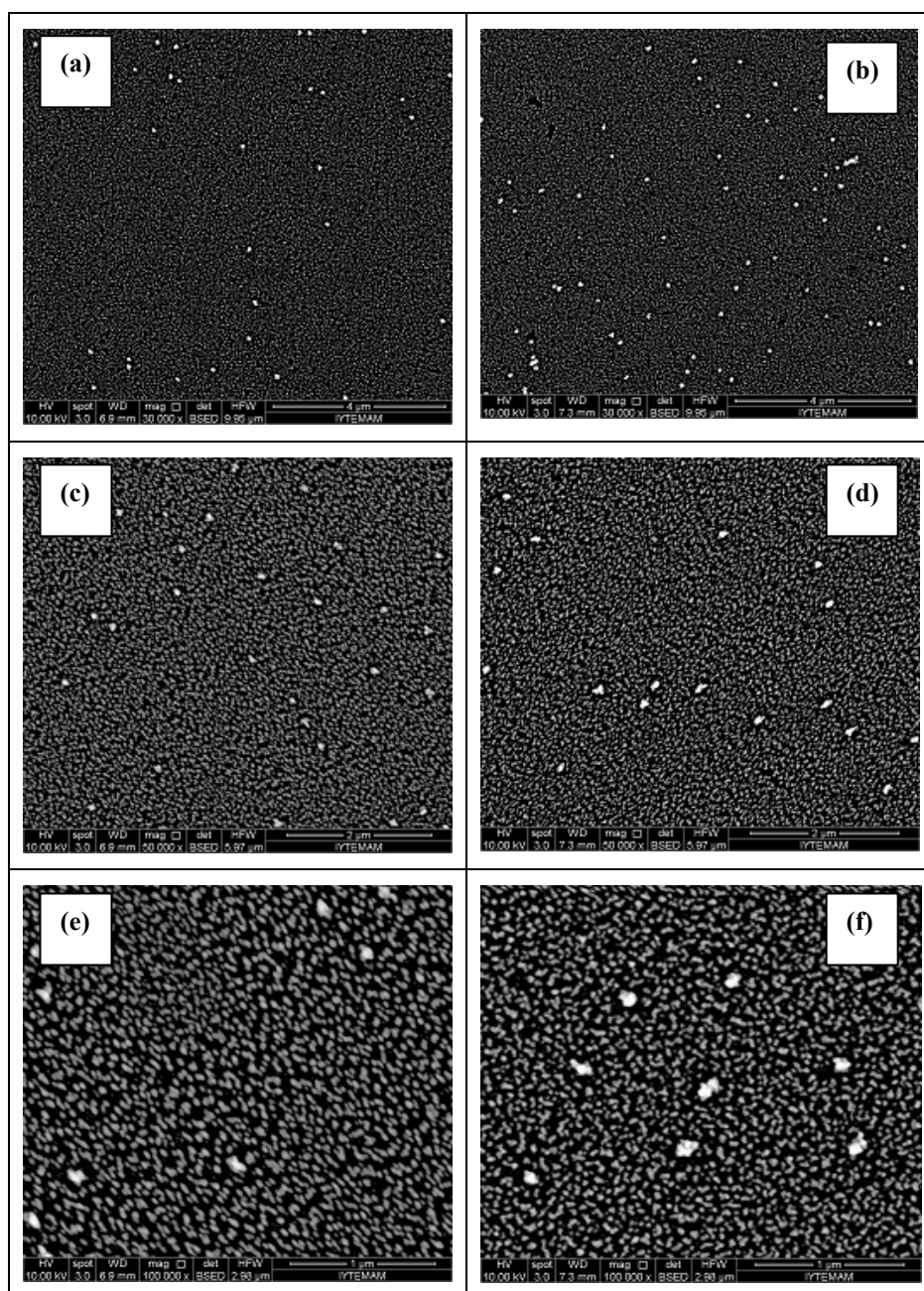
The interactions of Purolite C100 resin and gold film surface with mercury were investigated using scanning electron microscopy (SEM) and atomic force microscopy (AFM).

Although the Purolite C100 resin is not selective for mercury ions, it is observed that sorption of mercury(II) ions was occurred (Figure 3.46).

As seen from SEM images related to interaction of gold film surface with metallic mercury droplets which was formed reducing mercury(II) ions with hydrazine, a marked difference was not able to observe in terms of the surface images (Figure 3.47). It was attributed that atomic numbers of mercury and gold elements are close (Au 79, Hg 80).



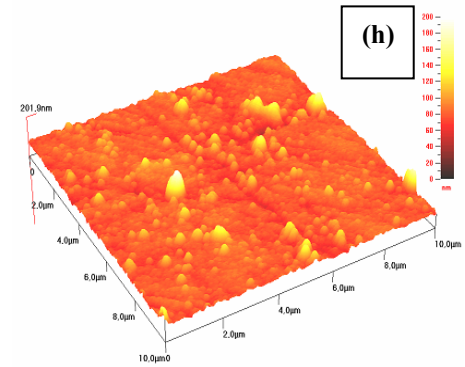
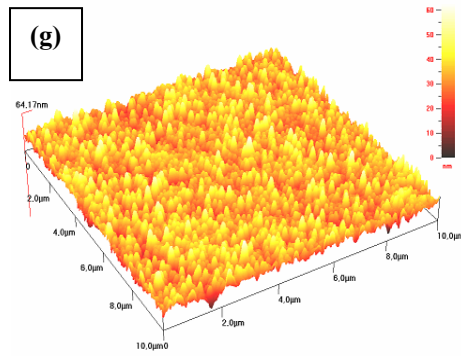
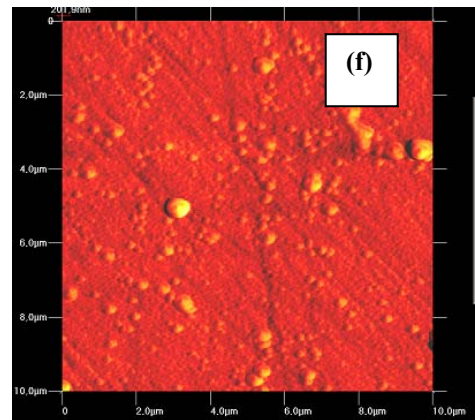
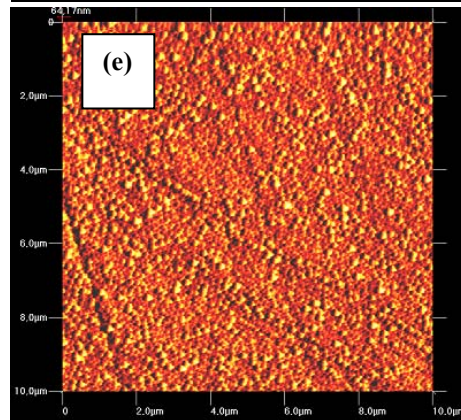
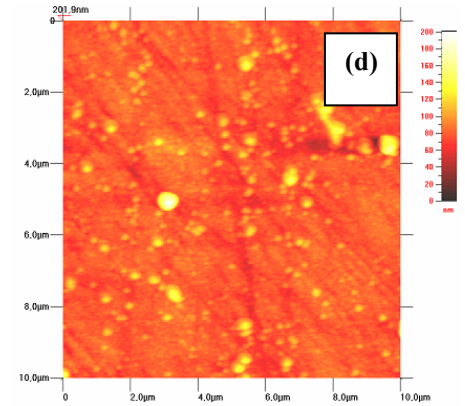
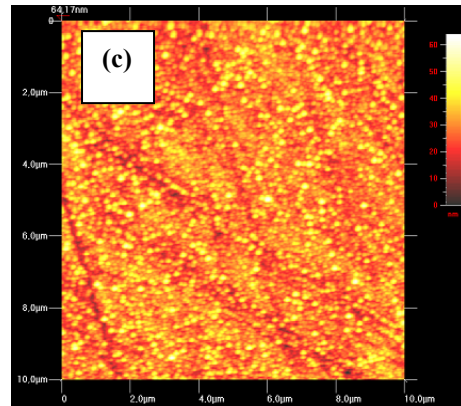
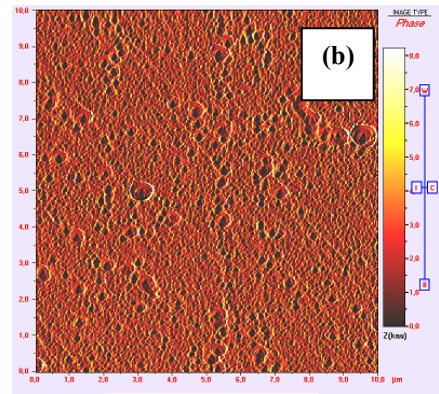
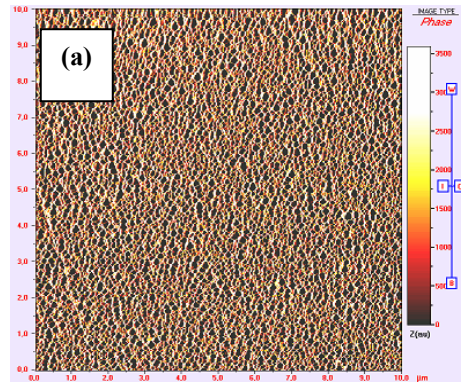
**Figure 3.46.** SEM images of Purolite C100 resin before sorption (size  $\leq 45\mu\text{m}$ ) magnified by (a) 10000, (c) 30000 times, and after sorption of Hg (II) ions (b) 10000, (d) 30000 times. Under the experimental conditions  $\text{pH}$ : 7.50,  $m_r$  : 6.0 mg,  $t_{\text{ads}}$  : 20 min Hg(II) concentration:  $5 \times 10^{-8}$  M.



**Figure 3.47.** SEM images of gold film surface magnified by (a) 20000, (c) 50000, (e) 100000 times, and after applied centrifugation procedure to reduced mercury with hydrazine (b) 20000, (d) 50000, (f) 100000 times. Conditions of formation GFE:  $2.5 \times 10^{-5}$  M  $\text{Au}^{3+}$ , 0.5 M  $\text{HClO}_4$ ,  $E_{\text{dep}}$ : -500 mV and  $t_{\text{dep}}$ : 100 s. Experimental conditions ( $C_{\text{hdy}}$ : 0.07 M,  $\text{pH} < 1$  (0.5 M  $\text{HClO}_4$ ),  $t_{\text{cent}}$ : 7 min,  $v_{\text{cent}}$ : 3000 rpm,  $\text{Hg(II)}$  concentration:  $5 \times 10^{-8}$  M).

Firstly, AFM images were taken for gold film electrode surface which was formed under conditions given in Section 2.3.1.1. Then, AFM images of amalgamated electrode surface were taken after the centrifugation process was applied to reduced mercury with hydrazine (Section 2.3.1.2) in the presence of  $5 \times 10^{-8}$  M mercury(II) ions (Figure 3.48).





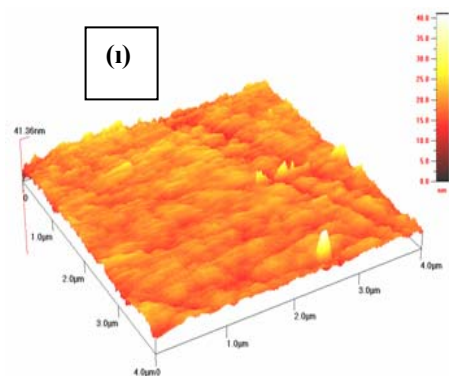


**Figure 3.48.** (a) Phase mode, (c) wave mode, (e) wave mode shaded, (g) wave mode 3D, of AFM images for GFE. (b) Phase mode, (d) wave mode, (f) wave mode shaded, (h) wave mode 3D, of AFM images for GFE after applied centrifugation procedure to reduced mercury with hydrazine, (i) bare GCE.

AFM images obtained in different modes of GFE surfaces were compared with absence (before centrifugation) and presence (after centrifugation) of metallic mercury in Figure 3.48. The initially roughness of GFE was 64.17 nm. The roughness value of 201.9 nm was obtained after centrifugation procedure was applied for  $5 \times 10^{-8}$  M mercury(II) concentration. This situation shows that the Hg particles, transformed to metallic form by reduction with hydrazine, were collected to the electrode surface via centrifugation and the surface was more roughness owing to amalgam with gold.

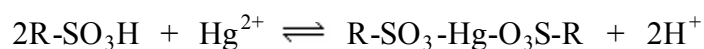
#### 4. CONCLUSION

High sensitivity of stripping techniques results from preconcentration of the analyte on the small volume of the microelectrode so the accumulation time, for relatively highly concentrated solutions, should be limited for avoiding saturation and the amount of deposited analyte should be kept about 2% of the bulk solution (Monk, 2002). In addition to this, the accumulation time must be long enough for the preconcentration process of dilute solutions to give a signal. It is evident that the peak current levels increase when more analyte is collected on the electrode surface. Also centri-voltammetric method provides the combined benefit of centrifugation and voltammetry. The significance difference and advantage of this method is that the preconcentrated analyte is not a small portion of the bulk solution as it is the usual case for ASV measurements.

In this thesis, to develop a method for more sensitive and reproducible determination of Hg(II) ions, it was intended that working with a reducing agent (hydrazine) and a carrier material (Purolite C100) which have never used in the centri-voltammetric method which implied the enrichment and separation procedures.

Mercury ions were first reduced to metallic mercury with hydrazine. Then, they were collected by a centrifugal force on the gold film electrode surface and applied stripping step ex-situ. Owing to the higher molecular weight of metallic mercury droplets was collected on GFE surface by creating amalgam with gold and by a centrifugation without any carrier material. This case was evidenced by the increased surface roughness of GFE in AFM images after centrifugation procedure. In these applications, reliable results are depended upon mainly on the performance of mercury reduction reaction and the reproducible the formation GFE and preconcentration step. The performance of hydrazine as a reducing agent was found better than NaBH<sub>4</sub> in the previously reported method (Ürkmez 2004; Ürkmez et al., 2009), especially aspect of reproducibility. When NaBH<sub>4</sub> was used, peak related to mercury was split and decreased; use of hydrazine has highly removed this splitting by adjusting initial pH of the reduction medium. Additionally, the peak current value of mercury was increased.

In second step of thesis, the centri-voltammetric method was applied with Purolite C100 that was non selective as a carrier materials for mercury ions. For this purpose, a new special cell named “centri-voltammetric cell” was designed. Interaction between the Hg(II) ions and Purolite C100 was allowed and then centri-voltammetric procedure was carried out in-situ. Resin enriched with mercury(II) was collected at the electrode surface by the aid of centrifugal forces. This situation was evidenced by comparing SEM images of resin which was applied sorption procedure or not. The following ion exchange reaction was suggested between Hg<sup>2+</sup> ions and Purolite C100, similarly reaction of other metal cations:



The effects of experimental parameters were investigated and calibration graphs were obtained under the optimal conditions for proposed two centri-

voltammetric methods by using hydrazine and Purolite C100. Calibration curves of Hg(II) concentrations ranging from  $1.0 \times 10^{-8}$  M to  $1.0 \times 10^{-10}$  M and  $1.0 \times 10^{-7}$  M to  $5.0 \times 10^{-11}$  M were found in a logarithmically linear fashion, respectively. Their equations were as follows:

$$\text{with hydrazine} \quad \log i_p = -0.3467 \log C_{\text{Hg(II)}} + 6.0912 \quad (R^2: 0.9869)$$

$$\text{with Purolite C100} \quad \log i_p = -0.3047 \log C_{\text{Hg(II)}} + 5.9119 \quad (R^2 : 0.9937)$$

The accuracy of the centri-voltammetric analysis methods using hydrazine and Purolite C100 was tested with ICP-MS method. Relative percentage errors of the proposed methods were 10.3%, 6.3%, respectively while that of ICP-MS was 2.8%. The reproducibility values were found as 1.39% and 1.78% when hydrazine and Purolite C100 were used, respectively. When Purolite C100 resin was used as a carrier material, Hg(II) levels of as low as  $5 \times 10^{-11}$  M was able to measure.

Since centri-voltammetric method with Purolite C100 was more advantageous in terms of sensitivity, selectivity, and ease of application, interferences of Cd(II), Pb(II), Cu(II) and Fe(III) ions on the mercury signal were investigated in this method. When these ions concentration was more dilute than  $1 \times 10^{-9}$  M, it was not observed any interference effect. LOD and LOQ were calculated as  $1 \times 10^{-13}$  M and  $5.8 \times 10^{-12}$  M from the standard deviation of peak current values for  $5.0 \times 10^{-11}$  M Hg(II) solution, respectively. The centrifugation step carries out the bulk collection leading to a higher sensitivity.

The developed centri-voltammetric method using Purolite C100 was applied to spring water without any pre-treatment with considering interference effects by standard addition. The obtained results were compared with that of ICP-OES measurements. Average recovery value was 88%. Proximity of determined mercury(II) concentrations in spring water samples with both methods set forth accuracy of the proposed method.

These values proved that the developed centri-voltammetric method by using Purolite C100 is reliable, low cost, and easy applicable. Various carrier materials and reducing agents can be employed to improve the selectivity and the sensitivity of this method in future.

## REFERENCES

- Abo-Farha, S. A., Abdel-Aal, A.Y., Ashour, I. A. and Garamon, S. E.,** 2009, Removal of some heavy metal cations by synthetic resin purolite C100, *J. Hazard. Mater.*, 169:190-194pp.
- Abollino, O., Giacomino, A., Malandrino, M., Marro, S. and Mentasti, E.,** 2009, Voltammetric determination of methylmercury and inorganic mercury with an home made gold nanoparticle electrode, *J. Appl. Electrochem.*, 39:2209-2216 pp.
- Abollino, O., Giacomino, A., Malandrino, M., Piscionieri, G. and Mentasti, E.,** 2008, Determination of mercury by anodic stripping voltammetry with a gold nanoparticle-modified glassy carbon electrode, *Electroanalysis*, 20, 1:75-83pp.
- Agilent Technologies,** 7700 Series ICP-MS - 360° interactive animation, [http://www.chem.agilent.com/en-US/Products/Instruments/icp-ms/Pages/7700\\_animation.aspx](http://www.chem.agilent.com/en-US/Products/Instruments/icp-ms/Pages/7700_animation.aspx) (Date accessed: 27 July 2010)
- Allibone, J., Fatemian, E. and Walker, P. J.,** 1999, Determination of mercury in potable water by ICP-MS using gold as a stabilising agent, *J. Anal. At. Spectrom.*, 14:235-239 pp.
- Augelli, M.A., Munoz, R.A.A., Richter, E.M., Cantagallo, M.I. and Angnes, L.,** 2007, Analytical procedure for total mercury determination in fishes and shrimps by chronopotentiometric stripping analysis at gold film electrodes after microwave digestion, *Food Chem.*, 101:579-584 pp.
- Bonfil, Y., Brand, M. and Kirowa-Eisner, E.,** 2000, Trace determination of mercury by anodic stripping voltammetry at the rotating gold electrode, *Anal. Chim. Acta*, 424:65-76 pp.
- Cañada Rudner, P., Garcia de Torres, A., Cano Pavón, J.M. and Sanchez Rojas, F.,** 1998, On-line preconcentration of mercury by sorption on an anion-exchange resin loaded with 1,5-bis[(2-pyridyl)-3-sulphophenyl methylene] thiocarbonohydrazide and determination by cold-vapour inductively coupled plasma atomic emission, *Talanta*, 46:1095-1105 pp.
- Capelo, J. L., Lavilla, I. and Bendicho, C.,** 2000, Room temperature sonolysis-based advanced oxidation process for degradation of organomercurials: Applications to determination of inorganic and total mercury in waters by flow injection-cold vapor atomic absorption spectrometry, *Anal. Chem.*, 72:4979-4984.
- Chen, J. P. and Lim, L. L.,** 2002, Key factor in chemical reduction by hydrazine for recovery of precious metals, *Chemosphere*, 49:363-370 pp.
- Chiarle, S., Ratto, M. and Rovatti, M.,** 2000, Mercury removal from water by ion exchange resins adsorption, *Wat. Res.*, 11, 34:2971-2978 pp.
- Dai, H.P. and Shui, K. K.,** 1996, Voltammetric studies of electrochemical pretreatment of rotating-disc glassy electrodes in phosphate buffer, *J. Electroanal. Chem.*, 419:7-14 pp.

## REFERENCES (continued)

**Elsholz, O., Frank, C., Matyschok, B., Steiner, F., Wurl, O., Stachel, B., Reincke, H., Schulze, M., Ebinghaus, R. and Hempel, M.,** 2000, On-line determination of mercury in river water at the German monitoring station Schnackenburg/Elbe, *Fresenius J. Anal. Chem.*, 366:196-199 pp.

**Engstrom, R.C.,** 1982, Electrochemical pretreatment of glassy carbon, *Anal. Chem.*, 54:2310-2314 pp.

**EPA,** 1997, Aqueous mercury treatment, *Capsule Report*, EPA16251R971004.

**EPA,** (United States Environmental Protection Agency), 1996, Mercury in aqueous samples and extracts by anodic stripping voltammetry(ASV), Method 7472.

**Ermakov, S.S., Borzhitskaya, A.V and Moskvina, L.N.,** 2001, Electrochemical polishing of the surface of a gold electrode and its effect on the sensitivity of the stripping voltammetric determination of mercury(II), *J. Anal. Chem.*, 56:542-545 pp.

**Erdugan, E., Vardar, H., Ürkmez, İ. and Gökçel H. İ.,** 2009, Investigation of centri-voltammetric behavior of terbutaline at glassy carbon and carbon paste electrodes, *8th International Electrochemistry Meeting*, October 8-11, Antalya, Türkiye.

**Faller, C., Stojko, N.Y., Henze, G. and Brainina, K. Z.,** 1999, Stripping voltammetric determination of mercury at modified solid electrodes. Determination of mercury traces using PDC/Au(III) modified electrodes, *Anal. Chim. Acta*, 396:195-202 pp.

**Fernandez, C., Conceição, A. C. L., Rial-Otero, R., Vaz, C., and Capelo, J. L.,** 2006, Sequential flow injection analysis system on-line coupled to high intensity focused ultrasound: Methodology for trace analysis applications as demonstrated for the determination of inorganic and total mercury in waters and urine by cold-vapour atomic absorption spectrometry, *Anal. Chem.*, 78:2494-2499 pp.

**Filho, N. L. D. and Carmo, D. R.,** 2006, Study of an organically modified clay: Selective adsorption of heavy metal ions and voltammetric determination of mercury(II), *Talanta*, 68:919-927 pp.

**Giacomino, A., Abollino, O., Malandrino, M. and Mentasti, E.,** 2007, Parameters affecting the determination of mercury by anodic stripping voltammetry using a gold electrode, *Talanta*, 75:266-273 pp.

**Gil, S., Lavilla, I. and Bendicho, C.,** 2006, Ultrasound-promoted cold vapor generation in the presence of formic acid for determination of mercury by atomic absorption spectrometry, *Anal. Chem.*, 78:6260-6264 pp.

## REFERENCES (continued)

**Gil, S., Lavilla, I. and Bendicho, C.,** 2007, Green method for ultrasensitive determination of Hg in natural waters by electrothermal-atomic absorption spectrometry following sono-induced cold vapor generation and 'in-atomizer trapping', *Spectrochim. Acta, Part B*, 62:69-75 pp.

**Hassel, A. W., Fushimi, K. and Seo, M.,** 1999, An agar-based silver/silver chloride reference electrode for use in micro-electrochemistry, *Electrochem. Commun.* 1:180-183 pp.

**Hatle, M.,** 1987, Determination of mercury by differential pulse anodic stripping voltammetry with various working electrodes, *Talanta*, 34:1001-1007 pp.

**Hernandez, O., Castro, V. and Arias, J. J.,** 1991, Preconcentration of mercury(II) with a chelating resin modified with chromotrope-2R, *Anal. Sci.*, 7:341-344 pp.

**Kirgöz, Ü. A., Tural, H. and Ertaş, F. N.,** 2004, A new procedure for voltammetric lead determination based on coprecipitation and centrifugation preconcentration, *Electroanalysis*, 9, 16:765-768 pp.

**Kirgöz, Ü. A., Tural, H. and Ertaş, F. N.,** 2005, Centri-voltammetric study with amberlite XAD-7 resin as a carrier system, *Talanta*, 65:48-53 pp.

**Koçak, S.,** 2009, Centri-voltammetric molybdenum determination and electrochemical polyoxo-molybdate formation and its characterization, PhD. Thesis, *Ege Univ. Grad. Sc. Nat. Appl. Sci.*, 154p.

**Koçak, S., Ertaş, F. N. and Tural, H.,** 2008, Centri-voltammetric determination of molybdenum(VI) in the presence and absence of 8-hydroxyquinoline, *6th Aegean Anal. Chem. Days, October, 9-12, Denizli*. Book of Abstracts: 119.

**Kołodnyńska, D., Hubicki, Z. and Gęca, M.,** 2008, Application of a new-generation complexing agent in removal of heavy metal ions from aqueous solutions, *Ind. Eng. Chem. Res.*, 47:3192-3199 pp.

**Korolczuk, M.,** 1997, Sensitive and selective determination of mercury by differential pulse stripping voltammetry after accumulation of mercury vapour on a gold plated graphite electrode, *Fresenius J Anal Chem*, 357: 389-391 pp.

**Korolczuk, M. and Rutyna, I.,** 2008, New methodology for anodic stripping voltammetric determination of methylmercury, *Electrochem. Commun.*, 10:1024-1026 pp.



## REFERENCES (continued)

- Kubáň, P., Houserová, P., Kubáň P., Hauser, P. C. and Kubáň, V.,** 2007, Sensitive capillary electrophoretic determination of mercury species with amperometric detection at a copper electrode after cation exchange preconcentration, *J. Sep. Sci.*, 30:1070-1076pp.
- Labatzke, T. and Schlemmer, G.,** 2004, Ultratrace determination of mercury in water following EN and EPA standards using atomic fluorescence spectrometry, *Anal. and Bioanal. Chem.*, 378:1075-1082 pp.
- Leopold, K., Foulkes, M. and Worsfold, P.J.,** 2009, Gold-coated silica as a preconcentration phase for the determination of total dissolved mercury in natural waters using atomic fluorescence spectrometry, *Anal. Che.*, 81: 3421-3428 pp.
- Leopold, K., Harwardt, L., Schuster, M. and Schlemmer, G.,** 2008, A new fully automated on-line digestion system for ultra trace analysis of mercury in natural waters by means of FI-CV-AFS, *Talanta*, 76:382-388pp.
- Lindquist, O. Jernelöv, A. Johannson, K. and Rodhe, R.,** 1984, Mercury in the Swedish environment, *National Environment Board*, 105p.
- Locatelli, C. and Melucci, D.,** 2010, Sequential voltammetric determination of mercury(II) and toxic metals in environmental bio-monitors: application to mussels and clams, *Intern. J. Environ. Anal. Chem.*, 1, 90:49-63 pp.
- Locatelli, C. and Torsi, G.,** 2003, Analytical procedures for the simultaneous voltammetric determination of heavy metals in meals, *Microchem. J.*, 75:233-240 pp.
- Lu, J., He, X., Zeng, X., Wan, Q. and Zhang, Z.,** 2003, Voltammetric determination of mercury(II) in aqueous media using glassy carbon electrodes modified with novel calix[4]arene, *Talanta*, 59: 553-560 pp.
- Meucci, V., Laschi, S., Minunni, M., Pretti, C., Intorre, L., Soldani, G. and Macsini, M.,** 2009, An optimized digestion method coupled to electrochemical sensor for the determination of Cd, Cu, Pb and Hg in fish by square wave anodic stripping voltammetry, *Talanta*, 77:1143-1148 pp.
- Mizuike, A.,** 1983, Enrichment Technique for Inorganic Analysis, Springer Verlag, Berlin, 144p.
- Mojica, E. R. E. and Mecra, F. E.,** 2005, Anodic stripping voltammetric determination of mercury(II) using lectin-modified carbon paste electrode, *J. Appl. Sci.*, 5, 8:1461-1465 pp.
- Monk, P.M.S.,** 2002, Fundamentals of Electroanalytical Chemistry, Wiley, Chichester. 361p.
- Monteagudo, J. M. and Ortiz, M. J.,** 2000, Removal of inorganic mercury from mine waste water by ion exchange, *J. Chem. Technol. Biotechnol.*, 75: 767-772 pp.



## REFERENCES (continued)

**Moreno, R. G. M., Oliveira, E., Pedrotti, J. J. and Oliveira, P. V.,** 2002, An electrochemical flow-cell for permanent modification of graphite tube with palladium for mercury determination by electrothermal atomic absorption spectrometry, *Spectrochim. Acta, Part B*, 57: 769-778 pp.

**Morita, M., Yoshinaga J. and Edmonds, J. S.,** 1998, The determination of mercury species in environmental and biological samples, *Pure & Appl. Chem.*, 8, 70:1585-1615 pp.

**Murillo, M., Carrión, N., Chirinos, J., Gammiero, A. and Fassano, E.,** 2001, Optimization of experimental parameters for the determination of mercury by MIP/AES, *Talanta*, 54:389-395 pp.

**New Mexico State University,** College of Arts and Sciences, Dept. Chem. and Biochem.,

[http://www.chemistry.nmsu.edu/Instrumentation/NMSU\\_Optima2100A.html](http://www.chemistry.nmsu.edu/Instrumentation/NMSU_Optima2100A.html)

(Date accessed: 27 July 2010).

**Okçu, F., Ertaş, F. N., Gökçel, H. İ. and Tural, H.,** 2005, Anodic stripping voltammetric behavior of mercury in chloride medium and its determination at a gold film electrode, *Turk J. Chem.*, 29:355-366 pp.

**Okçu, F., Ertaş, H. and Ertaş, F. N.,** 2008, Determination of mercury in table salt samples by on-line medium exchange anodic stripping voltammetry, *Talanta*, 75:442-446 pp.

**Osipova, E.A., Sladkov, V. E., Kamenev A. I., Shkinev, V.M. and Geckeler, K.E.,** 2000, Determination of Ag(I), Hg(II), Cu(II), Pb(II), Cd(II) by stripping voltammetry in aqueous solutions using complexing polymers in conjunction with membrane filtration, *Anal. Chim. Acta*, 404:231-240 pp.

**Pavlogeorgatos, G. and Kikilias, V.,** 2002, The importance of mercury determination and speciation to the health of the general population, *Global Nest: the Int. J.*, 4:107-125 pp.

**Purolite ion exchange resin,** [www.purolite.com](http://www.purolite.com) ( Date accessed: 15 June 2009).

**Public Health Statement,** 1990, Mercury, USA.

**Radulescu, M. C. and Danet, A. F.,** 2008, Mercury determination in fish samples by chronopotentiometric stripping analysis using gold electrodes prepared from recordable CDs, *Sensors*, 8:7157-7171 pp.

**Roa-Morales, G., Ramírez-Silva, M. T., González, R. L., Galicia, L. and Romero-Romo, M.,** 2005, Electrochemical characterization and determination of mercury using carbon paste electrodes modified with cyclodextrins, *Electroanalysis*, 17, 8:694-700 pp.

## REFERENCES (continued)

**Romanenko, S. V. and Larina, L. N.**, 2005, A choice of optimal surface modifier of carbon electrodes for mercury determination by stripping voltammetry, *J. Electroanal. Chem.*, 583:155-161 pp.

**Salaun, P. and Berg C. M. G.**, 2006, Voltammetric detection of mercury and copper in seawater using a gold microwire electrode, *Anal. Chem.*, 78:5052-5060pp.

**Santos, J. S., Guàrdia, M., Pastor, A. and Santos, M. L. P.**, 2009, Determination of organic and inorganic mercury species in water and sediment samples by HPLC on-line coupled with ICP-MS, *Talanta*, 80:207-211pp.

**Sarzanini, C., Sacchero, G., Aceto, M., Abollino, O. and Mentasti, E.**, 1994, Ion chromatographic separation and on-line cold vapour atomic absorption spectrometric determination of methylmercury, ethylmercury and inorganic mercury, *Anal. Chim. Acta*, 284:661-667 pp.

**Settle, F.**, 1997, Handbook of Instrumental Techniques for Analytical Chemistry, Prentice Hall, Upper Saddle River, 995p.

**Sousa, M. F. B. and Bertazzoli R.**, 1996, Preconcentration and voltammetric determination of mercury(II) at a chemically modified glassy carbon electrode, *Anal. Chem.*, 68:1258-1261 pp.

**Švarc-Gajić, J., Suturović, Z., Marjanović, N. and Kravić, S.**, 2006, Determination of mercury by chronopotentiometric stripping analysis using glassy carbon vessel as a working electrode, *Electroanalysis*, 18, 5:513-516 pp.

**Šenkál, B. F. and Yavuz, E.**, 2006, Crosslinked poly(glycidyl methacrylate)-based resin for removal of mercury from aqueous solutions, *J. Appl. Poly. Sci.*, 101:348-352 pp.

**Tanaka, H., Nakagawa, T., Okabayashi, Y., Aoyama, H., Tanaka, T., Itoh, K., Chikuma, M., Saito, Y., Sakurai, H. and Nakayama, M.**, 1987, Development of functional resins by modification of ion-exchange resins and their application to analytical chemistry, *Pure & Appl. Chem.*, 4, 59:573-57 pp.

**Tonle, I. K., Ngamenia, E. and Walcarius A.**, 2005, Preconcentration and voltammetric analysis of mercury(II) at a carbon paste electrode modified with natural smectite-type clays grafted with organic chelating groups, *Sensors and Actuators B*, 110:195-203 pp.

**Ugo, P., Zampieri, S., Moretto L. M. and Paolucci, D.**, 2001, Determination of mercury in process and lagoon waters by inductively coupled plasma-mass spectrometric analysis after electrochemical preconcentration: comparison with anodic stripping at gold and polymer coated electrodes, *Anal. Chim. Acta*, 434:291-300 pp.

## REFERENCES (continued)

- Ürkmez, İ.**, 2004, Alternative technique for mercury determination: centri-voltammetry, MSc. Thesis, *Ege Univ. Grad. Sc. Nat. Appl. Sci.*, 52p.
- Ürkmez, İ., Gökcel, H. İ., Ertaş, F. N. and Tural H.**, 2009, Centrifugation: an efficient technique for preconcentration in anodic stripping mercury analysis using gold film electrode, *Microchim. Acta*, 167:225-230 pp.
- Vardar, H.**, 2008, Investigation of centri-voltammetric behavior of some heavy metals, MSc. Thesis, *Ege Univ. Grad. Sc. Nat. Appl. Sci.* 76p.
- Vladimirovna, Z. A.**, 2006, The improvement of anodic stripping voltammetric (ASV) method of cadmium and mercury determination, MSc. Thesis, *Luleå University of Technology*, 37p.
- Wang, J.**, 2006, Analytical Electrochemistry, Third Edition, Wiley-VCH Pub., New Jersey, 250p.
- Wang, L. and Tien, H.**, 1994, Determination of lead, arsenic and mercury in cosmetic formulations at modified electrodes, *Inter. J. Cosm.c Sci.*, 16:29-38pp.
- Watson, C. M., Dwyer, D. J., Andle, J. C., Bruce, A. E. and Bruce, M. R. M.**, 1999, Stripping analyses of mercury using gold electrodes: irreversible adsorption of mercury, *Anal. Chem.*, 71:3181-3186pp.
- WHO** (World Health Organization), 1989, Mercury - environmental aspects, Environmental Health Criteria, Geneva, 86p.
- WHO** (World Health Organization), 1990, Methylmercury, Environmental Health Criteria, Geneva, 101p.
- WHO** (World Health Organization), 1990, International Programme on Chemical Safety, Geneva, Switzerland, 168p.
- Wikipedia**, 2010, [en.wikipedia.org/wiki/Centrifuge](http://en.wikipedia.org/wiki/Centrifuge) (Date access: 8 April 2010)
- Wiatrowski, H.A., Ward, P.M. and Barkay T.**, 2006, Novel reduction of mercury(II) by mercury-sensitive dissimilatory metal reducing bacteria, *Environ. Sci. Technol.*, 40:6690-6696pp.
- Widmann, A. and Berg, C. M. G.**, 2005, Mercury detection in seawater using a mercaptoacetic acid modified gold microwire electrode, *Electroanalysis*, 17, 10:825-831pp.
- Willard, H. H. and Boldyreff, A. W.**, 1930, Determination of mercury as metal by reduction with hydrazine or stannous chloride, *J. Am. Chem. Soc.*, 52, 2: 569-574pp.
- Willard, H. H., Merritt, L. L., Dean, J. A. and Settle, F. A.**, 1981, Instrumental Methods of Analysis, D. Van Nostrand Company, New York, 1030p.

## REFERENCES (continued)

**Wu, J., Li, L., Shen, B., Cheng, G., He, P. and Fang, Y.,** 2010, Polythymine oligonucleotide-modified gold electrode for voltammetric determination of mercury(II) in aqueous solution, *Electroanalysis*, 22, 4:479-482pp.

**Wu, Q., Apte, S. C., Batley, G. E. and Bowles, K. C.,** 1997, Determination of the mercury complexation capacity of natural waters by anodic stripping voltammetry, *Anal. Chim. Acta*, 350:129-134pp.

**Wuilloud, J. C. A., Wuilloud, R. G., Silva, M. F., Olsina, R. A. and Martinez, L. D.,** 2002, Sensitive determination of mercury in tap water by cloud point extraction pre-concentration and flow injection-cold vapor inductively coupled plasma optical emission spectrometry, *Spectrochim. Acta Part B*, 57:365-374pp.

**Wurl, O., Elsholz, O. and Ebinghaus, R.,** 2000, Flow-system device for the on-line determination of total mercury in seawater, *Talanta*, 52:51-57pp.

**Xu, H., Zeng, L., Xing, S., Shi, G., Xian, Y. and Jin, L.,** 2008, Microwave-radiated synthesis of gold nanoparticles/carbon nanotubes composites and its application to voltammetric detection of trace mercury(II), *Electrochem. Commun.*, 10:1839-1843pp.

**Zen, J.M. and Chung, M. J.,** 1995, Square-wave voltammetric stripping analysis of mercury(II) at a poly(4-vinylpyridine)/gold film electrode, *Anal. Chem.*, 67:3571-3577pp.

**Zierhut, A., Leopold, K., Harwardt, L. and Schuster, M.,** 2010, Reagenzienfreie bestimmung von quecksilberspuren in wasserproben, *Umweltwiss Schadst Forsch*, 22:72-77pp.

**Zierhut, A., Leopold, K., Harwardt, L., Worsfold, P. and Schuster, M.,** 2009, Activated gold surfaces for the direct preconcentration of mercury species from natural waters, *J. Anal. Atom. Spectrom.*, 24:767-774pp.

## APPENDICES

*Appendix 1:* The operation sequence and the programme of voltammetric formation of GFE in DC mode

Method : goldfilmipek.mth OPERATION SEQUENCE  
Title : Mercury determination

|    | <u>Instructions</u> | <u>t/s</u> | <u>Main parameters</u> |                   | <u>Auxiliary parameters</u> |            |
|----|---------------------|------------|------------------------|-------------------|-----------------------------|------------|
| 1  | SMPL/M              |            | V.fraction             | 20.000 mL         | V.total                     | 21.0 mL    |
| 2  | RDE                 |            | Rot. speed             | 1600 /min         |                             |            |
| 3  | DOS>M               |            | Soln.name              | HClO <sub>4</sub> | V. add                      | 1.00 mL    |
| 4  | DOS>M               |            | Soln.name              | Au                | V. add                      | 0.1 MmL    |
| 5  | PURGE               | 300        |                        |                   |                             |            |
| 6  | Q PURGE             |            |                        |                   |                             |            |
| 7  | CONDC               |            | U. start               | -600 mV           | Rate 1                      | 1000 mV/s  |
|    |                     |            | U. end                 | 800 mV            | Rate 2                      | 10000 mV/s |
|    |                     |            | Cycles                 | 100               |                             |            |
| 8  | SEGMENT             |            | Segm. name             | Prp-100           |                             |            |
| 9  | CONDC               |            | U. start               | -600mV            | Rate 1                      | 1000 mV/s  |
|    |                     |            | U. end                 | 800 mV            | Rate 2                      | 10000 mV/s |
|    |                     |            | Cycles                 | 10                |                             |            |
| 10 | SEGMENT             |            | Segm. name             | Prp-100           |                             |            |
| 11 | CONDC               |            | U. start               | -600mV            | Rate 1                      | 1000 mV/s  |
|    |                     |            | U. end                 | 800 mV            | Rate 1                      | 10000 mV/s |
|    |                     |            | Cycles                 | 10                |                             |            |
| 12 | SEGMENT             |            | Segm. name             | Prp-100           |                             |            |
| 13 | CONDC               |            | U. start               | -600mV            | Rate 1                      | 1000 mV/s  |
|    |                     |            | U. end                 | 800 mV            | Rate 1                      | 10000 mV/s |
|    |                     |            | Cycles                 | 10                |                             |            |
| 14 | MEAS                | 120        | u.meas                 | 0 mV              |                             |            |
| 15 | END                 |            |                        |                   |                             |            |

Method : goldfilmipek.mth SEGMENT  
Prp-100

|   | <u>Instructions</u> | <u>t/s</u> | <u>Main parameters</u> |           | <u>Auxiliary parameters</u> |         |
|---|---------------------|------------|------------------------|-----------|-----------------------------|---------|
| 1 | RDE                 |            | Rot.speed              | 1600 /min |                             |         |
| 2 | STIR                |            | Rot.speed              | 1600 /min |                             |         |
| 3 | DCTMODE             |            | t.step                 | 0.30 s    | t.meas                      | 40.0 ms |
| 4 | MEAS                | 100        | U.meas                 | -500 mV   |                             |         |
| 5 | QSTIR               | 2.0        |                        |           |                             |         |
| 6 | END                 |            |                        |           |                             |         |

**APPENDICES (continued)**

*Appendix 2:* The operation sequence and the programme of voltammetric stripping measurement in DP mode.

| Method : ipek2.mth |                     | OPERATION SEQUENCE    |                        |           |                             |
|--------------------|---------------------|-----------------------|------------------------|-----------|-----------------------------|
| Title              |                     | : determination of Hg |                        |           |                             |
|                    | <u>Instructions</u> | <u>t/s</u>            | <u>Main parameters</u> |           | <u>Auxiliary parameters</u> |
| 1                  | DOS/M               |                       | V.added                | 20.000 mL |                             |
| 2                  | REM                 |                       | 10.mL buffer           |           |                             |
| 3                  | SMPL/M              |                       | V.fraction             | 0.100 mL  | V.total 20.0 mL             |
| 4                  | PURGE               | 0.1                   |                        |           |                             |
| 5                  | QPURGE              | 0.1                   |                        |           |                             |
| 6                  | SEGMENT             |                       | Segm.name              | pol       |                             |
| 7                  | END                 |                       |                        |           |                             |

| Method : ipek2.mth |                     | SEGMENT    |                        |         |                             |
|--------------------|---------------------|------------|------------------------|---------|-----------------------------|
|                    |                     | pol        |                        |         |                             |
|                    | <u>Instructions</u> | <u>t/s</u> | <u>Main parameters</u> |         | <u>Auxiliary parameters</u> |
| 1                  | RDE                 |            | Rot.speed              | 0 /min  |                             |
| 2                  | DPMODE              |            | U.ampl                 | 50 mV   | t.meas 20.0 ms              |
|                    |                     |            | t.step                 | 0.60 s  | t.pulse 40.0 ms             |
| 3                  | SWEEP               | 182        | U.start                | -1000mV | U.step 6 mV                 |
|                    |                     |            | U.end                  | 800 mV  | Sweep rate 10 mV/s          |
| 4                  | END                 |            |                        |         |                             |

## **CIRRICULUM VITAE**

### **PERSONEL INFORMATION**

**Name:** İpek ÜRKMEZ

**Date of Birth:** 06.02.1977

**Place of Birth:** İZMİR/ Selçuk

**Nationality:** T.C

**Gender:** Female

**Marital Status:** Single

### **MAILING ADDRESS**

Ege University Faculty of Sciences

Department of Chemistry, Division of Analytical Chemistry.

35100 Bornova -İZMİR –TURKEY

**Phone:** +90 232 3884000

**Fax:** +90 232 3888264

**Email:** [iurkmez@yahoo.com](mailto:iurkmez@yahoo.com)

**Home address:**

Gerçek Sit. Bloc 4/6 Kadınlar Denizi

Kuşadası- AYDIN

**EDUCATION**

➤ September 2000 – 2004

M.Sc. Degree, Ege University Graduate School of Natural and Applied Sciences,  
Department of Analytical Chemistry, Bornova, IZMIR

➤ September 1995 – July 2000

B.Sc. Degree in Chemistry  
Faculty of Science, Ege University, Bornova, IZMIR

**LANGUAGES**

English reading and writing

**THESIS**

I. URKMEZ, “*Determination of Mercury II Ions by Centri Voltammetric Technique*” Ege University Graduate School of Natural and Applied Sciences  
Department of Analytical Chemistry M.Sc. Thesis, August, 2004

**PUBLICATION**

Ürkmez, İ., Gökcel, H. İ., Ertaş, F. N. and Tural H., 2009, Centrifugation: an efficient technique for preconcentration in anodic stripping mercury analysis using gold film electrode, *Microchim. Acta*, 167:225-230.